MICROCOPY RESOLUTION TEST CHART

NATIONAL BUREAU OF STANDARDS 1963 A

LEVEL

AD A109703

EFFECTS OF SURFACE CONDITIONS ON
CARRIER TRANSPORT IN III-V COMPOUNDS

R.W. Grant, S.P. Kowalczyk, J.R. Waldrop, W.A. Hill, and E.A. Kraut
Rockwell International Corporation
Microelectronics Research and Development Center
1049 Camino Dos Rios
Thousand Oaks, California 91360

DTIC
SELECTED
JAN 1 8 1982

H

November 1981

Final Report for the period
September 1, 1978 through March 1, 1981

DTIC FILE COPY

AVIONICS LABORATORY
AIR FORCE WRIGHT AERONAUTICAL LABORATORIES
AIR FORCE SYSTEMS COMMAND
WRIGHT-PATTERSON AIR FORCE BASE, OHIO 45433

01 15 82

NOTICE

When Government drawings, specifications, or other data are used for any purpose other than in connection with a definitely related Government procurement operation, the United States Government thereby incurs no responsibility nor any obligation whatsoever; and the fact that the government may have formulated, furnished, or in any way supplied the said drawings, specifications, or other data is not to be regarded by implication or otherwise as in any manner licensing the holder or any other person or corporation, or conveying any rights or permission to manufacture use, or sell any patented invention that may in any way be related thereto.

This report has been reviewed by the Office of Public Affairs (ASD/PA) and is releasable to the National Technical Information Service (NTIS). At NTIS, it will be available to the general public, including foreign nations.

This technical report has been reviewed and is approved for publication.

DIETRICH W. LANGER
Project Engineer
Electronic Research Branch
Avionics Laboratory

FOR THE COMMANDER

PHILIP E. STOVER, Chief
Electronic Research Branch
Avionics Laboratory

"If your address has changed, if you wish to be removed from our mailing list, or if the addressee is no longer employed by your organization please notify AFWAL/AADR, W-PAFB, OH 45433 to help us maintain a current mailing list."

Copies of this report should not be returned unless return is required by security considerations, contractual obligations, or notice on a specific document.

REPORT DOCUMENTATION PAGE	READ INSTRUCTIONS BEFORE COMPLETING FORM

1. REPORT NUMBER	2. GOVT ACCESSION NO.	3. RECIPIENT'S CATALOG NUMBER
AFWAL-TR-81-1200	AD-A109703	

4. TITLE (and Subtitle)	5. TYPE OF REPORT & PERIOD COVERED
EFFECTS OF SURFACE CONDITIONS ON CARRIER TRANSPORT IN III-V COMPOUNDS	Final Report 09/01/78 through 03/1/81
	6. PERFORMING ORG. REPORT NUMBER ERC41012.102FR

7. AUTHOR(s)	8. CONTRACT OR GRANT NUMBER(s)
R.W. Grant, S.P. Kowalczyk, J.R. Waldrop, W.A. Hill, and E.A. Kraut	F33615-78-C-1532

9. PERFORMING ORGANIZATION NAME AND ADDRESS	10. PROGRAM ELEMENT, PROJECT, TASK AREA & WORK UNIT NUMBERS
Rockwell International Microelectronics Research & Development Center 1049 Camino Dos Rios, Thousand Oaks, CA 91360	P.E. 61102F Project No. 2306R180

11. CONTROLLING OFFICE NAME AND ADDRESS	12. REPORT DATE
Air Force Wright Aeronautical Laboratories Avionics Laboratory (AFWAL/AADR) Wright-Patterson Air Force Base, Ohio 45433	November 1981
	13. NUMBER OF PAGES 105

14. MONITORING AGENCY NAME & ADDRESS(If different from Controlling Office)	15. SECURITY CLASS. (of this report)
	Unclassified
	15a. DECLASSIFICATION/DOWNGRADING SCHEDULE

16. DISTRIBUTION STATEMENT (of this Report)

Approved for public release; distribution unlimited.

17. DISTRIBUTION STATEMENT (of the abstract entered in Block 20, if different from Report)

18. SUPPLEMENTARY NOTES

19. KEY WORDS (Continue on reverse side if necessary and identify by block number)

XPS, GaAs, surface chemistry, band bending, surface potential, oxidation, contactless C-V probe, thermal cleaning, defect model, interface Fermi-level, annealing, deposited materials.

20. ABSTRACT (Continue on reverse side if necessary and identify by block number)

Surface chemical and potential measurements carried out by XPS (x-ray photo-emission spectroscopy) are reported for several GaAs materials. The GaAs samples had (100) and (110) orientations, n- and p-type doping, and both bulk and VPE grown materials were studied. Various surface treatments which included chemical etching, annealing, oxidation, gas exposure, and deposition of materials were investigated. The thermal cleaning process was shown to be associated with the surface chemical reaction $As_2O_3 + 2GaAs \rightarrow Ga_2O_3 + (4/x)As_x\uparrow$.

DD FORM 1473, EDITION OF 1 NOV 65 IS OBSOLETE

A variation in GaAs interface Fermi-level position of up to 0.7 eV was observed. The difference in interface Fermi-level position for n- and p-type samples subjected to identical surface treatments was observed to be nearly constant at $\approx$ 0.3 eV. A single defect model with multiple charge states is suggested as the simplest explanation for the observed interface-potential variations. Progress toward the development of a contactless C-V apparatus is described.

TABLE OF CONTENTS

LIST OF FIGURES

LIST OF FIGURES (Continued)

LIST OF TABLES

I. INTRODUCTION

This is the final report for Contract No. F33615-78-C-1532, entitled "Effects of Surface Conditions on Carrier Transport in III-V Compounds." The report describes work that was performed on the 30-month contract which was initiated in September 1978. Work that was reported previously in four interim reports associated with this contract is included here. In addition, activities pursued during the last 6-month phase of the contract are reported.

As GaAs microwave technology moves toward higher frequency and smaller dimension devices, the importance of surface-potential stability and control of the surface potential so as to minimize surface band bending at the active layer—gate interface of an FET increases. Also, for many years there has been interest in a GaAs MIS technology. The development of such a technology, has been limited by the absence of a stable GaAs—insulator interface which does not exhibit large hysteresis effects and which permits inversion and accumulation to be obtained. The identification of such an interface could have considerable influence on future GaAs device technology. The nature and properties of the GaAs interface states is a key element in learning how to control GaAs interface properties so as to maximize device performance.

The primary approach to studying GaAs interface characteristics followed in this program was to correlate surface chemistry and surface potential by means of x-ray photoemission spectroscopy (XPS). By utilizing XPS to study GaAs surfaces on which the selvedge thickness is on the order of the XPS photoelectron escape depth, both the surface chemistry and surface potential can be determined from a single measurement. Thus the GaAs surface chemistry can be altered and the corresponding effect on surface potential can be directly determined.

Section II of this report describes the XPS apparatus and measurement technique that wereutilized to correlate GaAs surface chemistry and poten-

1

tial. Characterization and initial surface preparation of GaAs samples is also discussed. Section III presents all of the experimental results obtained from XPS studies in this program. Included in this section are studies of thermally treated surfaces, oxidized surfaces, surfaces intentionally exposed to gases or on which materials were deposited, and samples with different doping type. Section IV develops a model to interpret the correlation of surface potential with surface chemistry and doping type observed experimentally. This model associates the interface states responsible for Fermi-level pinning and thus the observed surface potential with multiple charge states of a single GaAs interfacial defect. Section V describes progress toward the development of a C-V apparatus which could permit the determination of interface-state densities without physically contacting a sample. Two papers were published based on work supported by this contract; these papers are reproduced in the appendix.

II. APPLICATION OF XPS FOR GaAs SURFACE POTENTIAL MEASUREMENTS

The most frequent and well known application of XPS is the determination of surface chemistry by analysis of the chemical shift.[1] XPS can also be used to measure surface potential and interface band bending,[2] although this application has not received widespread attention. Much of the work carried out as part of this contract involved studies of the relationship between GaAs surface chemistry and surface potential. Consequently, in Section II.A we discuss the XPS apparatus; in Section II.B the XPS measurement technique that was used to determine GaAs surface potentials is described. Application of the technique requires knowledge of the sample doping characteristics. Properties and initial surface preparation of the GaAs samples utilized in this work are summarized in Section II.C.

II.A   XPS Apparatus

The XPS measurements discussed throughout this report were obtained by using a Hewlett-Packard 5950A XPS spectrometer with monochromatic Al Kα radiation (1486.6 eV). The XPS system includes a bakeable ultrahigh vacuum (UHV) custom-built sample preparation chamber. By combining ion-, cryo-, and Ti-sublimation-pumping it is possible to obtain a system base pressure of $<10^{-10}$ torr. However, because many of the experiments carried out during this work involved exposure of GaAs surfaces to various gasses, sample heating, and evaporation of various materials onto sample surfaces, the typical system pressure during most of the XPS experiments was in the low 10^{-9} to high 10^{-10} torr range.

A schematic diagram of the XPS system is shown in Fig. 1. The sample preparation chamber has several features which were used in this work. The instrumentation includes a low energy electron diffraction (LEED) system, a rastered ion sputter gun, a general purpose multi-source evaporation system with a shutter to interrupt the beam, and a quartz crystal film thickness deposition monitor. The sample is attached to a movable rod which incorporates a long UHV bellows assembly.

The sample holder has a heater with an attached thermocouple temperature monitor. There is a substantial temperature drop between the measured thermocouple temperature and the sample surface temperature. By comparing our measured temperature at which a GaAs surface can be thermally cleaned with results of others,[3] we estimate that our measured temperatures are ≈20% too high. Consequently, all sample temperatures given in this report have been reduced by ≈20% to provide a more consistent basis to compare results. A temperature controller which utilizes the thermocouple as a monitor, was used to regulate the sample temperature between room temperature and ≈600°C. The GaAs samples were attached to a Mo sample platen by In. This sample platen was mechanically attached to the sample heater.

As part of this program, an evaporator capable of depositing small amounts of semiconducting or insulating compounds on GaAs surfaces was

3
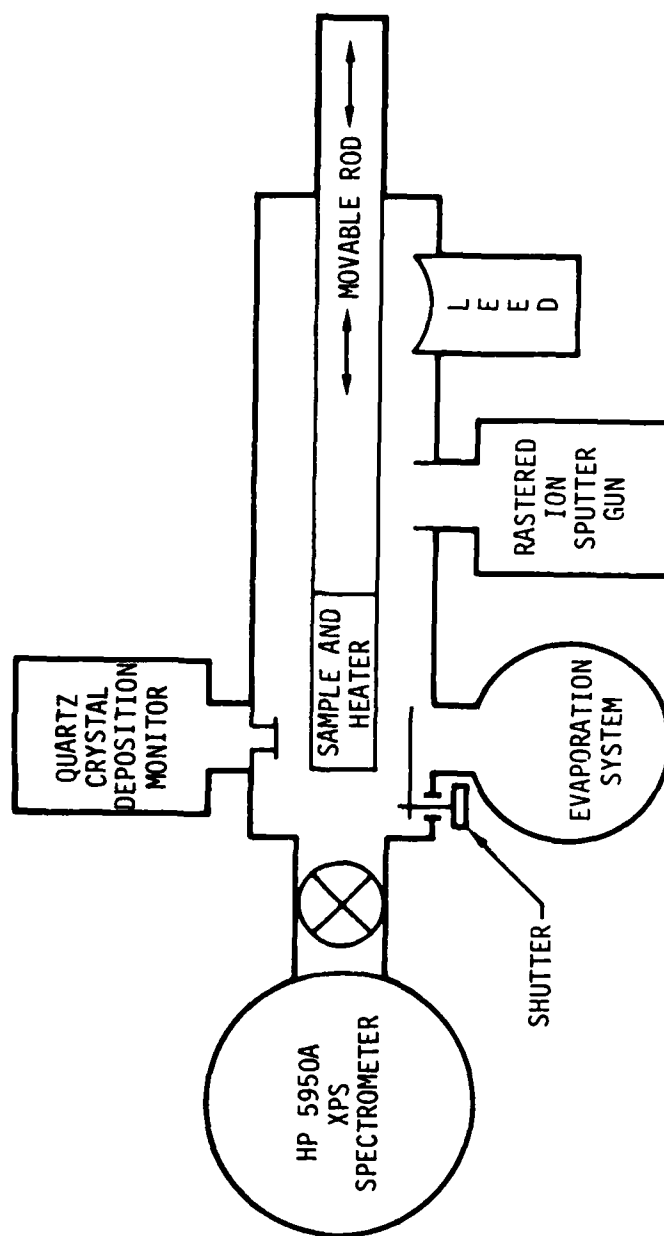
Fig. 1 Schematic diagram which illustrates essential components of XPS apparatus.

4

developed. The evaporator consisted of a small resistively heated quartz ampoule which was mounted in the XPS sample preparation chamber in close proximity to the sample surface (≈1 in.) to minimize the amount of evaporated material required to produce thin layers on the GaAs surfaces within the UHV system.

II.B   Surface Potential Measurement Technique

In this Section, the use of XPS as a potential monitoring technique is described. This application is illustrated in Fig. 2 which shows a schematic band diagram for n-type GaAs. The interface (or band-bending) potential is V_{BB} and for no band bending (a flatband condition), $V_{BB} = 0$. The other parameters shown in Fig. 2, namely E_c^{GaAs}, E_F, $E_{v,}^{GaAs}$, E_{As3d}^{GaAs}, q, W, E_B are the conduction-band minimum, the Fermi energy, the valence-band maximum, the As3d core-level binding energy, the electronic charge, the depletion width, and the binding energy referenced to E_F. The notation (b) and (i) refers to bulk- and interface-quantities, respectively, and $\Delta = E_F - E_v$.

As mentioned in Section II.A, the XPS measurements discussed throughout this report were all obtained by using monochromatic Al Kα radiation (1486.6 eV). The escape depths for the Ga3d and As3d photoelectrons excited by this radiation are ≈25Å.[4] Thus, if only a thin (thickness comparable to the escape depth) layer of material is present on a GaAs surface, it is possible to observe As3d and Ga3d photoelectrons originating from the GaAs; in Fig. 2, this thin layer is shown as ≈20Å. For this case $E_{As3d}^{GaAs}(i)$ or $E_{Ga3d}^{GaAs}(i)$ is measured. If the GaAs is only moderately doped ($\lesssim 10^{17}$ cm^{-3}), W ≈10^3Å and thus band bending will not complicate the interface core-level binding energy measurement. On the other hand, if the doping density is too low, the sample resistivity could become large enough that charging effects would complicate the XPS measurements. Consequently, a doping density in the 10^{16} cm^{-3} range is very suitable for XPS surface-potential measurements.

From Fig. 1 it is clear that the position of E_F at the interface, $\Delta(i)$, is given as

5
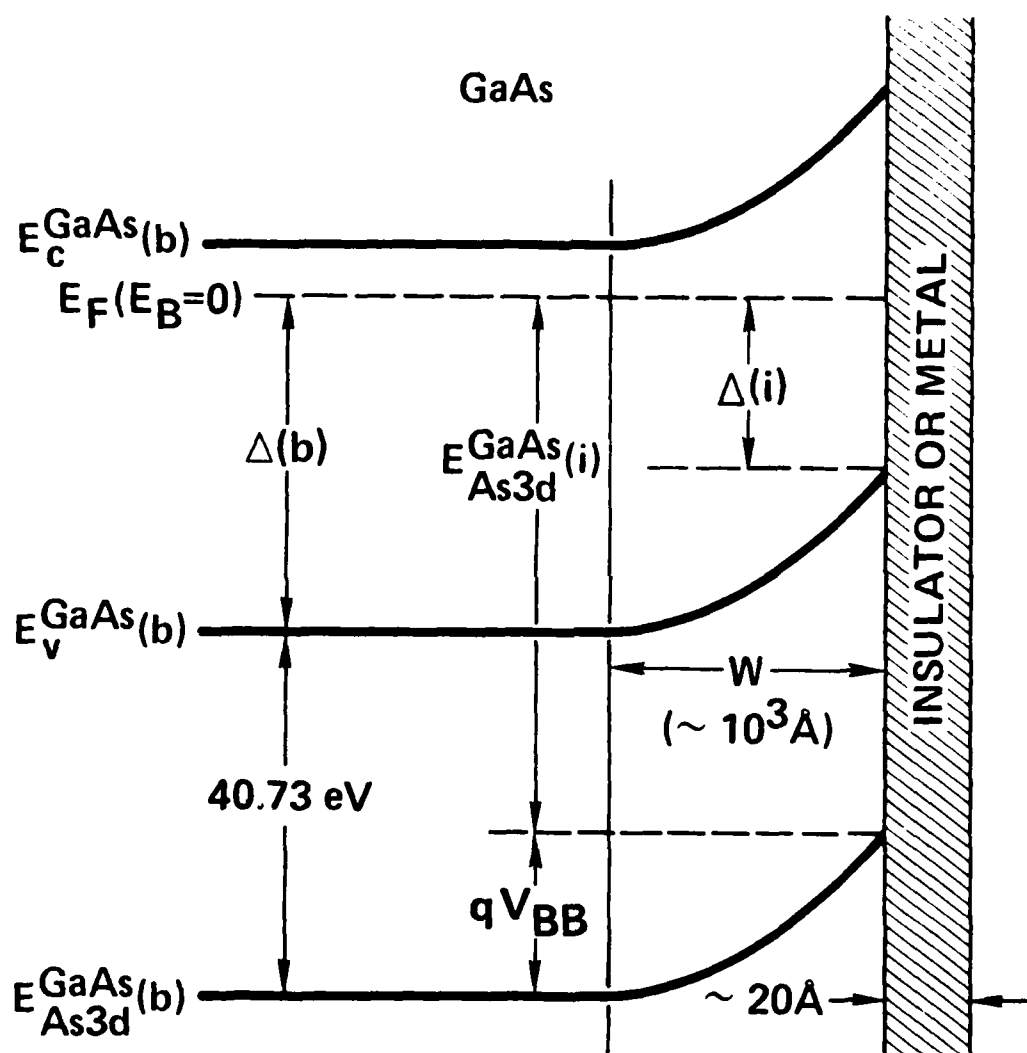
Fig. 2 Schematic energy-band diagram which illustrates the XPS measurement
of band bending.

6

$$\Delta(i) = E_{As3d}^{GaAs}(i) - (E_{As3d}^{GaAs} - E_v^{GaAs}) \tag{1}$$

or equivalently

$$\Delta(i) = E_{Ga3d}^{GaAs}(i) - (E_{Ga3d}^{GaAs} - E_v^{GaAs}) \quad . \tag{2}$$

The interface potential is

$$qV_{BB} = \Delta(b) - \Delta(i) \quad . \tag{3}$$

A key parameter needed to determine $\Delta(i)$ is the core-level to valence-band maximum binding-energy difference. For the Ga3d and As3d core levels in GaAs, these quantities have recently been determined with high precision.[5]

$$E_{As3d}^{GaAs} - E_v^{GaAs} = 40.73 \pm 0.02 \text{ eV} \tag{4}$$

$$E_{Ga3d}^{GaAs} - E_v^{GaAs} = 18.81 \pm 0.02 \text{ eV} \quad . \tag{5}$$

To determine a change in interface potential, $\delta\, qV_{BB}$, it is only necessary to determine a change in interface core-level binding energy $\delta\, E_{As3d}^{GaAs}(i)$ or $\delta\, E_{Ga3d}^{GaAs}(i)$; it is clear from Fig. 2 that

$$\delta\, qV_{BB} = \delta\, E_{As3d}^{GaAs}(i) = \delta\, E_{Ga3d}^{GaAs}(i) \quad . \tag{6}$$

However, to determine an absolute value for qV_{BB} it is necessary to measure $E_{As3d}^{GaAs}(i)$ on an absolute binding-energy scale referenced to E_F. For this purpose, an Au overlayer (with thickness $>10^3$Å) was evaporated onto a sample surface at the conclusion of an experiment. The absolute binding-energy scale was established by indexing the observed peak position of the Au4$f_{7/2}$ line to 84.00 ± 0.01 eV.[6] Care must be taken to ensure that the Au overlayer is thick enough to establish bulk properties as for very thin layers the Au4$f_{7/2}$ line binding energy is observed to depend on layer thickness (see e.g., Ref. 7).

In the following sections several studies which involve XPS observations of $\Delta(i)$ variations will be presented. Here we show one example of the ease with which large variations in $\Delta(i)$ can be directly observed. In Fig. 3a is shown the As3d core level for an n-type GaAs (100) sample which was thermally cleaned at ~570°C in vacuum, oxidized at ~460°C by exposure to 2×10^4 L (Langmuir) of O_2 to form a Ga_2O_3-GaAs interface, and subsequently stored in vacuum at room temperature for 16 hrs. This same sample was then thermally cleaned by heating in vacuum at ~570°C and a few monolayers of Au were evaporated onto the room temperature sample surface (Fig. 3b). The vertical lines in Fig. 3 indicate the center of the peak width at half peak height. The large variation (0.7 eV) in $E_{As3d}^{GaAs}(i)$ and thus $\Delta(i)$ is obvious from the figure.

II.C   GaAs Sample Characterization and Initial Surface Preparation

Most of the GaAs samples utilized in this work were bulk grown although a few vapor phase epitaxial (VPE) layers were also studied. The electrical characteristics of the GaAs samples are documented in Section II.C.1. The initial GaAs surface preparation to remove mechanical polishing damage and to prepare the samples for insertion into the XPS system is mentioned in Sec. II.C.2.

II.C.1   Electrical Characterization

The GaAs bulk samples utilized in this work were purchased from Crystal Specialties Inc. Both n- and p-type materials were studied. The crystallographic orientations were (100), (110), and (111). The specifications for the samples as provided by Crystal Specialties are given in Table 1. The heavily doped n-type material (boule #3548) was used as substrate for the VPE grown samples. As mentioned in Sec. II.B, for the XPS surface-potential measurements, it is desirable to keep the carrier concentration $\lesssim 10^{17}$ cm^{-3} so that potential variations within the photoelectron escape depth will not complicate the $\Delta(i)$ measurement.
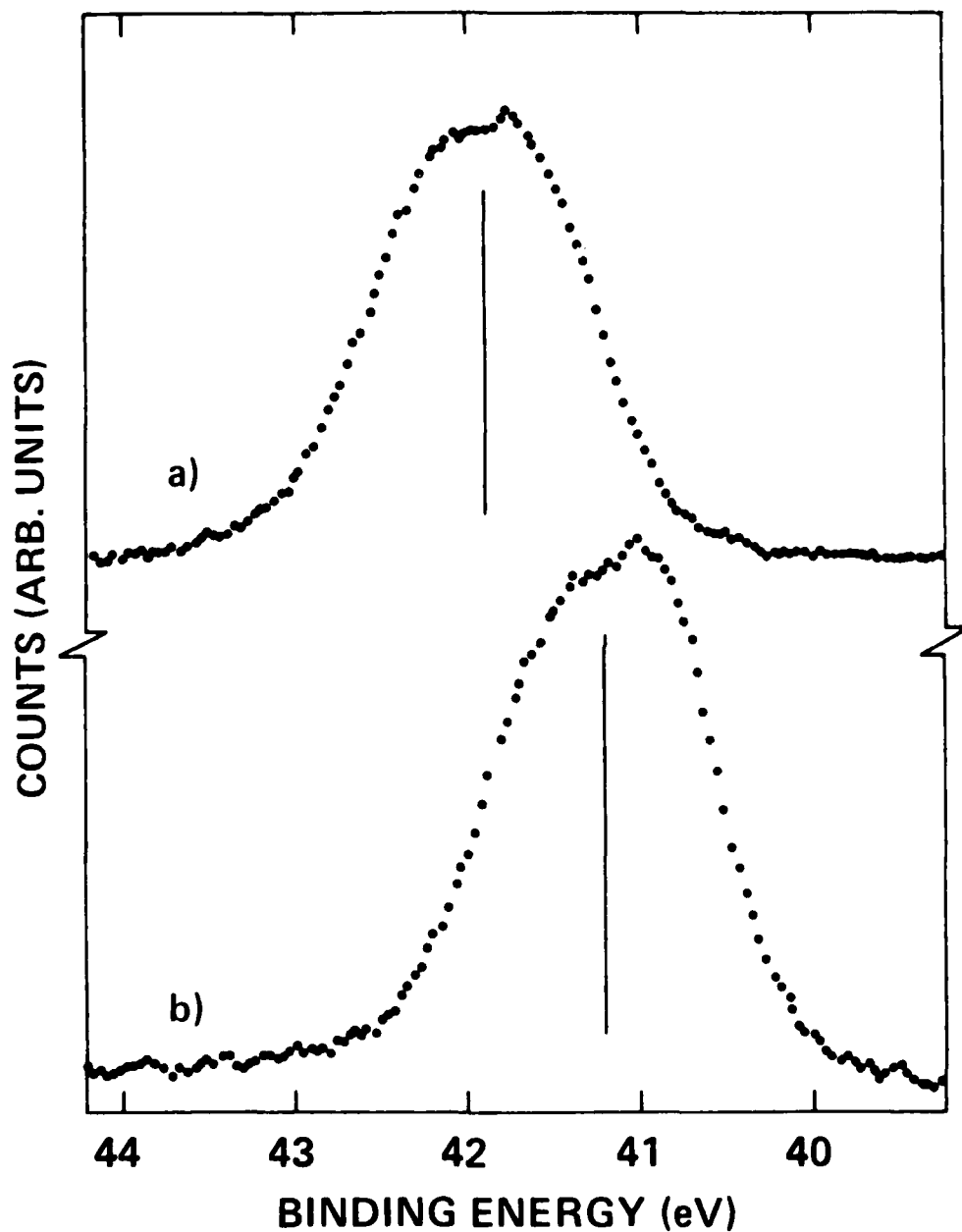
Fig. 3   XPS spectra in the region of the As3d core level for an n-type GaAs (100) sample with two different surface treatments. a) The sample was thermally cleaned at ≈570°C, oxidized at ≈460°C by exposure to 2×10^4 L O_2 and stored in vacuum for 16 hours. b) The sample was thermally cleaned at ≈570°C followed by the deposition of 2-5 monolayers of Au. The E_B difference of 0.7 eV between the two vertical lines is a direct measure of the $\Delta(i)$ difference.

Table 1

Sample Characteristics as Supplied by Vendor

Boule #	Crystal-lographic Orientation	Carrier Concentration (cm^{-3})	Mobility $(cm^2/volt-sec)$	Etch Pit Density (cm^2)
3691	(100)	(p) 9×10^{16} Cd doped	180	9500
3686	(100) (110)	(n) 6×10^{16} Te doped	3500	8800
3548	(100)	(n) 3×10^{17} Sn doped	3000	6400
3630	(100)	(p) 2×10^{16} Zn doped	230	3200
3782	(110) (111B)	(p) 2×10^{16} Cd doped	210	6000

The GaAs material specifications supplied by Crystal Specialties (Table 1) were verified for some of the samples by our own electrical measurements. These measurements which are summarized in Table 2 included room temperature Hall-effect, capacitance-voltage, and van der Pauw measurements. For boules #3630 and #3782 the doping type was confirmed although analysis of the carrier concentration was not carried out.

A few measurements were also carried out on VPE samples which were grown by the Microwave Section of MRDC (Thousand Oaks). The samples (designated as VPE #1100) were 3 μ thick, n-type, and had a carrier concentration of 4×10^{16} cm^{-3}. This material was grown on substrates from boule #3548 which had a (100) orientation.

10

Table 2
Measured Material Characteristics

Boule #	Carrier Concentration (Hall effect) (cm^{-3})	Carrier Concentration (C-V) (cm^{-3})	Mobility (Hall effect) ($cm^2/volt\text{-}sec$)	Bulk Resistivity (Van der Pauw) (ohm-cm)
3691	(p) 1.4×10^{16}	2×10^{16}	200	2.2
3686	(n) 1.6×10^{17}	$\approx 1 \times 10^{17}$ [a]	3400	1.2×10^{-2}
3548	(n) 3.0×10^{17}	3.8×10^{17}	3300	6.2×10^{-3}

[a] C-V measurements on samples from this boule yielded a range of values from 0.5 to 2×10^{17} cm^{-3}.

II.C.2   Initial Surface Preparation

The final surface treatment of the bulk grown GaAs samples as supplied by Crystal Specialties was a chemical mechanical polish designed to produce a surface flatness of ≈ 1 μ/in. To remove possible residual mechanical polishing damage, the bulk grown samples were first degreased in detergent, rinsed in deionized water, and then etched in a freshly prepared (4:1:1) H_2SO_4:H_2O_2:H_2O solution for about 1 min. This freshly prepared solution which is quite warm ($\approx 60°C$) has an etching rate of ≈ 1 μ/min. At the conclusion of the etch, the samples were quenched in deionized H_2O. The samples were then attached to Mo sample platens with In which required heating in air to $\approx 160°C$. The time inverval between etching and insertion of the samples into the XPS spectrometer was usually <10 min. The etching procedure just described is referred to throughout this report as the initial chemical etch.

For consistency of initial surface preparation, the VPE grown samples were also given a similar initial chemical etch. However, because the epitaxial layer was only 3 μ thick, the samples were only etched for a few seconds to avoid complete removal of the layer.

III.   RELATIONSHIP BETWEEN GaAs SURFACE POTENTIAL AND SURFACE CHEMISTRY

In this section XPS measurements of GaAs surface chemistry and sur-
face potential are reported. Section III.A describes measurements on n-type
materials which demonstrate reproducible variations in surface potential for
several thermal and oxidation surface treatments. Also reported in this
section are measurements which involve depositions of thin semiconducting or
insulating layers. In Section III.B XPS measurements on bulk grown p-type
GaAs materials are presented. Similarities between surface-potential vari-
ations on n- and p-type materials were noted and thus in the latter part of
this program a considerable effort was made to study the correlation of
surface-potential variations as a function of surface chemistry for both
doping types. These studies are presented in Sec. III.C.

III.A   XPS Measurements on n-type GaAs Samples

The majority of XPS measurements carried out as part of this contract
were performed on bulk grown n-type ($\approx 1 \times 10^{17}$ cm^{-3}) GaAs (100) material from
boule #3686. In this section we describe results on surfaces prepared by
several different methods. The studies include a few results for VPE grown
epitaxial layers.

III.A.1   Thermal and Oxidation Studies

Correlations of surface chemistry and surface potential are described
in the first part of this section. In addition, a new view of the surface
chemistry associated with thermal cleaning of a GaAs surface is presented
here.

III.A.1a. Surface-Potential Variations

A typical series of XPS spectra in which surface potential varia-
tions with surface treatment are directly observed is shown in Fig. 4. The E_B
region which includes both the As3d (≈ 41 eV) and Ga3d (≈ 19 eV) core levels is

12
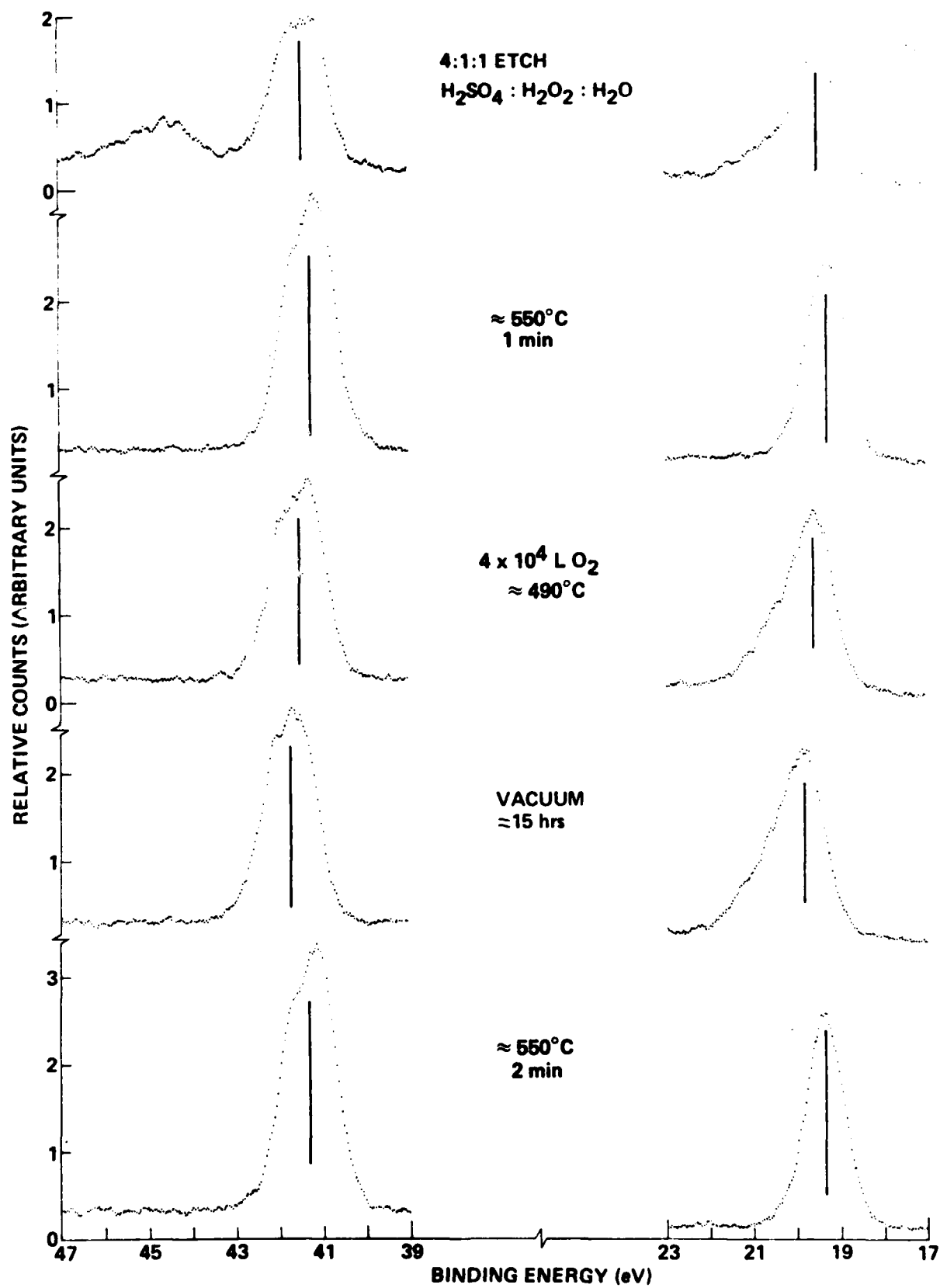
Fig. 4   XPS spectra of n-type GaAs (100) surfaces after the treatments indicated in the figure.

13

covered. The vertical lines shown in the figure indicate the approximate centroid of the Ga3d and As3d lines which are associated with GaAs. These centroids shift rigidly together as the surface potential varies which justifies the use of XPS as a surface-potential monitoring technique (a similar result was also reported in Ref. 8).

The chemically etched sample (top spectrum) exhibits oxidized forms of both As and Ga on the surface. The chemical shift of the As3d level in the oxidized As relative to GaAs ($\Delta E_B \approx 3.2$ eV) and of the Ga3d level in the oxidized Ga relative to GaAs ($\Delta E_B \approx 0.95$ eV) suggests that the oxides are primarily As_2O_3 and Ga_2O_3.[9] This sample was heated to $\approx 550°C$ (1 min) and cooled to room temperature before obtaining the second spectrum shown in Fig. 4. The surface contaminants C and O were removed by this treatment. In this case both $E_{As3d}^{GaAs}(i)$ and $E_{Ga3d}^{GaAs}(i)$ have decreased substantially which corresponds to an increased surface band bending. The sample was then exposed to 4×10^4 L of dry O_2 at $\approx 490°C$ and subsequently cooled to room temperature. This treatment caused Ga_2O_3 to appear on the surface (note the high binding-energy shoulder on the Ga3d peak in the third spectrum of Fig. 4) which was accompanied by a significant decrease in band bending. Subsequent storage of the sample in vacuum ($\approx 10^{-9}$ torr) for about 15 hours (see fourth spectrum of Fig. 4) resulted in a further substantial decrease in surface band bending. A final heat cleaning treatment (see bottom spectrum of Fig. 4) at $\approx 550°C$ (2 min) and subsequent cooling to room temperature produced a surface band bending similar to that observed in the second spectrum. The relative changes in E_{As3d}^{GaAs} referenced to the average value observed on the thermally cleaned surface are given in Table 3. This experiment clearly demonstrates that the thermal cleaning procedure produces a surface on which V_{BB} can be altered by means of chemical reactions.

As noted in Table 3, the band bending and thus the surface charge is lowest for the surface which had only Ga_2O_3 present and which was stored in vacuum ($\approx 10^{-9}$ torr) for several hours. Another series of experiments was

Table 3

Annealing and Oxidation of GaAs
n-Type GaAs (100), Boule #3686
(Same sample as studied in Fig. 4)

Treatment	Relative As3d Binding Energy in GaAs (eV)[a]	Remarks
Chem. etch	+0.16	$As_2O_3 + Ga_2O_3$
≈550°C	-0.03	Clean
4×10^4 L O_2 at ≈490°C	+0.29	Ga_2O_3
Vacuum ≈15 hrs at 25°C	+0.47	
≈550°C	+0.04	Clean

[a]Uncertainty ±0.05 eV

carried out to determine the absolute $E_{As3d}^{GaAs}(i)$ by the method discussed in Section II.B. The initial surface was prepared for this study by heating a sample to ≈400°C within the XPS system to remove all As oxides followed by vacuum storage, also within the system, for 2 days at room temperature. The binding energy on an absolute scale for this initial surface is given in Table 4. At the conclusion of the series of experiments reported in Table 4, a thick Au overlayer was evaporated onto the sample in situ. The binding energy of the As3d peak in GaAs, $\Delta(i)$, and the associated line width are given in Table 4 after several oxidation and thermal treatments (in each case the sample was cooled to near room temperature for the XPS measurements). The thermally cleaned surface was prepared several times on this sample. The As3d binding energy is observed to scatter by almost 0.1 eV. This suggests that it may be difficult to prepare a completely reproducible surface by thermal cleaning even though characteristic LEED patterns were observed on all the cleaned surfaces. The results in Table 4 show that in each case where Ga_2O_3

Table 4

Oxidation and Thermal Treatment of GaAs
n-Type GaAs (100), Boule #3686

Treatment	As3d Binding Energy in GaAs (eV)[a]	Δ(i) (eV)	As3d Line Width in GaAs (eV)	Remarks
≈400°C; Vacuum 2 Days at 25°C	41.95	1.22	1.41	Ga_2O_3; no As_2O_3
≈440°C	41.82	1.09	1.39	Ga_2O_3
≈540°C	41.64	0.91	1.43	Ga_2O_3; no LEED
≈550°C	41.41	0.68	1.39	Clean; LEED
6×10^4 L O_2 at 25°C; ≈480°C	41.44	0.71	1.39	No oxides
6×10^4 L O_2 at ≈490°C	41.71	0.98	1.39	Ga_2O_3; no As_2O_3
≈550°C	41.46	0.73	1.38	Trace of residual oxygen; no LEED
≈560°C	41.40	0.67	1.35	Clean; LEED
Vacuum 12 hrs at 25°C	41.48	0.75	1.31	
≈560°C	41.45	0.72	1.35	Clean; LEED
6×10^4 L O_2 at ≈200°C	41.49	0.76	1.37	Ga_2O_3
≈560°C	41.36	0.63	1.35	Clean; LEED
6×10^4 L O_2 at ≈360°C	41.51	0.78	1.41	Ga_2O_3
≈560°C	41.37	0.64	1.35	Clean; LEED

[a]Accuracy is ±0.05 eV

16

is formed on the surface, a sizable decrease in band bending relative to the thermally cleaned surface results. A possible minor exception is the oxidized surface formed by O_2 exposure at ~200°C. If elemental As is formed in the oxidation process, it may be that it is not completely removed from the surface at this lower temperature.

The binding energies given in Table 4 can be used to evaluate the surface charge. In the following analysis, the depletion approximation is assumed. The conduction-band minimum to Fermi-energy position in the bulk is[10]

$$E_c - E_F = kT \ln (N_c/N_D) \tag{7}$$

where k is the Boltzmann constant, T is the absolute temperature, N_c is the effective conduction-band density of states and N_D is the donor density. For $N_D \approx 10^{17}$ cm^{-3}, $E_c - E_F = 0.04$ eV. The surface charge, Q_{ss}, is given by

$$Q_{ss} = (2 \ q \ \varepsilon_s \ N_D |V_{BB}|)^{1/2} \tag{8}$$

where ε_s is the semiconductor permittivity.

The surface which had been heated to ~400°C and stored in vacuum for 2 days had an As3d binding energy (given in Table 4) of 41.95 eV. As indicated in Eq. 4, the recently determined value for $E_{As3d}^{GaAs} - E_v^{GaAs}$ is 40.73 eV. Because E_F in the bulk is 1.43-0.04 = 1.39 eV above E_v, from Fig. 2 it is seen that $|q \ V_{BB}| = 1.39 - (41.95-40.73) = 0.17$ eV. From equation (8), this leads to a surface charge of 0.76×10^{-7} $coul/cm^2$ or 4.8×10^{11} $electrons/cm^2$. This value is much larger than the 10^{10} $electrons/cm^2$ characteristic of the SiO_2/Si interface.

The results reported in this section show that the low V_{BB} can be obtained for a n-type GaAs (100) surface either by thermal cleaning followed by high temperature oxidation and room temperature vacuum storage or by thermal removal of the initial As_2O_3 at ~400°C followed by room temperature vacuum storage.

17

The vacuum storage phenomena was investigated further in an indepen-
dent set of experiments. Bulk samples of n-type GaAs (100) and (110)
both from boule #3686 were mounted side by side on a single Mo sample
platen. The vacuum storage phenomena was only investigated on the (100)
sample; we will return to a discussion of the (110) results in Sec. III.C.2.
The results of these experiments are presented in Table 5. The initial
chemically etched surface was thermally cleaned at ≈560°C. This surface was
oxidized at ≈420°C to form Ga_2O_3 and stored in vacuum for 25 hrs. The usual
large decrease in V_{BB} was observed. Subsequent storage in vacuum for an
additional 43 hrs produced no change in V_{BB}; however an anneal at ≈420°C
markedly increased V_{BB}. The surface was then thermally cleaned at ≈560°C and
reoxidized at ≈420°C to form Ga_2O_3. The Δ(i) monotonically drifts with
storage time to the same low value as was previously observed. At this point
the sample was again thermally cleaned and reoxidized to form Ga_2O_3 on the
surface. During the previous 2 vacuum storage sequences, an ion gauge had
been used in the sample preparation chamber to monitor the residual gas pres-
sure (≈1 × 10^{-9} torr). The sample was now stored in vacuum for 22 hrs but
with the ion gauge turned off. Previous work reported in the literature[11] has
demonstrated remarkable differences in surface reactivity due to excited gas
species produced by the presence of an ion gauge. In this experiment we again
observed a decrease in V_{BB} with vacuum storage; however, the maximum change in
V_{BB} was less than with the ion gauge on. Further work would be needed to
substantiate if this is a real effect. At this point, the samples were again
thermally cleaned and thin deposits of Au were evaporated onto the surfaces.
The results of these experiments are discussed in Sec. III.C.2.

The surface potential of an initially prepared Ga_2O_3 surface was
studied several times throughout this report; it is observed to vary sub-
stantially from sample to sample and as noted in Table 5 to change with vacuum
storage time. The drift with vacuum storage time may explain the scatter in
Δ(i) observed on the initially prepared Ga_2O_3 surfaces as no attempt was made
to carry out the XPS measurements at a constant time interval following sur-
face preparation.

18

Table 5

Vacuum Storage Phenomenon and Au Deposition Study
n-Type GaAs (100) and (110), Boule #3686

Treatment	As3d Binding Energy in GaAs (eV)[a]		Δ(i) (eV)		Remarks
	(100)	(110)	(100)	(110)	
Chem. etch	41.60		0.87		As_2O_3 + Ga_2O_3
≈560°C	41.39		0.66		Clean, LEED
≈420°C 5 × 10^4 L O_2	41.41		0.68		Ga_2O_3
25 hrs vacuum	41.67		0.94		Ion gauge on
68 hrs vacuum	41.68		0.95		Ion gauge on
≈420°C	41.50		0.77		
≈560°C	41.35		0.62		Clean
≈420°C 5 × 10^4 L O_2	41.42		0.69		Ga_2O_3
0.5 hr vacuum	41.45		0.72		Ion gauge on
1.75 hrs vacuum	41.50		0.77		Ion gauge on
3 hrs vacuum	41.52		0.79		Ion gauge on
5 hrs vacuum	41.54		0.81		Ion gauge on
8 hrs vacuum	41.58		0.85		Ion gauge on
22 hrs vacuum	41.66		0.93		Ion gauge on
≈560°C	41.35		0.62		Clean, LEED
≈420°C 5 × 10^4 L O_2	41.40		0.67		Ga_2O_3
6 hrs vacuum	41.54		0.81		Ion gauge off
22 hrs vacuum	41.54		0.81		Ion gauge off
≈560°C	41.33	41.39	0.60	0.66	Clean, LEED
≈1 Monolayer Au	41.38	41.42	0.65	0.69	
≈3 Monolayers Au	41.18	41.19	0.45	0.46	

[a] Accuracy ±0.05 eV

In the next section, the surface chemistry associated with the
thermal cleaning of GaAs is discussed.

III.A.1b Surface Chemistry Associated with Thermal Cleaning

In this section the results of a series of XPS experiments related
to thermally cleaning a chemically etched GaAs (100) surface are reported.
The sample was heated at a specific temperature for five minutes followed by
cooling to room temperature before the XPS analysis. Each successive anneal
was at a higher temperature. The As3d, Ga3d, 01s, and C1s XPS photoelectron
lines were monitored during the experiment. The small amount of initial
surface C contamination decreased below a detectable value at ≈240°C. Oxygen
was removed from the surface at ≈550°C. The initial surface exhibited both
As_2O_3 and Ga_2O_3 as can be seen in the XPS spectra obtained with this surface
which are shown at the top of Figs. 5 and 6. In Table 6, the relative peak
areas above background associated with the As3d line in both GaAs and As_2O_3,
the total Ga3d line, and the total 01s line are given. Also, the As3d binding
energy in GaAs relative to the thermally cleaned surface and the associated
line width (full-width at half-maximum intensity) are given.

The As_2O_3 decreases slowly between ≈240 and ≈450°C. The spectra in
the middle of Figs. 5 and 6 show the Ga3d and As3d lines after the ≈530°C
annealing treatment. The As_2O_3 is clearly absent; however, the Ga_2O_3 com-
ponent has apparently increased. The spectra at the bottom of Figs. 5 and 6
show the Ga3d and As3d lines after thermally cleaning the surface.

To investigate the apparent increase in Ga_2O_3 which accompanies the
decrease in As_2O_3, the spectra at the top and middle of Fig. 5 were analyzed
further. The Ga3d line shape associated with the thermally cleaned GaAs
surface (bottom of Fig. 5) was fitted to the low binding-energy side of the
peak at the top and middle of Fig. 5 and was subtracted from this experimental
peak shape to obtain the peak shape associated with the oxide. The results of
this analysis are shown in Figs. 7 and 8. The ratio of Ga3d in Ga_2O_3 to Ga in
GaAs increases from 0.31 to 0.54 between Figs. 7 and 8. The apparent chemical

20
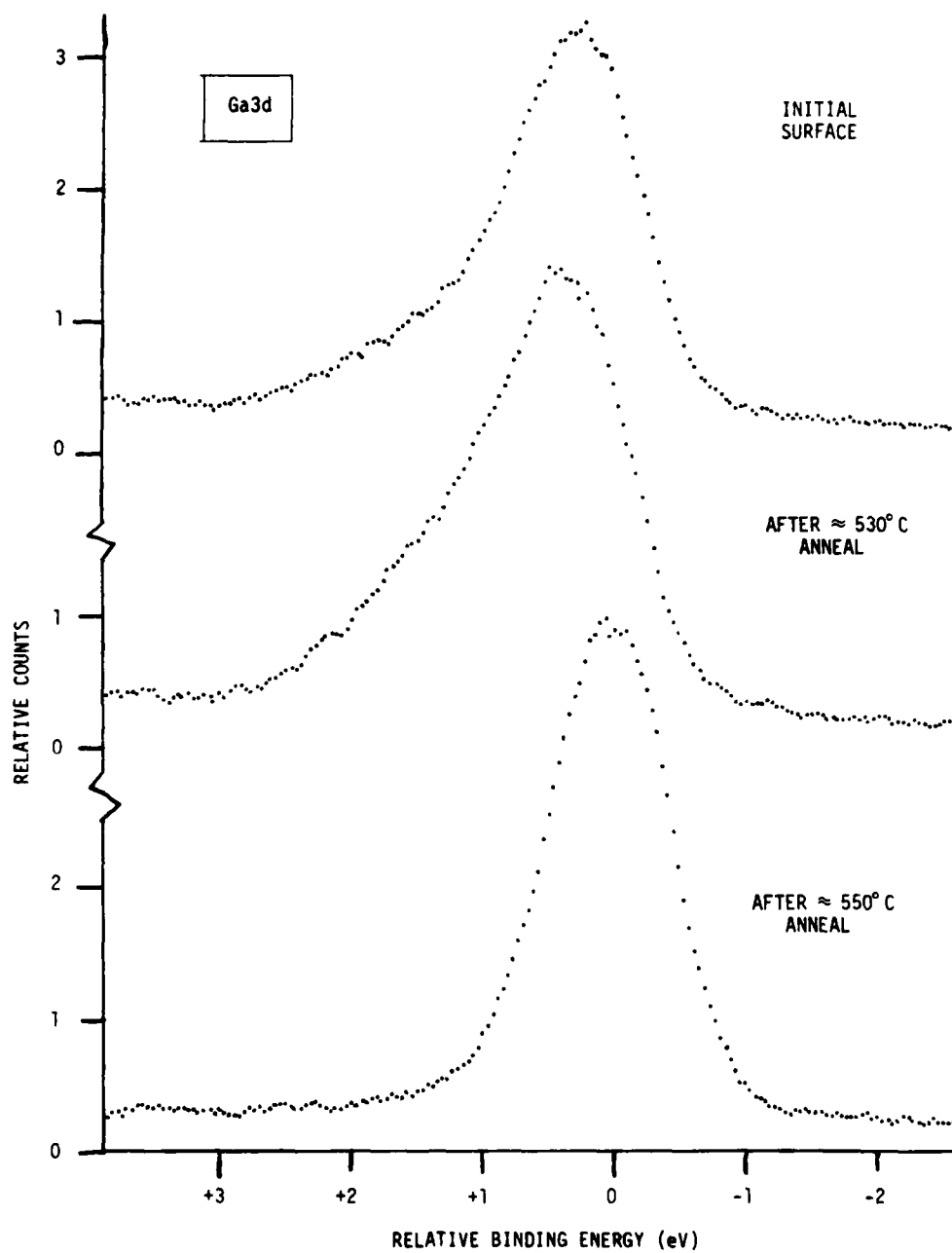
Fig. 5   XPS spectra of n-type GaAs (100) surface in the energy region of the Ga3d core level. Binding-energy scale is referenced to centroid of peak in spectrum at bottom.

21
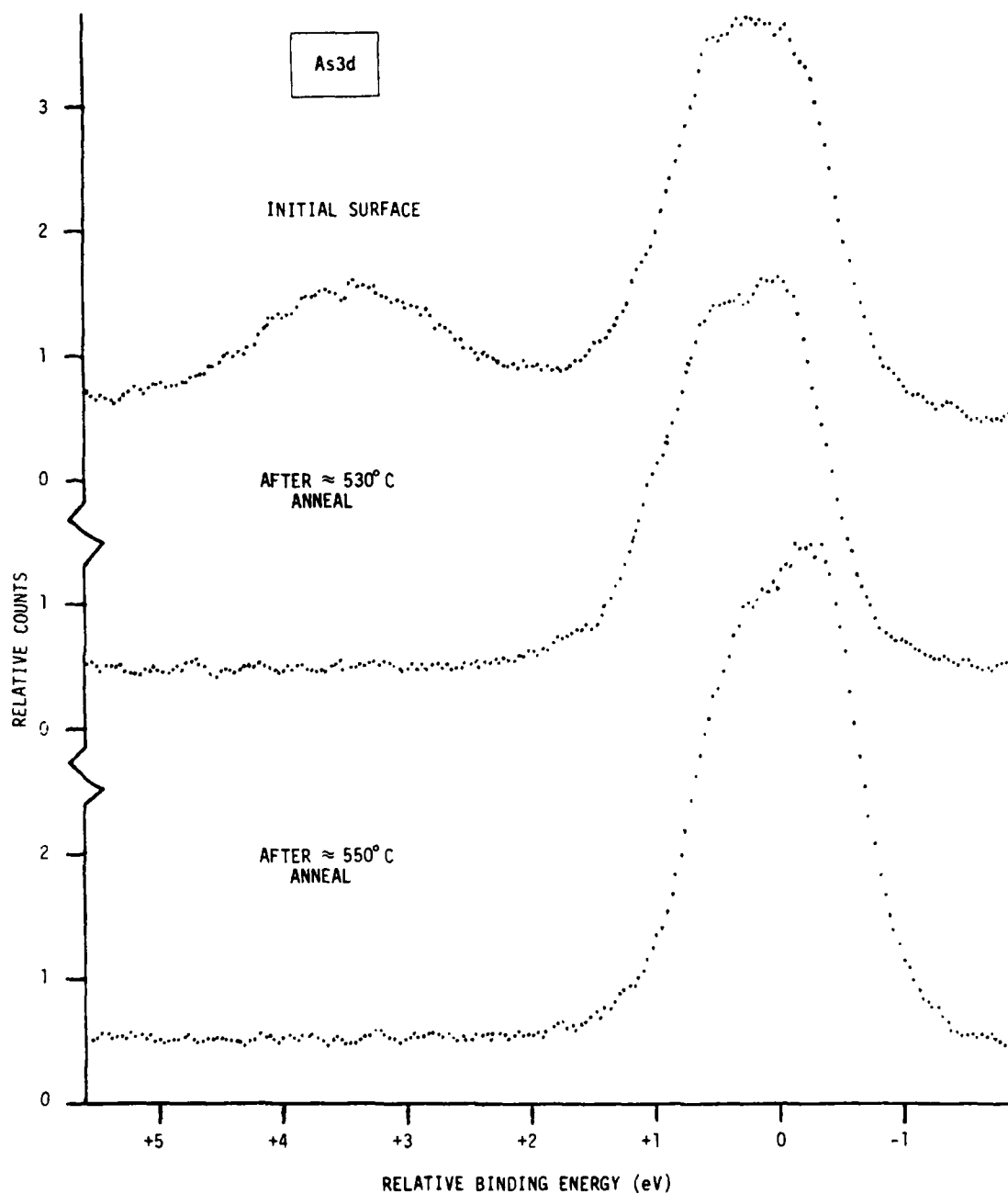
Fig. 6   XPS spectra of n-type GaAs (100) surface (same sample as Fig. 5) in
the energy region of the As3d core level. Binding-energy scale is
referenced to centroid of peak in spectrum at bottom.

22

Table 6

Annealing of Oxidized GaAs Surface
n-Type GaAs (100), Boule #3686

Treatment	Relative As3d Binding Energy in GaAs (eV)	As3d Line Width in GaAs (eV)	As3d Peak Area in GaAs	As3d Peak Area in As_2O_3	Total As3d Peak Area	Total Ga3d Peak Area	Total O1s Peak Area
Initial Surface	0.24	1.45	.383	.143	.526	.293	.839
≈80°C	0.20	1.44	.371	.142	.513	.250	.917
≈160°C	0.17	1.43	.382	.149	.531	.285	.819
≈240°C	0.12	1.46	.382	.106	.488	.293	.722
≈280°C	0.11	1.50	.367	.081	.448	.306	.689
≈320°C	0.13	1.43	.366	.058	.424	.302	.754
≈370°C	0.16	1.44	.352	.036	.388	.344	.748
≈410°C	0.16	1.44	.343	.020	.363	.341	.715
≈450°C	0.24	1.43	.354	0	.354	.384	.728
≈490°C	0.30	1.44	.368	0	.368	.400	.728
≈530°C	0.30	1.43	.376	0	.376	.375	.631
≈550°C	0	1.39	.470	0	.470	.332	0
≈500°C O_2 6 × 10^4 L	0.33	1.42	.409	0	.409	.381	.553
Vacuum 7.5 hrs	0.44	1.40	.452	0	.452	.445	.566
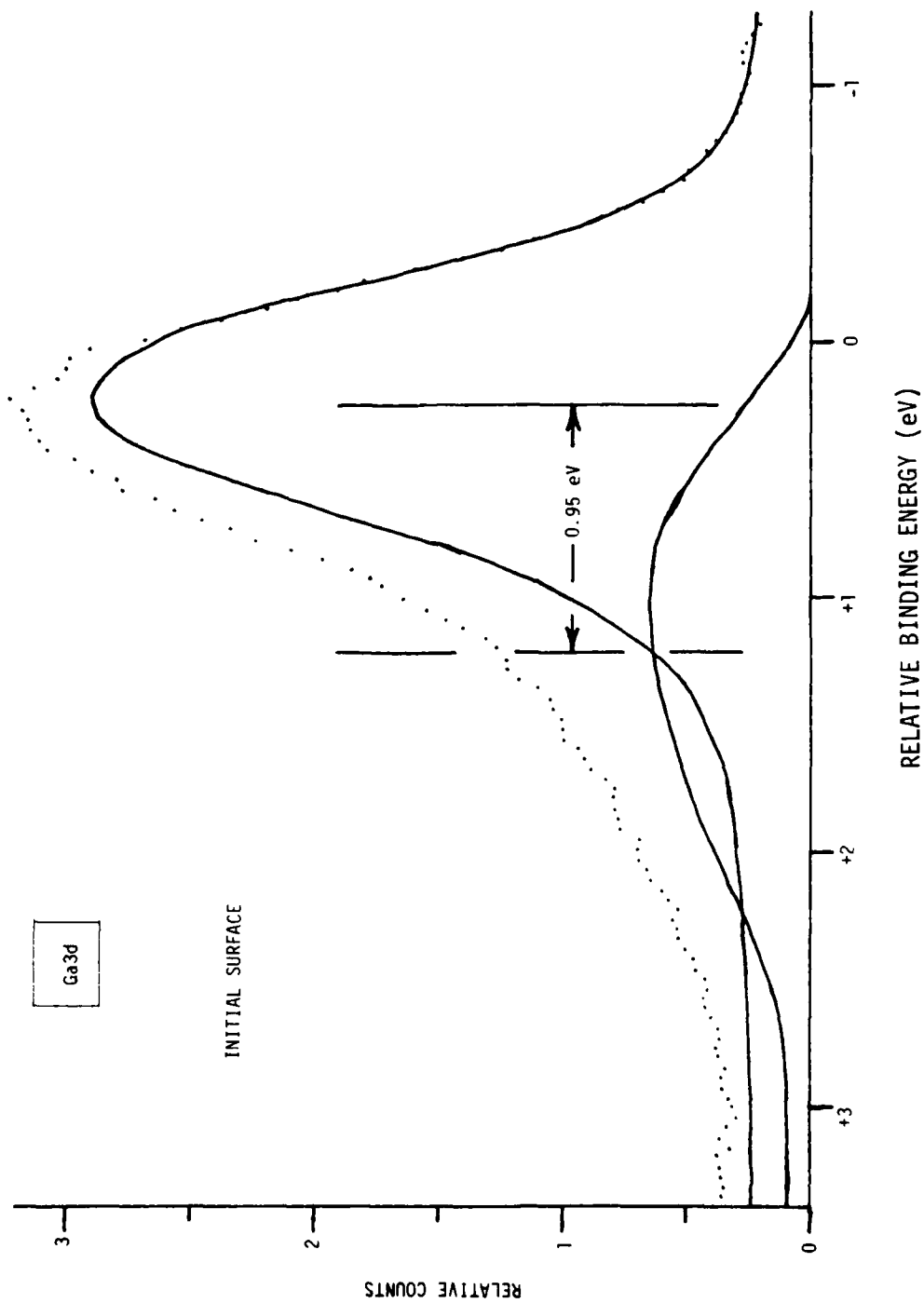
Fig. 7   Analysis of spectrum shown at top of Fig. 5.

24
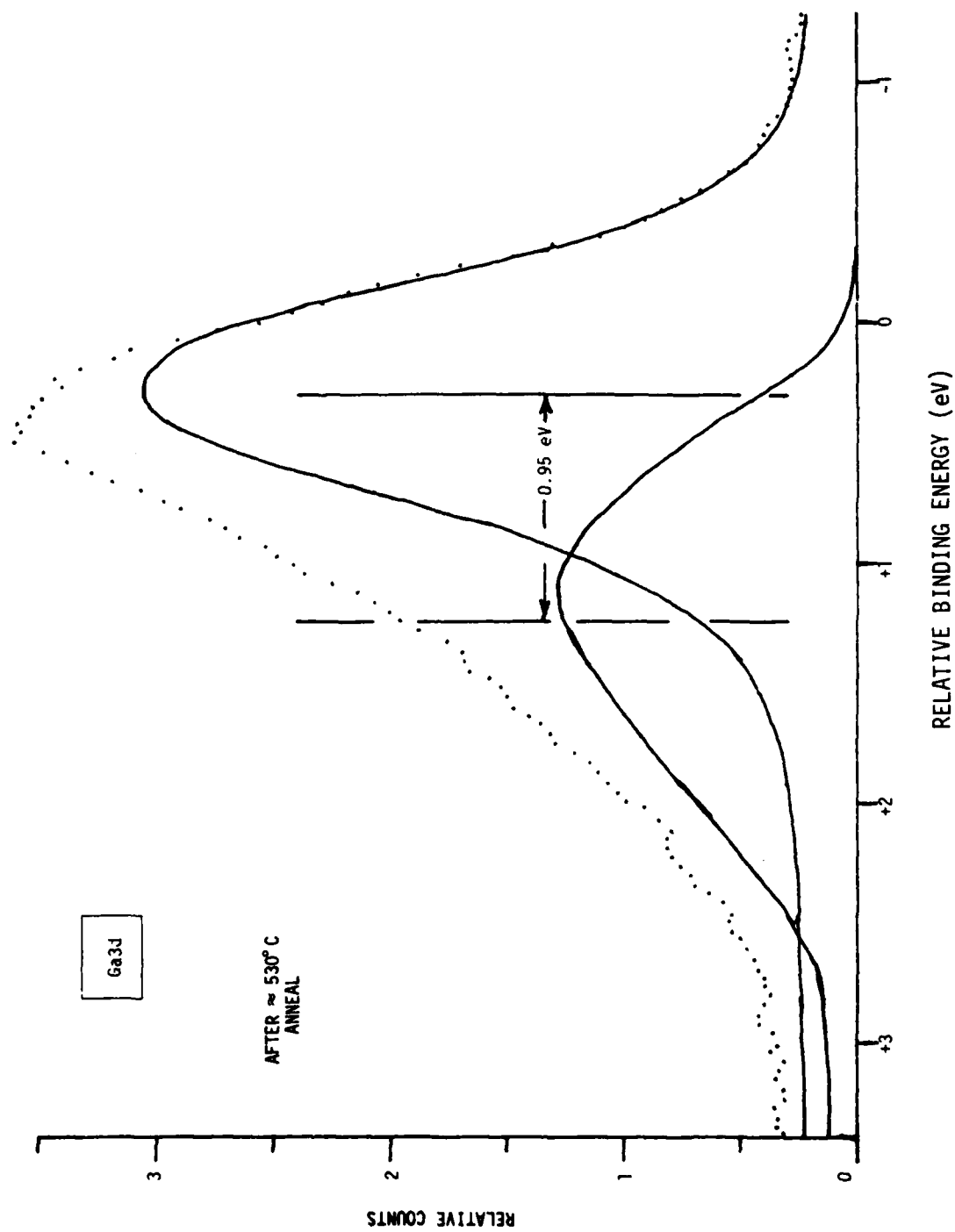
Fig. 8   Analysis of spectrum shown in middle of Fig. 5.

25

shift of the Ga3d line in Ga_2O_3 relative to GaAs is 0.95 eV in both cases. In Fig. 9 the relative photoelectron peak areas (taken from Table 6) are plotted as a function of the annealing temperature. As previously noted, the As_2O_3 starts to decrease at ~240°C and is absent at ~450°C. There appears to be only a small loss of oxygen from the initial surface up to ~240°C. However, above ~240°C in the temperature range where As_2O_3 is being removed from the surface, the total O1s peak area remains essentially constant up to ~530°C. The total Ga3d peak area increases somewhat between ~240°C and ~530°C while the As3d peak area associated with GaAs is relatively constant. The total As3d peak area decreases substantially in this temperature interval.

The above results suggest a new view of the surface chemistry associated with thermally cleaning a GaAs surface. It is usually assumed (see e.g., Ref. 12) that As oxides are removed from the surface first due to the high volatility of these compounds. The XPS results reported here show that As is lost from the surface as elemental As (presumably as As_2 or As_4). In the process, additional Ga must be oxidized to form Ga_2O_3. These results suggest that a surface chemical reaction of the form

$$As_2O_3 + 2\ GaAs \rightarrow Ga_2O_3 + \frac{4}{x}\ As_x \uparrow \qquad (9)$$
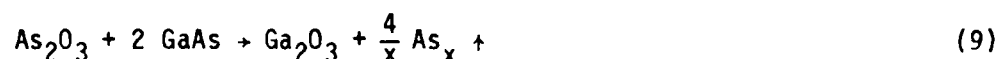
is associated with the removal of oxidized arsenic from the GaAs surface in the ~240°C to ~450°C temperature range. It is interesting to note that additional GaAs is consumed in this process.

The change in surface potential (as monitored by the relative As3d binding energy in GaAs) is shown at the bottom of Fig. 9. The bands initially bend up as the annealing temperature is increased to ~240°C. As the As_2O_3 is removed from the surface, the bands bend down past the initial position. When the Ga_2O_3 is removed from the surface, the bands bend up by ~0.3 eV. This thermally cleaned surface was reoxidized to form Ga_2O_3 by exposure to 6×10^4 L of O_2 at ~500°C. As indicated in Table 6, this resulted in a marked decrease in surface band bending which was further decreased by storage in

26
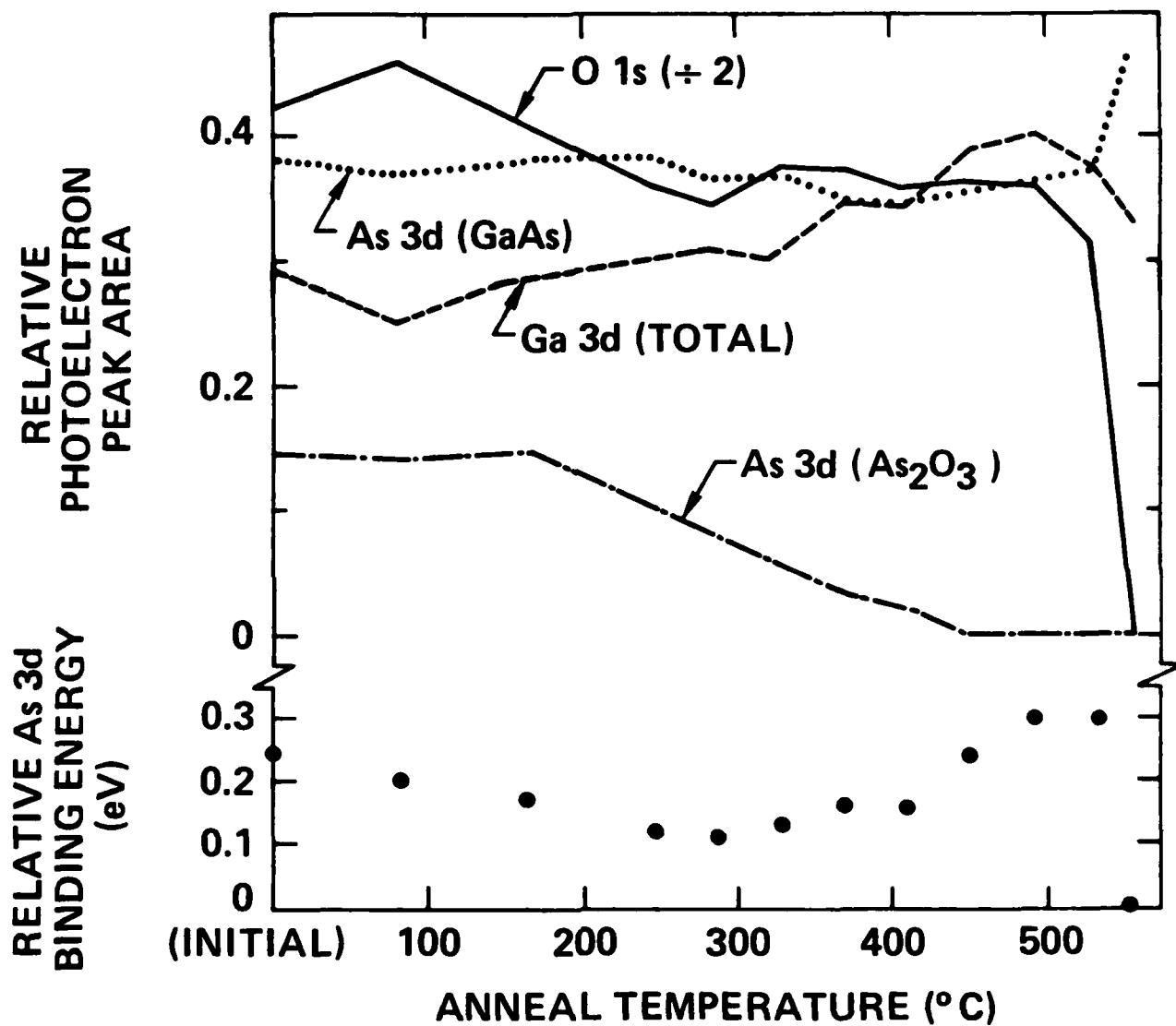
Fig. 9 Relative photoelectron peak areas and As3d binding energy vs annealing temperature. Data are from Table 6.

27

vacuum for 7.5 hours. Both of the results are consistent with the observations discussed in Sec. III.A.1a.

The same thermally induced solid-state reaction as suggested in Eq. (9), has been proposed[13] to explain the formation of elemental As at interfaces between GaAs and relatively thick ($\approx 10^3$A) anodic oxides. Interfaces prepared at room temperature which do not initially exhibit elemental As are observed to form elemental As rapidly at 450°C,[13] which, due to the thickness of the oxide, remains trapped at the interface. Recent condensed-phase diagram calculations,[14] have also shown that only elemental As and Ga_2O_3 can exist in thermodynamic equilibrium with GaAs, consistent with Eq. (9). There has been considerable recent interest in the electrical effect of the elemental As detected at the thermally annealed native-oxide/GaAs interface.[15,16] These elemental As atoms may be a major source of interface traps and thus play a significant role in determining the GaAs MOS characteristics.[17,18] The results of this section suggested the possibility of forming a useful GaAs-oxide interface by heat treating a native oxide of moderate thickness ($\lesssim 100$A). By annealing this oxide at ≈ 450°C it should be possible to form pure Ga_2O_3, evaporate the elemental As which is formed, and produce a new GaAs interface by consuming additional GaAs during the process. Observations reported in Sec. III.A.1a show that this process reduces Q_{ss}. An attempt to prepare such a sample is reported in Sec. III.A.2; however, as discussed in Sec. IV, the relatively small Q_{ss} observed on Ga_2O_3/GaAs interfaces for n-type material may not imply a relatively low interface-state density.

III.A.2 Water Vapor and Air Exposure Studies

In this section, XPS studies related to the exposure of GaAs (100) surfaces to H_2O vapor and air are reported. A pure H_2O vapor source was prepared by attaching a 12 in. long quartz tube containing liquid H_2O to a UHV leak valve. The H_2O was frozen with a dry ice/methanol bath and the tube was evacuated through the leak valve. Dissolved gases were removed by subsequent melting and freezing of the H_2O followed by evacuation of the tube.

28

The XPS results (relative As3d binding energies and line widths in GaAs) for a series of experiments in which a thermally cleaned sample was exposed to H_2O vapor are given in Table 7 (all XPS data were obtained at or near room temperature). Exposure to H_2O vapor at room temperature, ~240°C, ~360°C, and ~480°C caused no observable surface chemical reaction to occur. Also, only modest variations in surface potential were observed. Subsequent cleaning of the surface at ~560°C followed by exposure to a mixture of H_2O and O_2 at ~200°C also caused no noticeable surface reaction to occur. High temperature oxidation followed by vacuum storage caused a marked decrease in surface band bending which has been mentioned several times previously.

Two experiments are reported in Table 7 in which the surface was given an initial high temperature oxidation followed within a few minutes by H_2O vapor exposure after the sample had been cooled to near room temperature. In both cases the same marked decrease in band bending is observed as on the vacuum stored samples. A component of the residual gas in the ion pumped XPS system is H_2O vapor. Although with careful bakeout procedures, the base pressure of this system is in the high 10^{-11} torr range, the residual background H_2O pressure in more "typical" experiments is considerably higher. This suggests that the decrease in band bending associated with room temperature vacuum storage of surfaces oxidized at high temperature may be due to H_2O absorption and may explain why subsequent annealing of these surfaces increases the band bending.

The stability of the high temperature oxidized (100) surface to air exposure was investigated in a separate experiment; the XPS results on the relative As3d binding energy and line width in GaAs are given in Table 8. The usual marked decrease in band bending was observed following high temperature oxidation. The sample was subsequently exposed to laboratory air at 1 atmosphere for 1 hour. Contrary to the effect of exposure to pure H_2O vapor discussed above, this treatment resulted in an increase in surface band bending which may be associated with a change in the chemical state of the oxidized Ga. In Fig. 10 the Ga3d-and As3d-core levels observed by XPS on the surface

29

Table 7

H$_2$O and O$_2$ Exposure of GaAs Surface
n-Type GaAs (100), Boule #3686

Treatment	Relative As3d Binding Energy in GaAs (eV)	As3d Line Width in GaAs (eV)	Remarks
≈560°C	0	1.39	Clean, LEED
25°C Vacuum; 2 hrs	+0.03	1.37	
6 × 10³ L H$_2$O at 25°C	0	1.29	
3 × 10⁴ L H$_2$O at ≈240°C	-0.04	1.43	
6 × 10⁴ L H$_2$O at ≈360°C	-0.08	1.32	
3 × 10³ L H$_2$O at ≈480°C	+0.04	1.39	
≈560°C; 3 × 10³ L H$_2$O + O$_2$ at ≈200°C	-0.03	1.39	
≈560°C	-0.05	1.37	Clean
6 × 10⁴ L O$_2$ at ≈480°C	+0.09	1.36	Ga$_2$O$_3$
≈200°C Vacuum; 12 hrs	+0.49	1.34	
≈540°C	+0.02	1.32	Clean
6 × 10⁴ L O$_2$ ≈480°C	+0.23	1.39	Ga$_2$O$_3$
10⁵ L H$_2$O at ≈35°C	+0.44	1.37	
≈480°C	+0.22	1.36	
10⁴ L H$_2$O at ≈36°C	+0.41	1.35	
≈160°C	+0.24	1.42	
≈540°C	+0.15	1.44	Surface still oxidized

30

Ga3d

As3d

BINDING ENERGY (eV)

BINDING ENERGY (eV)

RELATIVE COUNTS
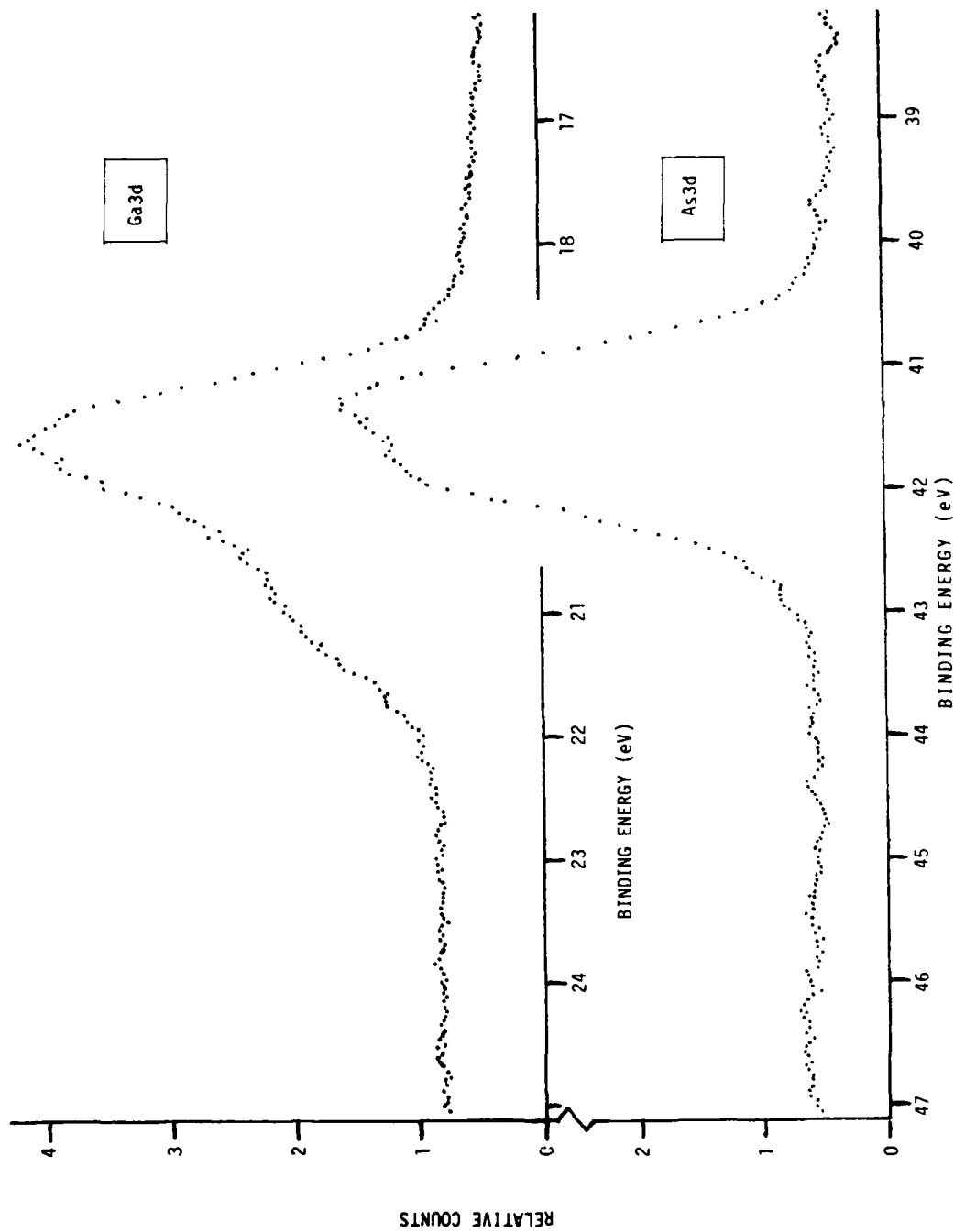
Fig. 10 XPS spectrum of oxidized n-type GaAs (100) surface which was exposed to air for 1 hr.

31

Table 8

Air Exposure of Oxidized GaAs Surface
n-Type GaAs (100), Boule #3686

Treatment	Relative As3d Binding Energy in GaAs (eV)	As3d Line Width in GaAs (eV)	Remarks
≈560°C	0	1.41	Clean; LEED
6×10^4 L O_2 at ≈480°C	+0.24	1.41	Ga_2O_3
Air at 25°C for 1 hour	+0.13	1.36	No As_2O_3; oxidized form of Ga may differ from previous treatment; see Fig. 11.

which had been exposed to air are shown. The high binding-energy shoulder observed on the Ga3d lines appears to have a larger shift relative to Ga in GaAs than those observed in Figs. 7 and 8. As in Figs. 7 and 8, a Ga3d line shape associated with Ga in thermally cleaned GaAs was fitted to the low binding-energy side of this experimental spectrum and subtracted from the data. The result is shown in Fig. 11. The center of the peak associated with the oxidized Ga has a larger binding-energy difference (by ≈0.2 eV) relative to GaAs than the binding-energy difference between Ga_2O_3 and GaAs. The O1s level on the air exposed surface is substantially shifted to higher binding energies than on the high temperature oxidized surface as can be seen in Fig. 12. If it is assumed that no change in interface dipole charge distribution occurs as a result of the air exposure, these results suggest that a different chemical form of Ga may exist on the air exposed surface. The initial surface with the very thin Ga oxide layer is not stable to room temperature air exposure.

A few capacitance-voltage measurements were performed with GaAs samples on which the initial surface was originally characterized by XPS. As
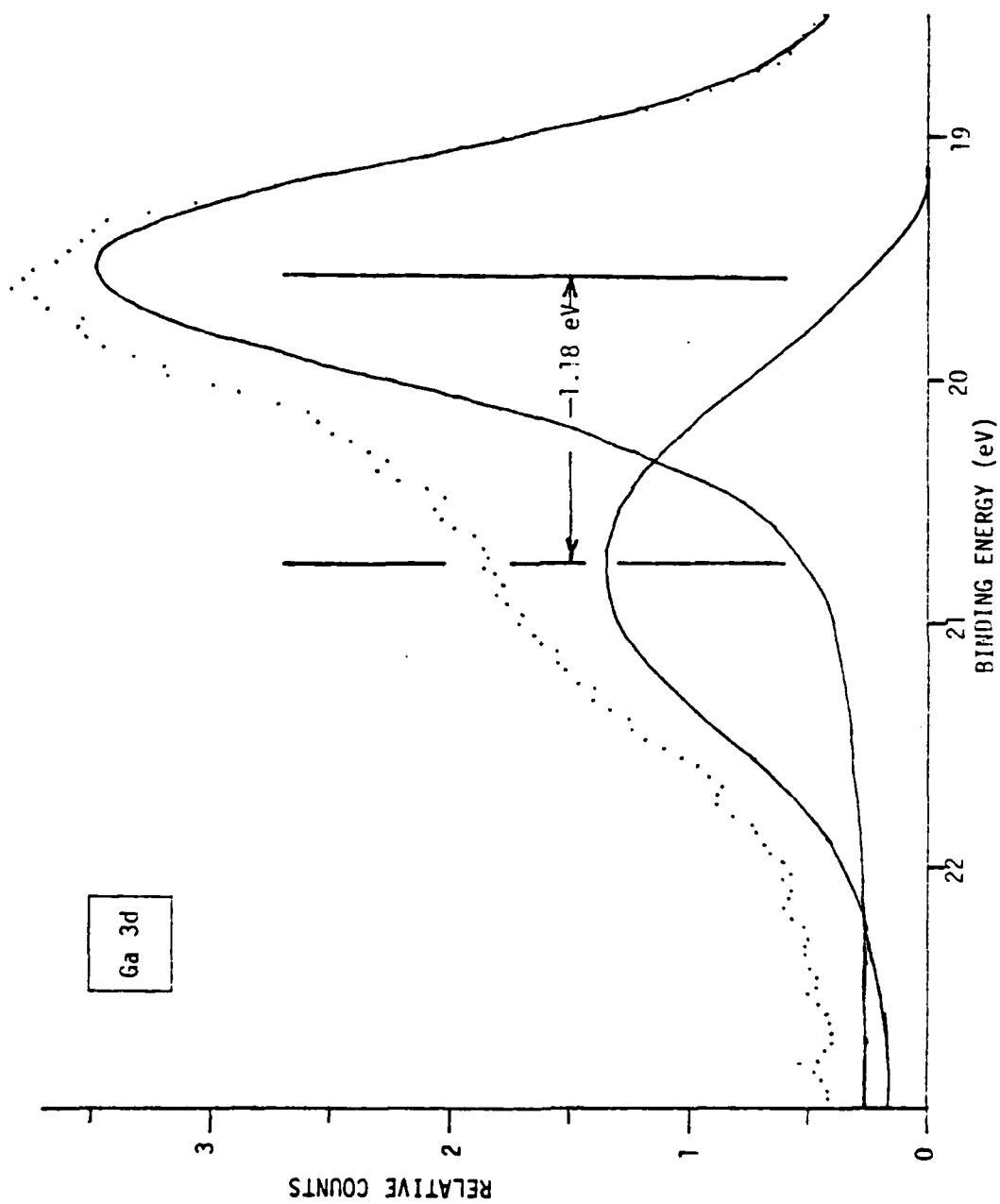
Fig. 11 Analysis of spectrum shown at top of Fig. 10.

33
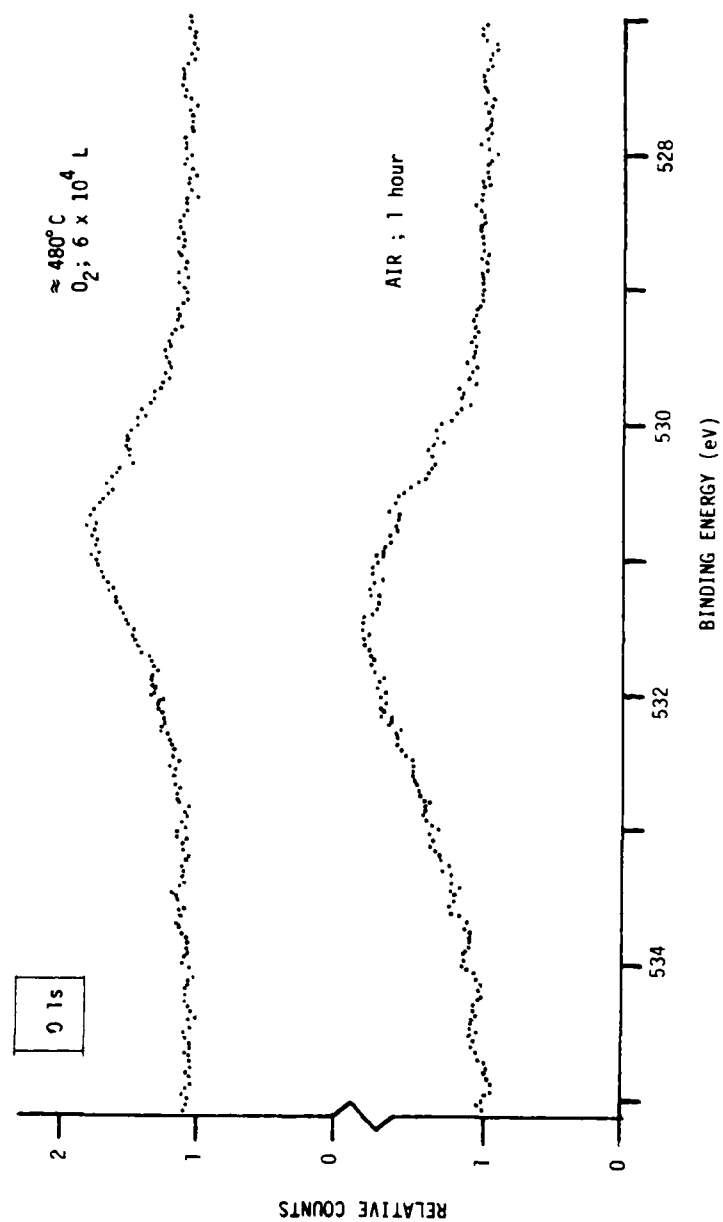
Fig. 12 XPS spectra in energy region of the O1s core level. Spectrum at top was obtained with an n-type GaAs (100) sample which was initially thermally cleaned at ≈560°C and subsequently oxidized by exposure to dry O₂ at ≈480°C; the spectrum at the bottom of figure was obtained after exposing this surface to air for 1 hr.

discussed in Sec. III.A.1a the GaAs (100) surface which is formed by high temperature oxidation to form only Ga_2O_3 on the surface has a relatively low Q_{ss}.

In an effort to electrically characterize the interface formed by the high temperature oxidation of GaAs (100), a sample was prepared in the XPS apparatus and characterized by XPS to be sure that only Ga_2O_3 was present on the surface. This sample was removed from the XPS system and transferred into a SiO_x evaporation system; the transfer required ~1 hour of air exposure. For comparison, an additional sample which was only given a 4:1:1 etch ($H_2SO_4:H_2O_2:H_2O$) was mounted in the SiO_x evaporation system next to the high temperature oxidized sample. About 1000Å of SiO_x was evaporated onto the samples followed by evaporation of metal dots through a contact mask.

Capacitance-voltage measurements were taken at 200 kHz. These data are shown in Fig. 13 where the two samples are identified as thermally oxidized (prepared in the XPS system) and etched (prepared with the 4:1:1 etch), respectively. The capacitance variation with applied voltage indicates that neither accumulation nor inversion took place for these samples. The apparent "flat-band" voltages were determined from $1/C^2$ plots as shown in Fig. 14. In these plots only depletion occurs. The inflection point is where a "flat-band" potential is produced because the depletion region has been diminished by the applied voltage. The "flat-band" voltage for the thermally oxidized sample is considerably higher than for the etched sample which indicates a possibly larger band bending at the thermally oxidized interface. This result coupled with the XPS studies reported above which attempted to duplicate the effect of 1 hour air exposure again show that the thermally oxidized surface is unstable in air.

III.A.3 Studies with Deposited Materials

XPS surface-potential measurements were carried out with thin overlayers of deposited materials in attempts to alter the interface potential by this means. The materials were deposited by using the quartz tube evaporator described in Sec.II.A. The first part of this section describes experiments
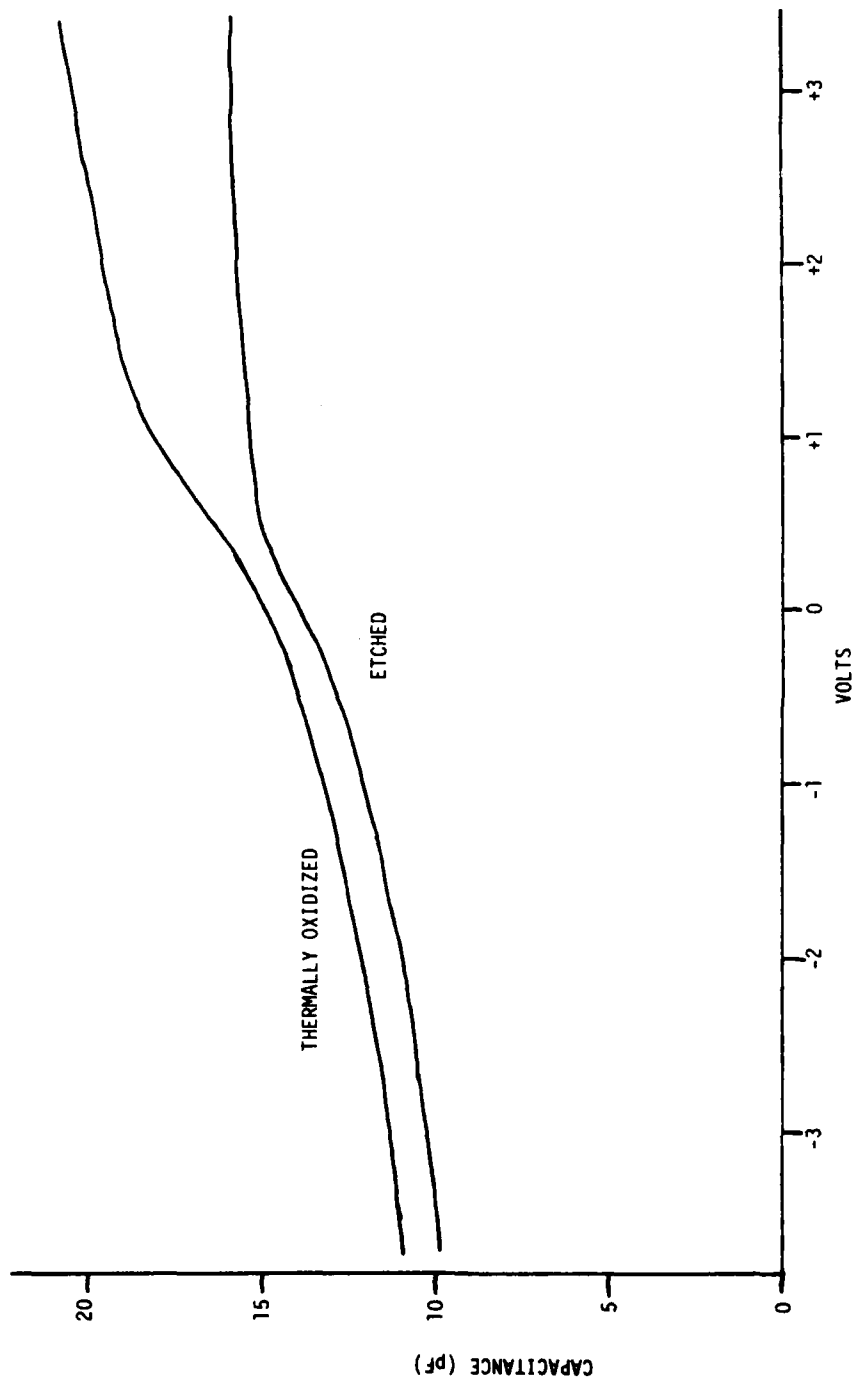
Fig. 13 Capacitance vs voltage for two n-type GaAs (100) samples prepared as described in Sec. III.A.2. Data were obtained at 200 kHz.

36
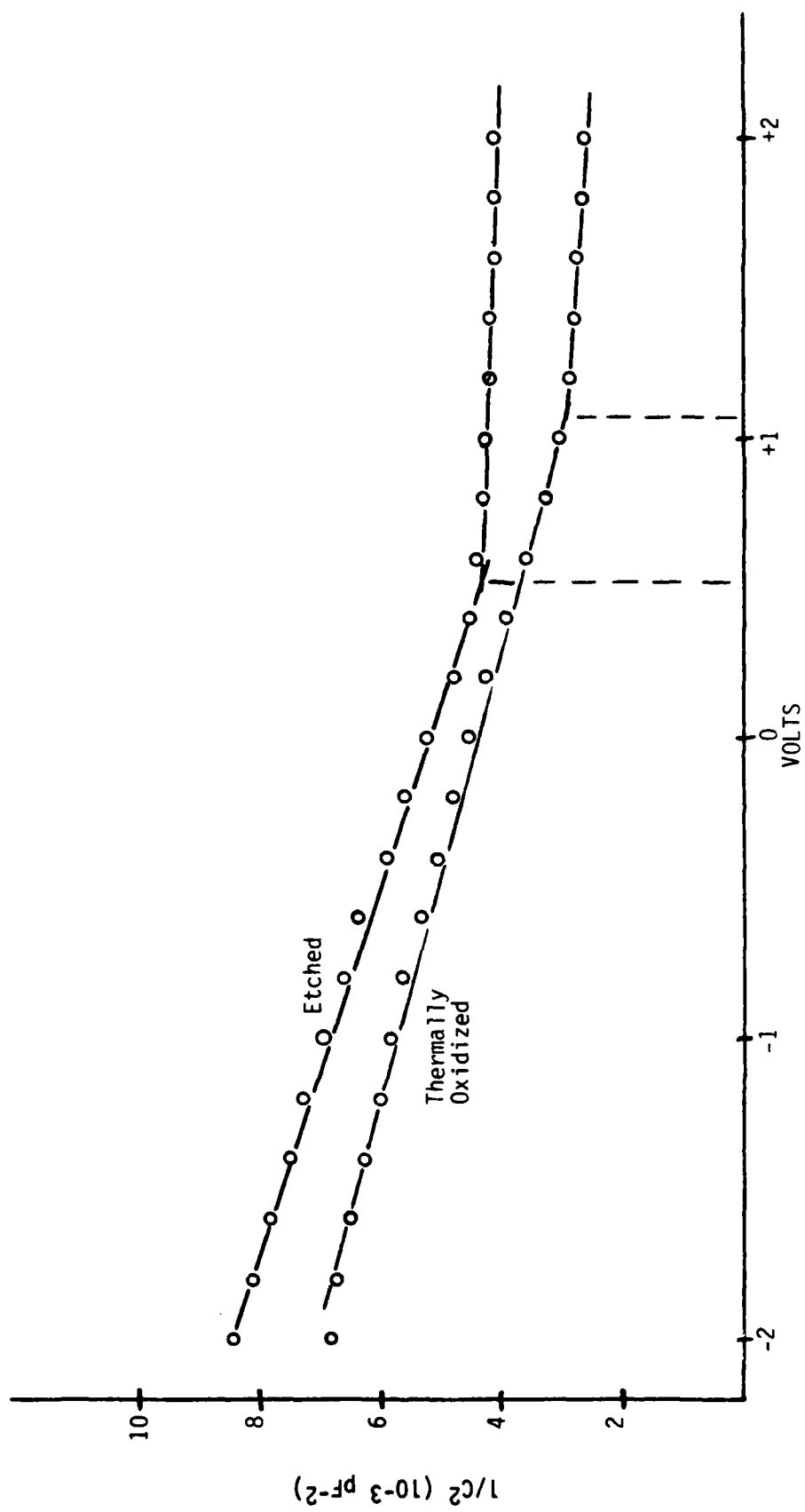
Fig. 14 $1/C^2$ vs voltage for the same samples studied in Fig. 13.

in which elemental As was evaporated onto bulk n-type (100) surfaces. Other deposited insulators are described in the second part of the section. All GaAs samples were from boule #3686.

a. <u>Elemental As</u>

Because As can easily be evolved from GaAs surfaces, it might be intuitively expected that As vacancies are a dominant defect near GaAs surfaces. An experiment was performed to determine if $\Delta(i)$ could be substantially altered by varying the surface concentration of As. In this experiment, a n-GaAs (100) surface was exposed to a As_2 beam. This beam was generated by heating GaAs in the quartz tube evaporator. The results are summarized in Table 9 which shows the relative shifts of As3d- and Ga3d-core levels as a function of increasing As overlayer thickness. The initial surface was thermally cleaned at ~550°C. This surface was then oxidized prior to As deposition, to form Ga_2O_3 which as discussed above produces a relatively small band bending on n-type GaAs. Four sequential As deposits were carried out; the relative As overlayer thickness can be assessed from the As3d/Ga3d intensity ratio which is given in Table 9. Little variation in the As3d binding energy is observed for all the deposits. There is a <u>chemical</u> shift of ~0.3 eV between As3d in elemental As and in GaAs (the E_B is larger in elemental As). Thus, although there does not appear to be a potential shift in the As3d line, this interpretation is complicated by the chemically shifted elemental As component. In fact, for the thicker As deposits, a substantial potential shift is observed in the Ga3d line. For the thickest As deposit the band bending in this n-type sample increases to nearly the same position as is observed on the thermally cleaned surface.

The final surface treatment of this sample was an ~ 300°C anneal. A substantial fraction of the elemental As was removed from the sample surface by this treatment as can be seen from the As3d/Ga3d intensity ratio. However, little further change in band bending was produced as determined by the lack of significant change in the Ga3d relative binding energy.

38

Table 9

Deposition of As on GaAs
n-Type GaAs (100), Boule #3686

Treatment Sequence	Intensity Ratio As3d/Ga3d	Relative Binding Energy (eV)[a]	
		Ga3d	As3d
≈550°C Anneal[b] (Clean, LEED)	-	0.00	0.00
Oxidation (Ga$_2$O$_3$)	1.34	+0.43	+0.27
1st As Deposit	1.38	+0.39	+0.27
2nd As Deposit	1.78	+0.37	+0.31
3rd As Deposit	2.29	+0.24	+0.27
4th As Deposit	3.48	+0.08	+0.27
≈300°C, 5 min	2.02	+0.04	+0.12

a - Accuracy is ± 0.06 eV.
b - Binding energies are relative to the values observed on this surface.

b. Other Materials

Experiments were carried out in which thin layers of CuBr, GeS, and SiO$_x$ were evaporated onto bulk grown n-type GaAs (100) surfaces. The results are briefly summarized in Table 10.

CuBr is a semiconducting material (E$_g$ = 3.0 eV) which has the interesting feature that it is lattice matched to and will grow epitaxially on GaAs (100) at room temperature. The band matching properties of this hetero-junction have been previously studied in this laboratory.[19] This epitaxially prepared heterojunction suggests the possibility of forming a low defect interface with a corresponding low interface-state density similar to the use

Table 10

Deposition of Materials on GaAs Surfaces
n-Type GaAs (100), Boule #3686

Deposited Material	Treatment	Relative As3d Binding Energy in GaAs (eV)	Remarks
	≈440°C	+0.34	Ga_2O_3
	≈550°C	0	Clean, LEED
CuBr	Epitaxial Growth at 25°C	+0.06	LEED
	≈560°C	0	Clean
GeS	Deposit at 25°C	+0.02	
GeS	≈280°C; Deposit at 25°C	+0.15	First deposit removed by ≈280°C treatment
	≈570°C	0	Clean
SiO_x	Deposit at ≈400°C	+0.05	

of oxidized $Ga_{1-x}Al_xAs$ layers for GaAs passivation.[20] A thin layer $\lesssim 20$Å of CuBr was grown epitaxially on this surface at room temperature. Only a small decrease in band bending was observed which suggests that the surface states associated with the surface charge present on the thermally cleaned surface are not removed by the room temperature epitaxial growth of CuBr.

GeS was evaporated onto a thermally cleaned GaAs (100) surface. The substrate was at room temperature. Essentially no change in band bending occurred. The GeS was subsequently removed from the surface by heating to

40

~280°C which was followed by an additional GeS deposit at room temperature. This procedure resulted in a significant decrease in band bending which suggests that a surface reaction may have occurred during the heat treatment.

Silicon monoxide was evaporated onto a thermally cleaned substrate which was at ~400°C during the deposit. Only a small decrease in band bending was observed at this interface.

The results reported in this section, although fragmentary, suggest that to produce a substantial alteration of surface potential a surface chemical reaction may be required as, for example, is produced by oxygen exposure at high temperature. Interfaces formed by reaction with S, P, and other non-metallic elements are clearly interesting possibilities.

III.A.4 VPE Grown Material

The experiments reported in this section were carried out to determine if there were any significant differences in the chemistry and (interfacial) surface potential for VPE samples (described in Sec. II.C.1) as compared to bulk n-type GaAs. The results of various treatments are listed in Table 11. The thermal treatment to about ~550°C results in converting a surface with mixed Ga- and As- oxides to one of solely Ga_2O_3. Further heat treatment at ~570°C removes the Ga_2O_3 from the surface and results in a clean GaAs(100) surface with a characteristic LEED pattern. Exposure of this clean surface to O_2 at elevated temperatures (~480°C) results in Ga_2O_3 formation and concomitant loss of the LEED pattern. These surface treatments result in a variation of the surface potential which closely mimics that observed for the surfaces of bulk samples. Namely, the Ga_2O_3 surface exhibits only a small band bending (~0.2 eV), while thermal cleaning results in a large band bending. Table 11 also summarizes results from the deposition of elemental As (see also Sec. III.A.3a) on the thermally cleaned surface at low substrate temperatures. Such depositions resulted in elemental As overlayers as detected by a 0.3 eV chemical shift of the As3d line to higher binding energy; however, no change in surface potential was observed. Thermal treatment resulted in the As being easily driven off.

41

Table 11

Several Treatments of VPE Grown GaAs
n-Type GaAs (100), VPE #1100[a]

Treatment	Relative As 3d Binding Energy in GaAs (eV)	Remarks
≈550°C	+0.2	Ga_2O_3
16 Hrs Vacuum	+0.3	---
≈570°C	0.0	Clean, LEED
2×10^4L H_2O (≈480°C)	0.0	---
2×10^4L O_2 (≈480°C)	+0.2	Ga_2O_3
≈560°C	0.0	Clean, LEED Ga3d/As3d ≈0.88
Deposit As° (25°C)	(+0.3)[b]	Ga3d/As3d ≈0.02 (No significant shift in Ga3d line)
≈560°C	0.0	Clean, LEED Ga3d/As3d ≈0.88
Deposit As° (≈65°C)	(+0.3)[b]	Ga3d/As3d ≈0.42 (No significant shift in Ga3d line)

[a] - ≈0.1 eV Binding-Energy Instability
[b] - Chemical Shift Due to As°

No significant differences in surface potential variation were noted between the VPE and bulk grown materials.

III.B XPS Measurements on p-Type GaAs Samples

Measurements were carried out on bulk p-type material (boule #3691) to compare the effects of surface treatments on surface chemistry and potential with the results of Sec. III.A on n-type materials. Also in this section

42

are described the results of a H_2O_2 surface treatment which produced a native oxide that contained As_2O_5.

1. Thermal and Oxidation Studies

Thermal and oxidation treatments similar to those reported in Sec. III.A.1a were carried out in a bulk grown p-type GaAs (100) sample. The results are summarized in Table 12. The chemistry of the p-type surface is similar to that for n-type described above. Heat treatment at ≈480°C produces a surface of Ga_2O_3, while further treatment at ≈560°C yields a clean surface with a characteristic LEED pattern. High temperature (≈480°C) oxidation results in a Ga_2O_3 covered surface. The magnitude of the surface-potential variations is similar to that observed for n-type material but the sign of the variation in band-bending potential is reversed, i.e., a surface treatment which causes an increased V_{BB} for n-type material produces a decreased V_{BB} for p-type material and vice versa. This surface-potential behavior as a function of treatment is discussed further in Sec. III.C where a more direct comparison of XPS results for n- and p-type samples is presented. As was noted in Sec. III.A.1a for n-type material, vacuum storage (≈10^{-9} torr, 16 hrs) also results in a surface-potential variation on p-type material. Finally, sputtering of the large V_{BB} surface with 1 keV Ar^+ followed by a ≈280°C anneal produced a large variation in $\Delta(i)$.

2. H_2O_2 Treatment to Form As_2O_5

The XPS experiments on band bending at oxidized GaAs surfaces described above have concerned two types of oxides: a) a mixture of As_2O_3 and Ga_2O_3 formed after the initial surface preparation procedure Sec. II.C.2 and b) Ga_2O_3 only, formed by heating the mixed oxide of (a) to ≈500°C or oxidation of a thermally cleaned sample in O_2 at this temperature. We have also investigated a third type of GaAs native-oxide covered surface, that formed by etching a sample in a 4:1:1 (H_2SO_4:H_2O_2:H_2O) solution, quenching with water, followed by storage overnight in a solution of H_2O_2 (30%) and H_2O. After the H_2O_2 treatment the sample was not heated before initial XPS examination.

43

Table 12

Several Surface Treatments of GaAs
p-Type GaAs (100), Boule #3691[a]

Treatment	Relative As3d Binding Energy in GaAs (eV)	Remarks
≈480°C	+0.3	Ga_2O_3
≈560°C	0.0	Clean, LEED
O_2 2×10^4L (≈480°C)	+0.2	Ga_2O_3
16 Hrs Vacuum	+0.3	---
Sputter 1 keV Ar^{+} Anneal ≈280°C	-0.1	No LEED (Small Ga_2O_3)

[a] - ≈0.1 eV Binding-Energy Instability

In Fig. 15, the upper XPS spectrum shows the As3d core-level peaks from the initial H_2O_2 treated surface of a p-type GaAs (100) sample. In addition to the peak from the underlying substrate [labeled As(GaAs)], a substantial peak chemically shifted by ≈ 4.5 eV and attributed to As_2O_5 (see Ref. 21) is also evident. The data indicate the presence of some As_2O_3 and the Ga3d core-level spectrum (not shown) indicated the substantial presence of Ga_2O_3. From the relative intensity of these two As peaks, in conjunction with an examination of the corresponding peaks associated with the Ga3d core levels, the estimated oxide thickness is 15-20Å and the composition consists of a As_2O_5, As_2O_3, and Ga_2O_3 mixture. This H_2O_2 treatment produced the thickest (by about a factor of 2) native oxide layer that was examined in this work. Also in Fig. 15, the lower As3d spectrum shows the result of a ≈340°C heat treatment. The initial As_2O_5 has been converted to As_2O_3 and there is an accompanying relatively large ≈0.35 eV increase in band bending (seen as a shift in the As(GaAs) peak). No change in Ga chemistry was observed after this ≈340°C heating. Thus, this surface is a mixture of As_2O_3 and Ga_2O_3.
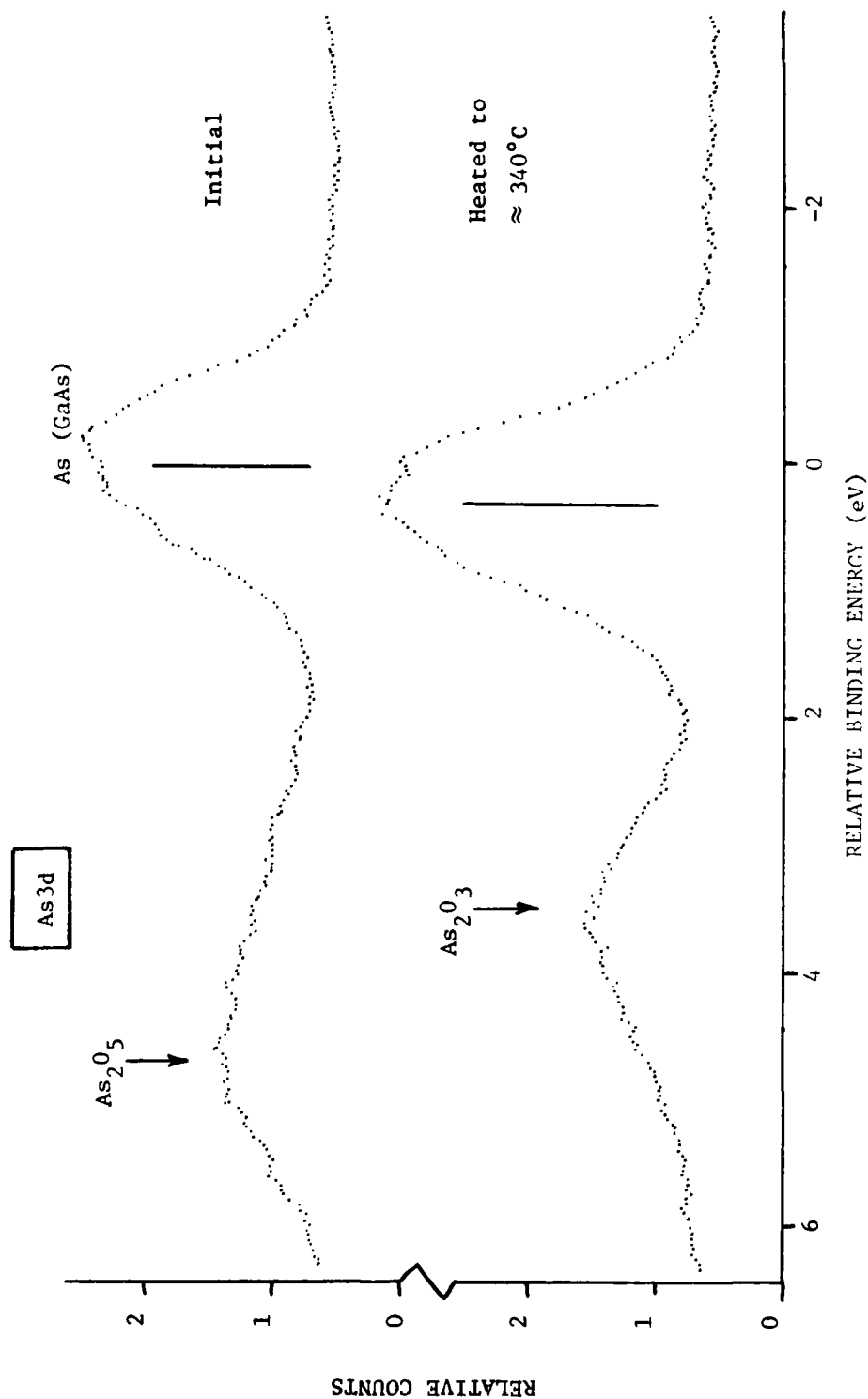
Fig. 15 XPS spectra of p-type GaAs (100) in the region of the As3d line. The spectrum at the top exhibits the substantial presence of As_2O_5 and was obtained after the sample was treated with H_2O_2 solution. The spectrum at the bottom is for the same surface after annealing at $\approx 340°C$; this treatment removed the As_2O_5 and produced more As_2O_3.

Next, the sample was heated to ≈550°C and a clean surface and characteristic LEED pattern was obtained. The potential shift associated with this step was ≈0.45 eV to lower band bending. The results are summarized in Table 13.

The same H_2O_2 treatment described above was also applied to a n-type GaAs (100) sample (boule #3686) and for completeness these results are also given in Table 13. Roughly similar results were obtained, except that the band-bending change when As_2O_5 was converted to As_2O_3 was somewhat smaller.

Table 13

Peroxide Treatment of GaAs
p-Type GaAs (100), Boule #3691
n-Type GaAs (100), Boule #3686

Doping	Treatment	Relative As3d Binding Energy in GaAs (eV)[a]	Remarks
p	H_2O_2	+0.1	As_2O_5 (As_2O_3) + Ga_2O_3
	≈340°C	+0.45	As_2O_3 + Ga_2O_3
	≈550°C[b]	0.0	Clean, LEED
n	H_2O_2	+0.3	As_2O_5 (As_2O_3) + Ga_2O_3
	≈320°C	+0.4	As_2O_3 + Ga_2O_3
	≈550°C[b]	0.0	Clean, LEED

a – Accuracy is ± 0.06 eV.
b – Binding energies are relative to the values observed on this surface.

III.C Correlation of n- and p-type GaAs Surface Potential Measurements

As noted in Sec. III.B.1, the variation in band-bending potential between n- and p-type surfaces is apparently correlated with the interesting feature than an increased V_{BB} for an n-type surface corresponds to a decreased band bending on a p-type surface and vice versa. In the first part of this section, experiments on n- and p-type GaAs (100) bulk samples from boules

46

#3686, 3691 and 3630 are described which were designed to explore this correlated potential variation. The results of these studies which confirmed the correlated surface-potential variation suggested that modifications of the popular Universal Defect Model (UDM) of Fermi-level pinning[22] were needed. Most previous studies of GaAs Fermi-level pinning reported in the literature have involved the (110) cleavage surface. In order to compare our results with these studies, experiments on n- and p-type GaAs (110) bulk samples from boules #3686 and 3782 were carried out and are reported in the second part of this section.

II.C.1   (100) Measurements

To facilitate comparison of the chemistry and surface-potential variations between n- and p-type GaAs(100), an n- and p-specimen were simultaneously given a chemical etch in the same solution and then mounted side by side on the same sample platen. Thus, as nearly as possible, both samples were exposed to the same chemical and thermal treatments. The results are shown in Fig. 16, where binding energies are reported on an absolute scale by the method described in Sec. II.B. As can be seen in Fig. 16, except for some small subtle ($\approx$0.1 eV) differences, the surface potentials for n- and p-type GaAs(100), as monitored by the As3d core-level binding energy, track together in a highly correlated manner as a function of surface treatment. It must be remembered, however, that when considering the band-bending potential, this behavior is opposite. For example, consider the clean surface; when exposed to 2×10^4 L O_2 at $\approx$460°C, the As3d core level shifts by 0.18 eV to higher binding energy for both n- and p-GaAs(100). However, in the case of n GaAs(100), this means the band bending is reduced by 0.18 eV, while in the case of p-GaAs(100) the band bending is increased by 0.18 eV. Another interesting aspect of Fig. 16 is that the surfaces can be prepared with at least several different surface potentials. This result may be in contradiction to the recently proposed UDM for surface Fermi-level pinning[22] which suggests a unique pinning position for the energy bands on n- and p-type samples. One final interesting observation concerns the effect of Au deposits

47
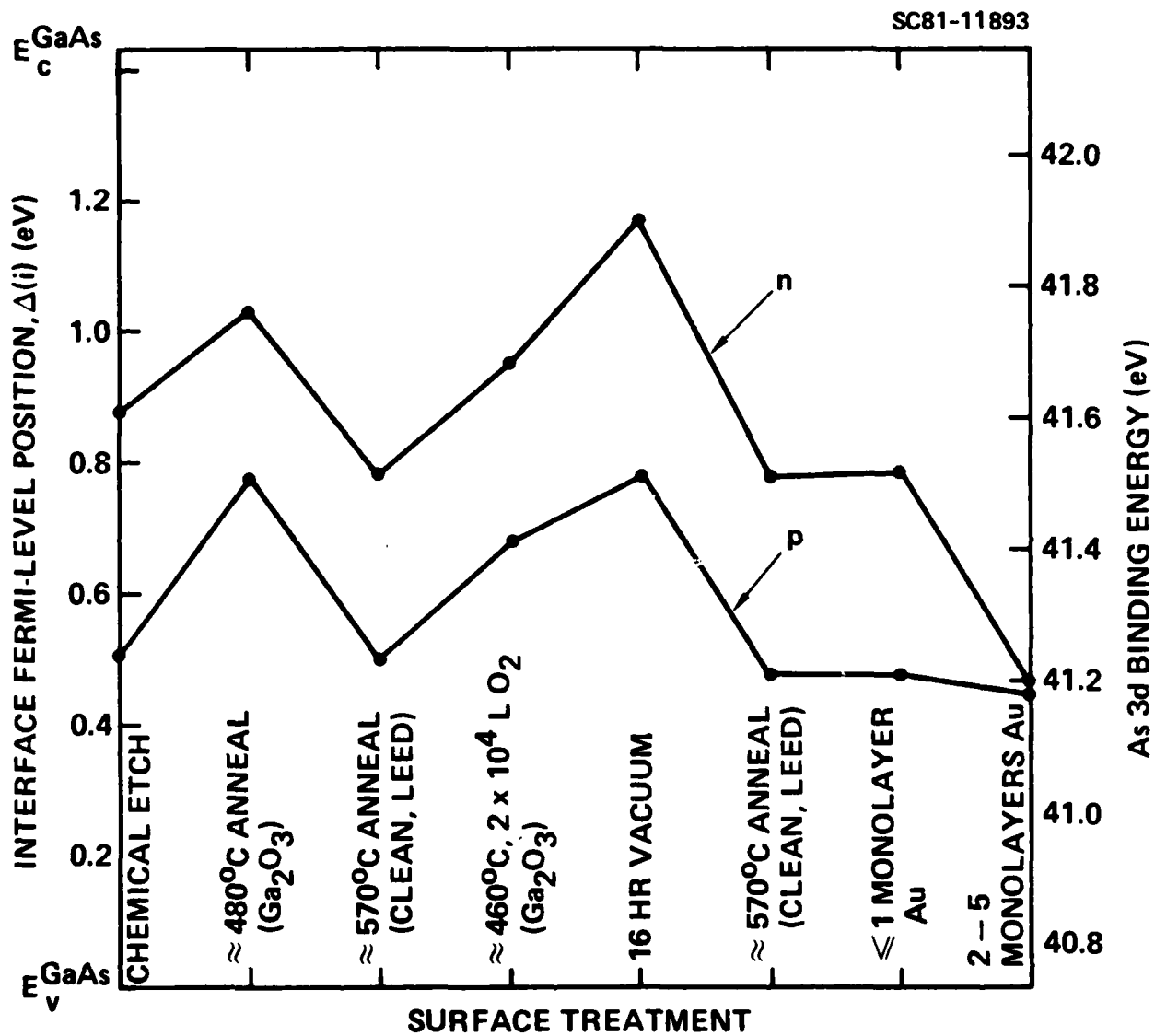
Fig. 16   Δ(1) observed for several surface treatments of n- and p-type GaAs
(100) samples.

on the surface. Before terminating the experiment with a thick Au deposit for a final absolute reference-energy determination, intermediate amounts of Au were deposited. At first only a small submonolayer amount of Au was deposited. The $Au4f_{7/2}$ binding energy had a 0.29 eV difference between n- and p-type GaAs, the same difference as observed for the As3d binding energy in n- and p-GaAs. This submonolayer deposit had little effect on the surface potential as seen in Fig. 16. Next, the Au deposit was increased to several monolayers. At this point the $Au4f_{7/2}$ binding energy on n-GaAs decreased by 0.82 eV, while on the p-GaAs the $Au4f_{7/2}$ binding energy decreased by 0.53 eV. Now the $Au4f_{7/2}$ binding energy was the same on both n- and p-GaAs, i.e., 84.20 eV. At this point, there is a large surface-potential shift in the n-type sample, which resulted in the same As3d binding energy for the n- and p-type samples (see Fig. 16). A final thick deposit of Au resulted in a further shift of the $Au4f_{7/2}$ by 0.20 eV to lower binding energy; it was observed that a small amount of As was present on top of the Au deposit. The variation in $Au4f_{7/2}$ binding energy with Au layer thickness was previously noted in Sec. II.B.

Several additional experiments were carried out to explore the highly correlated variation in surface potential for n- and p-type samples subjected to the same surface treatment. The same approach of monitoring samples mounted side-by-side on a single Mo platen was employed.

Figure 17 shows the variation in $E_{As3d}^{GaAs}(i)$ measured relative to the $E_{As3d}^{GaAs}(i)$ observed on the thermally cleaned n-type surface for three sets of n- and p-type samples. The error bars in Fig. 17 refer to relative error limits between the n- and p-type sample surfaces and between different surface treatments. The initial surfaces for sample set #1 were chemically etched and had a mixed oxide consisting of $Ga_2O_3 + As_2O_3$. These samples were heated to ~415°C to remove the As_2O_3 leaving only Ga_2O_3; the $\Delta(i)$ is observed to increase for both surfaces. The samples were then thermally cleaned at ~540°C which caused a decrease in $\Delta(i)$ for both surfaces. Deposition of a thin layer of Pd caused the $\Delta(i)$ for both surfaces to become nearly equal and have essentially the same value as observed on the thermally cleaned p-type surface.

49
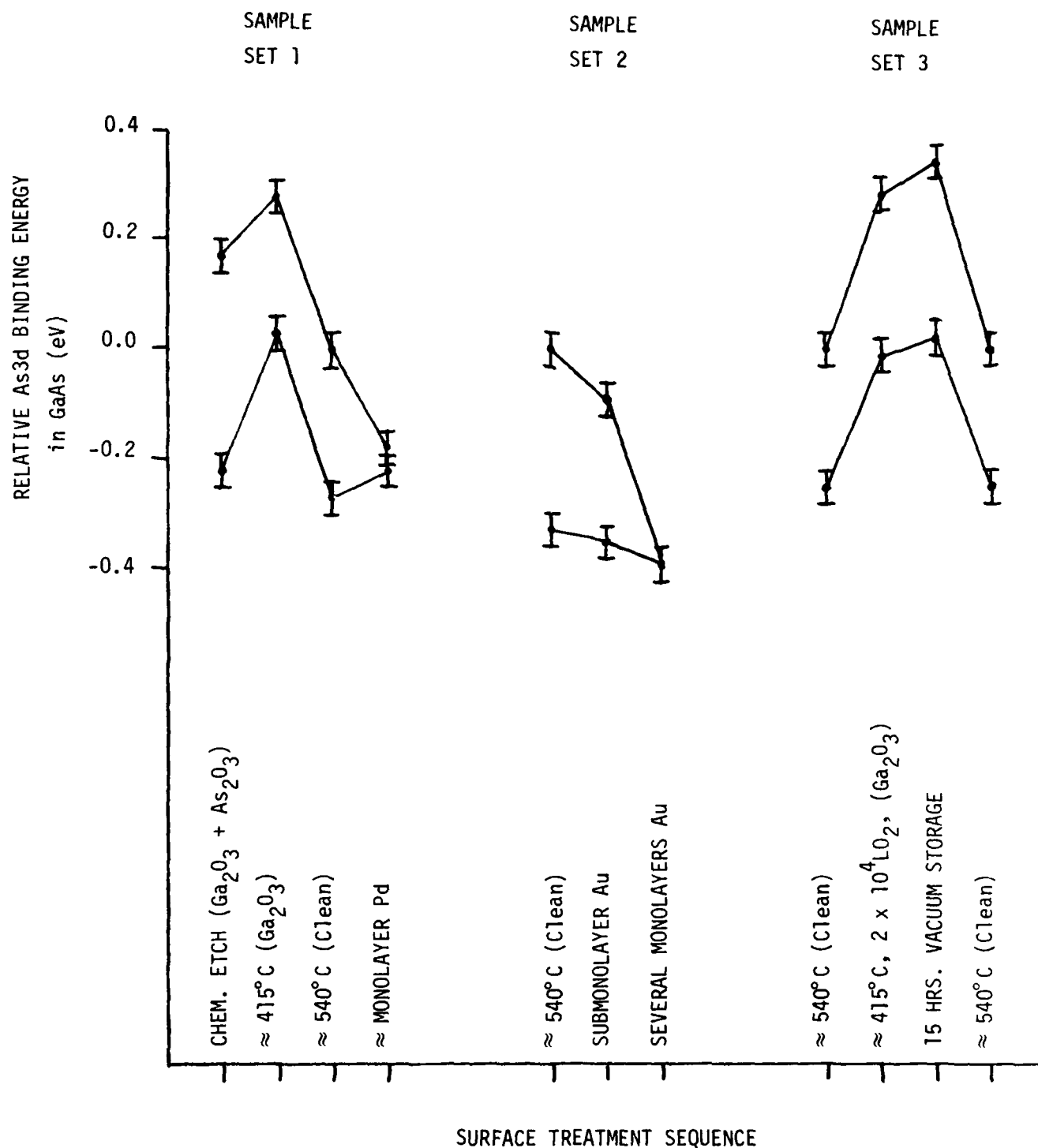
Fig. 17 Variation of Δ(i), relative to the value observed on the thermally cleaned n-type surface, for three sets of n- and p-type GaAs (100) samples. The surface treatment and resulting surface chemistry are given at the bottom of the figure.

50

For sample set #2 the initial surfaces were thermally cleaned at ≈540°C. Deposition of a submonolayer amount of Au caused only a small variation in surface potential; however, a thicker Au deposit caused $\Delta(i)$ to be the same for both surfaces and have a value nearly equal to that observed on the thermally cleaned p-type surface. This behavior is also observed in Fig. 16.

The inital surfaces for the third sample set shown in Fig. 17 were thermally cleaned at ≈540°C. These surfaces were oxidized to form Ga_2O_3 by exposure to 2×10^4 L of O_2 at ≈415°C which caused $\Delta(i)$ for both surfaces to increase. Vacuum storage for 15 hrs caused a small additional increase in $\Delta(i)$, a result which was noted in Sec. III.A.1a. A final thermal cleaning of these surfaces reproduced the initial $\Delta(i)$.

Two other n- and p-type sample sets were studied which again showed the highly correlated movement of $\Delta(i)$. Details of the experimental procedure prevented the difference in $\Delta(i)$ between the n- and p-type surfaces to be determined with reasonable accuracy, however, the relative change in As3d binding energy for the individual n- and p-type surfaces was measured with good accuracy. The results are given in Table 14. For sample set #4 the initial surfaces were prepared as described in Sec. II.C.2 and had the usual mixed oxides of Ga_2O_3 and As_2O_3. Heating these surfaces to ≈450°C removed the As_2O_3 and caused $\Delta(i)$ to increase for both surfaces.

The initial surfaces for sample set #5 were prepared as described in Sec. II.C.2 heated to ≈400°C to remove the As_2O_3 and stored in vacuum for 18 hrs. As noted in Sec. III.A.1a, this procedure produces the highest $\Delta(i)$ on n-type surfaces that we have observed. Thermally cleaning this sample set at ≈550°C caused $\Delta(i)$ for both surfaces to decrease. Reoxidizing the surface to form Ga_2O_3 by exposure to 6×10^4 L of O_2 at ≈450°C caused $\Delta(i)$ to increase for both surfaces.

51

Table 14

Annealing and Oxidation of GaAs
p-Type GaAs (100), Boule #3630
n-Type GaAs (100), Boule #3686

Sample Set #	Treatment	p-Type Relative As3d Binding Energy in GaAs (eV)[a]	n-Type Relative As3d Binding Energy in GaAs (eV)[a]	Remarks
4	Chem. Etch[b]	0.00	0.00	As_2O_3 + Ga_2O_3
	≈450°C	+0.15	+0.13	Ga_2O_3
5	Chem. Etch, ≈400°C, 18 hrs. vacuum	+0.15	+0.42	Ga_2O_3
	≈550°C[b]	0.00	0.00	Clean
	6×10^4 L O_2 at ≈450°C	+0.23	+0.24	Ga_2O_3

a - Accuracy is ± 0.05 eV.
b - Binding energies are relative to the values observed on this surface.

An additional set of experiments involved deposition of As_2 (again from a GaAs source) onto a n- and p-type sample which were mounted side by side on a single Mo platen. The initial surfaces had been prepared as described in Sec. II.C.2, and had a mixed oxide which consisted of As_2O_3 and Ga_2O_3. The difference in relative As3d-and Ga3d-binding energies between the n- and p-type surfaces was not determined. Consequently, in Table 15, the As3d-and Ga3d-binding energies have been normalized to the values observed on the thermally cleaned surfaces for each sample. Following the chemical etch, the samples were heated to ≈440°C to produce the Ga_2O_3 surface. This resulted in a decreased $\Delta(i)$ for both samples. The change in $\Delta(i)$ observed for the n-type sample in Table 15 is larger than that for the p-type sample possibly because the p-type surface was studied first and as noted in Sec. III.A.1a the potential shift on this surface takes place gradually over a period of several hours. The deposition of a thin (≈5Å) layer of As on this surface caused

Table 15

Several Treatments of GaAs
p-Type GaAs (100), Boule #3630
n-Type GaAs (100), Boule #3686

Treatment Sequence	p-Type		n-Type		Remarks
	Relative Ga3d Binding Energy in GaAs (eV)[a]	Relative As3d Binding Energy in GaAs (eV)[a]	Relative Ga3d Binding Energy in GaAs (eV)[a]	Relative As3d Binding Energy in GaAs (eV)[a]	
Chem. Etch	-0.07	-0.09	+0.04	+0.10	$As_2O_3 + Ga_2O_3$
≈440°C	+0.26	+0.13	+0.35	+0.32	Ga_2O_3
Deposited As°	+0.44	+0.43	+0.37	+0.38	≈5A thick
≈240°C	+0.42	+0.27	+0.41	+0.30	Removed ≈3/4 of As°
≈550°C	0.00	0.00	0.00	0.00	Clean, LEED
Deposited As°	+0.16	+0.35	-0.04	+0.19	≈6A thick
≈240°C	+0.09	-	-0.02	-	Removed ≈3/4 of As°
≈550°C	+0.02	-	-0.04	-	Clean, LEED
≈450°C, 6×10^4 L O_2	+0.35	+0.24	+0.28	+0.29	Ga_2O_3

a - Binding energies relative to the values observed on the thermally cleaned surface; accuracy is ± 0.05 eV.

little change in band bending on the n-type surface consistent with the results shown in Table 9. The apparent change in band bending noted on the p-type surface is probably only due to the vacuum storage effect noted previously. Annealing these surfaces at ≈240°C (which removed ≈3/4 of the elemental As from the surface) caused little change in band bending.

53

The samples were then thermally cleaned by annealing at ≈ 550°C. The usual large decrease in $\Delta(i)$ was observed for both samples. A thin (≈6A) layer of As was deposited onto these surfaces. Although little change in band bending was observed on the n-type surface, $\Delta(i)$ on the p-type surface increased substantially. With the assumption that $\Delta(i)$ for the n- and p-type thermally cleaned surfaces is separated by ≈0.3 eV (see Fig. 16), this shift would nearly make the $\Delta(i)$ for the p-type surface coincide with that observed on the thermally cleaned n-type surface (a result which is just opposite to that observed for Au and Pd deposits as noted in Figs. 16 and 17. Thermal annealing of the samples at ≈240°C removed about 3/4 of the elemental As and caused the bands to bend back to near the thermally cleaned position. A subsequent thermal cleaning of the surfaces reproduced the $\Delta(i)$ observed on the initial thermally cleaned surfaces. An additional thermal oxidation of these samples in O_2 at ≈450°C produced the usual increase in $\Delta(i)$ for both samples.

The experiments described in this section demonstrate that $\Delta(i)$ for n- and p-type surfaces subjected to identical treatments shift in the same direction (note that this means as the band bending is increasing for one surface it is actually decreasing for the other surface). The difference between the pinning position (resulting from a particular surface treatment) for n- and p-type samples is nearly constant and is ≈0.3 eV. Large variations in $\Delta(i)$ of up to 0.7 eV have been observed (Fig. 16). The deposition of several monolayers of Au on thermally cleaned surfaces causes $\Delta(i)$ to be the same for both n- and p-type samples and nearly equal to the $\Delta(i)$ observed on the thermally cleaned p-type (a similar result was obtained for the Pd deposition). The deposition of several monolayers of As on thermally cleaned surfaces caused $\Delta(i)$ again to be about the same for both n- and p-type samples; however in this case the $\Delta(i)$ is nearly equal to that observed on the thermally cleaned n-type surface (further study is needed to confirm the reproducibility of this As deposition result). These observations support the idea that the Fermi-level pinning position is being determined by defects. However, the UDM[22] appears to need modification to be consistent with these results. An alternative to the UDM which is consistent with both these results and the experimental results on which the UDM was based is presented in Sec. IV.

III.C.2 (110) Measurements

Most of the studies carried out in this contract involved GaAs (100) surfaces due to the expected greater device interest in this surface. However, to check the general nature of some of the observations (especially the correlated surface-potential variations reported in Sec. III.C.1), as few XPS measurements of surface-potential variations with surface treatment were carried out on (110) oriented samples. These measurements are discussed in this section. The (110) oriented bulk GaAs samples were from boules #3686 and 3782.

A set of surface-potential measurements was carried out on an n-type GaAs (110) surface. The initial sample surface was prepared as discussed in Sec. II.C.2. This treatment resulted in a surface which consisted of several monolayers of Ga_2O_3 and As_2O_3. The As_2O_3 was removed from the surface by heating at about 470°C. The surface was then thermally cleaned at ≈550°C. This surface exhibited a characteristic LEED pattern and no oxygen could be detected by XPS. The sample was then oxidized at ≈430°C in O_2 (2×10^4 L) to reform the Ga_2O_3 surface. This surface was stored overnight in vacuum; the final surface treatment involved an additional thermal cleaning at ≈540°C.

The relative binding energy of the As3d level was monitored by XPS to determine the relative surface potential. The results are shown in Table 16. The relative binding-energy scale is referenced to the average As3d binding energy observed on the thermally cleaned surfaces. The variation in surface potential is very similar to that reported for n-type GaAs (100) in Sec. III.A.1a.

A set of surface-potential experiments was also carried out on a GaAs (110) p-type surface. The sample was initially prepared as discussed in Sec. II.C.2. Consistent with previous results, this treatment produced a surface which consisted of several monolayers of the oxides As_2O_3 and Ga_2O_3. The sample was then annealed at ≈470°C to remove the As_2O_3 followed by thermal cleaning at ≈550°C. The surface was then reoxidized by exposing the sample to

55

Table 16

Annealing and Oxidation of GaAs
n-Type GaAs (110), Boule #3686

Treatment	Relative As3d Binding Energy in GaAs (eV)	Remarks
Chemical Etch	0.16	$As_2O_3 + Ga_2O_3$
≈470°C	0.21	Ga_2O_3
≈550°C	-0.04	Clean, LEED
2×10^4 L O_2 at ≈430°C	0.16	Ga_2O_3
≈10 hrs Vacuum	0.29	---
≈540°C	0.04	Clean

2×10^4 L of O_2 at ≈430°C. This sample was stored overnight in vacuum. The final surface treatment was an additional thermal cleaning at ≈540°C. In Table 17 are shown the relative As3d binding energies referenced to the thermally cleaned surface. There is a high degree of correlation of the surface potential changes with the data reported on the GaAs (110) n-type material (Table 16).

Experiments were also carried out in which n- and p-type samples were mounted side-by-side on a single Mo sample platen so that variations in surface treatments would be minimized. In Table 18 are shown the relative As3d binding energies for n- and p-type samples subjected to several surface treatments. The highly correlated movement in surface potential for the two samples can be clearly observed. The data in Table 18 have been normalized to the average binding-energy value observed on the thermally cleaned surfaces.

Table 17

Annealing and Oxidation of GaAs
p-Type GaAs (110), Boule #3782

Treatment	Relative As3d Binding Energy in GaAs (eV)	Remarks
Chemical Etch	0.06	As_2O_3 + Ga_2O_3
~470°C	0.21	Ga_2O_3
~550°C	0	Clean, LEED
2×10^4 L O_2 at ~430°C	0.12	Ga_2O_3
~10 hrs Vacuum	0.19	---
~540°C	0	Clean

Table 18

Annealing and Oxidation of GaAs
n-Type GaAs (110), Boule #3686
p-Type GaAs (110), Boule #3782

Treatment	Relative As3d Binding Energy in n-Type GaAs (eV)	Relative As3d Binding Energy in p-Type GaAs (eV)	Remarks
Chemical Etch	0.06	-0.03	Ga_2O_3 + As_2O_3
~470°C	0.16	0.16	Ga_2O_3
~550°C	-0.04	-0.06	Clean, LEED
~430°C 2×10^4 L O_2	0.08	0.19	Ga_2O_3
12 hrs Vacuum	0.27	0.25	---
~540°C	0.04	0.06	Clean, LEED

57

In another experiment, thin layers of Al were evaporated on n- and p-type samples mounted side by side on the same sample platen. The results of these experiments are given in Table 19. The data have again been normalized to the binding-energy value observed on the thermally cleaned surface.

Table 19

Deposition of Al on GaAs
n-Type GaAs (110), Boule #3686
p-Type GaAs (110), Boule #3782

Treatment	Relative As3d Binding Energy in n-Type GaAs (eV)	Relative As3d Binding Energy in p-Type GaAs (eV)	Remarks
≈550°C	0	0	Clean, LEED
≈1 Monolayer Al	0.02	0.01	
≈5 Monolayers Al	0.02	0.01	

At the conclusion of the experiment which produced the data in Table 18, a thick Au layer was deposited onto both sample surfaces. The average absolute binding energies (relative to the Fermi level) for the thermally cleaned n- and p-type surfaces were found to be 41.43 and 41.13 eV, respectively. In an additional independent experiment, another n- and p-type GaAs (110) sample set was thermally cleaned and again a thick Au layer was evaporated onto the sample surface. In this experiment, the absolute binding energies were observed to be 41.39 and 41.15 eV for the n- and p-type samples, respectively. By using the average values and the known value of 40.73 eV for the binding-energy difference between the As3d core level and E_v^{GaAs}, $\Delta(i)$ relative to E_v^{GaAs} is found to be 0.68 and 0.41 eV for the thermally cleaned n- and p-type GaAs (110) samples, respectively.

The data of Tables 16-19 have been used to determine $\Delta(i)$ for several surface treatments of n- and p-type GaAs (110) samples by using the 0.68 eV and

58

0.41 eV $\Delta(i)$ values observed on the thermally cleaned surfaces as a reference. The results are given in Table 20. Where more than one measurement exists, the average value is also given. The data in Table 20 are reproduced in Fig. 18.

Table 20

Interface Fermi-Level Position for Several Treatments of GaAs Surfaces
n-Type GaAs (110), Boule #3686
p-Type GaAs (110), Boule #3782

Treatment	n-Type $\Delta(i)$ (eV)		p-Type $\Delta(i)$ (eV)		Remarks
Chemical Etch	0.74 0.83	0.79	0.38 0.47	0.43	Ga_2O_3 + As_3O_3
≈470°C	0.83 0.89	0.86	0.57 0.62	0.60	Ga_2O_3
≈550°C	0.64 0.64	0.64	0.35 0.41	0.38	Clean, LEED
≈430°C 2 × 10^4 L O_2	0.75 0.83	0.79	0.60 0.53	0.56	Ga_2O_3
12 hrs vacuum	0.95 0.97	0.96	0.66 0.60	0.63	---
≈540°C	0.71 0.71	0.71	0.47 0.41	0.44	Clean, LEED
≈1 Monolayer Al	0.69		0.42		---
≈5 Monolayers Al	0.69		0.42		---

The correlated variation in surface potential between n- and p- type samples that was observed for (100) surfaces in Fig. 16 is again observed for (110) surfaces in Fig. 18. In Fig. 16 the last surface treatment involved deposition of a few monolayers of Au while in Fig. 18 that last surface treatment involved Al deposition. The behavior of these two metals as it effects
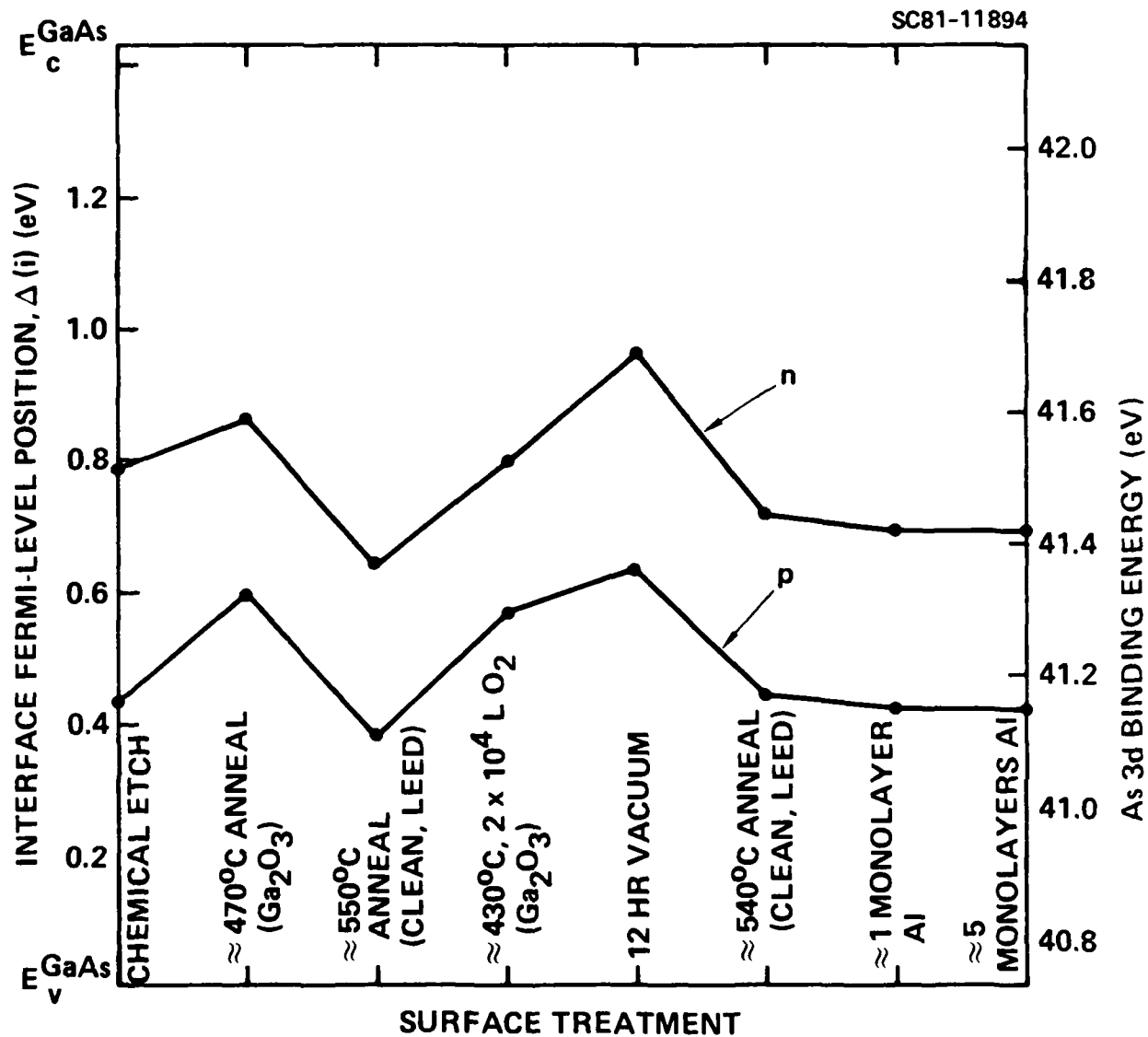
Fig. 18   Δ(i) observed for several surface treatments of n- and p-type GaAs (110) samples.

$\Delta(i)$ is quite different. In an independent experiment reported in Table 5, thin layers of Au were deposited onto n-type GaAs (100) and (110) samples which were mounted side by side on a single sample platen. The variation in $\Delta(i)$ for the two different crystallographic orientations is very similar.

A comparison of $\Delta(i)$ values for (100) and (110) samples which were subjected to similar surface treatments (Figs. 16 and 18) suggests that the (110) may be systematically lower by ≈0.1 eV. However, a comparison of the $\Delta(i)$ observed on thermally cleaned GaAs (100) surfaces in Tables 4 and 5 and Fig. 16 shows that considerable scatter occurs from sample to sample. In the one case where a (100) and (110) sample were studied under as nearly identical surface preparation conditions as possible (Table 5) the $\Delta(i)$ for the two samples were identical to within experimental error. Thus, without further work, significance should not be attached to this result.

For completeness, an experiment was also carried out on an n- and p-type GaAs (111B) sample set in an attempt to observe similar surface-potential variations. Unfortunately, the thermal cleaning treatment resulted in surface faceting.

IV. A SINGLE DEFECT MODEL INTERPRETATION OF THE GaAs SURFACE POTENTIAL MEASUREMENTS

Spicer et al[22] have proposed a universal pair of pinning levels which in GaAs arise from Ga and As vacancies. In their UDM, they suggest that these vacancies produce characteristic donor-and acceptor-levels at 0.5 and 0.75 eV (relative to E_v^{GaAs}), respectively. This model was based partly on the observation that the $\Delta(i)$ are independent of surface treatment for a specific doping type. Our experimental results agree with Ref. 22 for similar surface conditions but for treatments associated with the Ga_2O_3-GaAs interface, we observe different $\Delta(i)$. This seems to unambiguously require a modification of the UDM.

61

The fact that the difference between n-type and p-type $\Delta(i)$ remains nearly constant, although the average varies, suggests that the same defect may be involved throughout with levels shifted by the surface treatment. Otherwise, it would have to be assumed that not only did the high temperature oxidation followed by vacuum storage add new defects, but that this process also removed the old ones (a new empty level above the one which had pinned the n-type material would not increase $\Delta(i)$ if the original level is still present). Furthermore, it would have to be assumed that the added levels for the n-type and p-type samples differed in energy by about the same amount as the original levels. This would require a fortuitous coincidence if two different defects were involved for both n-type and p-type material. It would even seem to be a coincidence if one defect which produced n-type and p-type pinning were replaced by a single different defect which produced n-type and p-type pinning. It is therefore suggested that the observed highly correlated movement of $\Delta(i)$ on the n- and p-GaAs surfaces is the result of a single defect (such as an As vacancy[23]) which is responsible for all of the pinning levels and that the defect is affected by surface treatment. Thus, the high temperature oxidation treatment reported here may shift the energy levels associated with the defect by changing the local defect environment.

If the same defect is behaving as a donor and acceptor, it must exist in three charge states, either positive, neutral, or negative.[23] We may then associate an electron level with the addition of the first electron (+/0) and a higher level with the addition of the second (0/-). The energy difference in such levels is customarily called U and is assumed to arise from the Coulomb repulsion between two electrons in the same orbital. The differences in $\Delta(i)$ observed for GaAs are in fact on the order of a typical Coulomb shift; Baraff et al[24] predict a Coulomb U of ≈ 0.25 eV for the Si vacancy. The defect in GaAs cannot be a negative U center as is the vacancy in Si because for a negative U center the neutral state would be unstable. This would lead to a single $\Delta(i)$ for both n- and p-type GaAs since there is only a single energy level at which an electron is added or removed.

62

In n-type material, we assume that enough defects are in the negative charge state to produce the band bending necessary to pin $\Delta(i)$ at the (0/-) level; in p-type material enough defects are in the positive charge state to pin $\Delta(i)$ at the (+/0) level. Since (0/-) and (+/0) levels originate from the same defect, the number of each of these levels is of course equal on a particular surface.

The n- and p-GaAs surfaces on which several monolayers of Au (or Pd) were evaporated seem to be an anomaly. On these surfaces both n-type and p-type specimens have the same $\Delta(i)$ which is, within experimental error, the same as the $\Delta(i)$ observed on the thermally cleaned p-type surface. This suggests that the gold atoms have taken electrons from the neutral defects to produce positive defects and compensating negatively charged gold centers. This process in itself does not change $\Delta(i)$, but the positively charged defects can now take on electrons in n-type material which moves $\Delta(i)$ to the (+/0) level, in agreement with experiment. The fact that a heavy coverage of gold is required to accomplish this suggests that only a small fraction of the gold atoms are active (less than the number of defects, but enough to increase the band bending to the (+/0) level), perhaps those which enter the specimen interstitially. Previous experimental work has indicated that Au can form shallow acceptor levels in GaAs and cause n to p conversion.[25]

A single defect model (SDM) of Fermi-level pinning in GaAs accounts in a natural way for all of our experimental data and we believe, all of the data in Ref. 22. It is probably the simplest model which will accomplish this, but it is not conclusively proven. Furthermore, our results give no indication as to what the defect may be although an As vacancy would seem to be a reasonable possibility.

The model proposed here could have important implications for interface-state density control. It suggests that by means of surface treatments it may be possible to adjust $\Delta(i)$ within some interval. However, the observation that the interface-potential difference between a pair of n- and p-type samples remains nearly constant at ~0.3 eV suggests that the interface-

state density may be rather large despite a surface treatment that minimizes band bending on one or the other sample. This is because the minimum density of defects in the SDM is that required to trap the charge associated with the surface which has the largest band bending of the pair.

V. CONTACTLESS C-V APPARATUS DEVELOPMENT

As a possible supplementary probe of electrical interface properties, development of a contactless C-V technique was attempted. In this section we discuss the progress made toward this development. The first part of the section discusses the measurement technique. Our design and assembly of the apparatus is discussed in the second part of the section.

V.A   Measurement Technique

Capacitance vs voltage (C-V) measurements are a routine, established technique for investigating metal-insulator-semiconductor (MIS) structures. C-V curves yield valuable information about the band-bending magnitude in the semi-conductor at equilibrium, amount of interface charge, and time constants of interface-state occupation. It would be of use to develop a contactless C-V technique for investigating the characteristics of the ambient-semiconductor interface (be it air or vacuum) of GaAs in a manner analogous to that used for solid insulator-semiconductor interfaces. In this way the electrical charac-teristics resulting from a given surface treatment could be evaluated in a non-destructive manner by using a metal-air-semiconductor (MAS) arrangement.

In a C-V measurement a crucial parameter is C_{min}/C_0, the proportional change in measured C from accumulation to depletion, where C_0 is the capacitance between the electrode and the semiconductor, and C_{min} is the capacitance of the semiconductor depletion region in series with C_0 at the onset of inversion. It is easy to show that

$$C_{min}/C_0 = 1/[1 + (\epsilon_0 W_m/\epsilon_s d)]$$ (10)

64

where ε_0 and ε_s are the dielectric constants of insulator and semiconductor, respectively, W_m is the width of the depletion region at inversion, and d is the electrode to semiconductor spacing.

$$W_m = \{[4 \varepsilon_s k T \ln (N_D/n_i)]/q^2 N_D\}^{1/2} \text{ cm} \quad . \tag{11}$$

Rewriting Eq. (10) as

$$d = (\varepsilon_0 W_{min}/\varepsilon_s)[(C_0/C_{min})-1]^{-1} \quad , \tag{12}$$

we see that the electrode to sample spacing required for a given 'dip' in a C-V measurement is dependent only on the semiconductor doping and the ratio of gap to semiconductor dielectric constants. By using an air gap having $\varepsilon_s/\varepsilon_0 = 12$ rather than the usual solid dielectric having $\varepsilon_s/\varepsilon_0 \approx 3$ it is clear that to achieve the same C_{min}/C_0, d must be four times smaller for the same N_D. With GaAs, for a C_{min}/C_0 of 0.6 and $N_D = 1 \times 10^{16}$ cm^{-3}, the air gap must be d = 480Å. A lighter doping allows d to increase; for $N_D = 10^{15}$ cm^{-3}, d = 1200Å. Therefore, the MAS measurements would probably be best suited for use on $N_D <$ 10^{16} cm^{-3} material. At 1000Å, a disk electrode 50 mils in diameter gives a value for C_0 of 100 pF, a workable value for a C-V measurement.

A contactless C-V measurement needs to use an ~1 mm diameter electrode at a gap of <1000Å. The most desirable geometry has the electrode exactly parallel to the semiconductor surface, that is, d = constant. If d is not a constant, there will not be an equipotential at the semiconductor surface, thereby making the interpretation of a C-V measurement complex.

An expression is now derived for C_0 as a function of angle θ for a disk of radius R inclined to a conducting plane, with d the distance from the center of the disk to the plane. It will be shown that the function $C_0(\theta,d)$ provides the basis for a technique to align a contactless C-V measurement system. Ignoring any fringing field, which is justified for a $2R/d = 10^4$ geometry, $C_0(\theta)$ is given by

$$C_0(\theta) = 2\ \varepsilon_0 \int_{-R}^{R} \{[(R^2-x^2)^{1/2}]/(d + \theta x)\}\ dx \qquad (13)$$

or

$$C_0(\theta) = (2\ \varepsilon_0/d) \int_{-R}^{R} \{(R^2-x^2)^{1/2}/[1 + (\theta x/d)]\}\ dx \qquad (14)$$

For θ small, where $\theta R/d < 0.1$, which is the region of most interest, the $1/[1 + (\theta x/d)]$ term in the integral can be replaced by $1/[1 + (\theta x/d)] \approx 1 - (\theta x/d) + (\theta x/d)^2$ allowing Eq. 14 to be evaluated analytically. Upon integration,

$$C_0(\theta,d) = (\varepsilon_0\ \pi R^2/d)\ [1 + (R^2\theta^2/4d^2)] = C_0[1 + (R^2\theta^2/4d^2)] \qquad (15)$$

where C_0 is the gap capacitance at $\theta = 0$. One approach for alignment would be to vary θ mechanically while keeping d a constant and tuning for a minimum in $C_0(\theta)$. When $\theta = 0$, the gap dimension can be directly found by calculating $d = \varepsilon_0\pi R^2/C_0$. These alignment measurements would be made with the surface in accumulation. The alignment sensitivity in θ can be greatly enhanced by measuring dC/dθ; the derivative of Eq. 15 is

$$dC/d\theta = C_0 R^2\theta/2d^2 \quad . \qquad (16)$$

Therefore, if a measurement scheme to generate dC/dθ is devised, the sensitivity for detecting a null in θ is:

$$\theta = (2d^2/R^2 C_0)(dC/d\theta) = 5 \times 10^{-10}\ (dC/d\theta)(pF)^{-1} \quad . \qquad (17)$$

For R = 25 mils and d = 1000Å, C_0 = 108 pF. Therefore, θ is a very sensitive function of dC/dθ.

66

To fully assess the above result a way must be found to generate an electrical signal that is proportional to $dC/d\theta$. A possibility is to measure $dC/d\theta$ by means of a modulation scheme with lock-in amplifiers. This method is now briefly described. First, consider a θ with a small ac modulation impressed such that $\theta(t) = \theta + \Delta\theta \sin \omega_c t$, where ω_c is the frequency of the modulation and $\Delta\theta$ the amplitude. Substitution into Eq. 15 gives $C(t) = C_0[1 + k\theta(t)^2]$ where $k = R^2/4d^2$. A voltage $V(t) = V_0 \sin \omega_v t$ is also placed across the capacitor C_0. The resulting current through the capacitor is given by:

$$i = C(dV/dt) + V(dC/dt) \quad . \tag{18}$$

It is now assumed that $\omega_v \gg \omega_c$. For $V = V_0 \sin \omega_v t$ and $C = C_0[1 + k(\theta + \Delta\theta \sin \omega_c t)^2]$, where $k = R^2/4d^2$, R = radius of capacitor probe, and d = distance from surface,

$$dV/dt = \omega_v V_0 \cos \omega_v t \tag{19}$$

and

$$dC/dt = C_0[2k\theta\omega_c\Delta\theta \cos \omega_c t + k(\Delta\theta)^2 \omega_c \sin 2\omega_c t] \quad . \tag{20}$$

Ignoring terms involving $2\omega_c$ and assuming $k(\Delta\theta)^2 < k\theta^2 \ll 1$,

$$C = C_0[1 + 2\Delta\theta k\theta \sin \omega_c t] \tag{21}$$

$$C(dV/dt) = \omega_v V_0 C_0 \{\cos \omega_v t + \Delta\theta k\theta [\sin (\omega_v + \omega_c)t$$

$$- \sin (\omega_v - \omega_c)t]\} \tag{22}$$

and

$$V(dC/dt) = \omega_c V_0 C_0 \Delta\theta k\theta \ [\sin \ (\omega_v + \omega_c)t + \sin \ (\omega_v - \omega_c)t] \quad . \quad (23)$$

The terms involving θ appear at $\omega = (\omega_v + \omega_c)$ and $\omega = (\omega_v - \omega_c)$; if the measurement is made such that $\omega_v \gg \omega_c$, then $C(dV/dt) \gg V(dC/dt)$. Therefore, for $\omega_v \gg \omega_c$,

$$i \approx C(dV/dt) = \omega_v V_0 C_0 \ \{\cos \omega_v t + \Delta\theta k\theta \ [\sin \ (\omega_v + \omega_c)t$$

$$- \sin \ (\omega_v - \omega_c)t]\} \quad . \quad (24)$$

In other words, the current signal generated at ω_v is modulated at a frequency ω_c with an amplitude proportional to θ. The magnitude of the current appearing at ω_c after appropriate demodulation by two lock-in amplifiers in series (see Fig. 19) is a direct measure of θ: $i(\theta) = (\omega_v V_0 C_0 \Delta\theta k)\theta$. For $\omega_v \approx 5 \times 10^4$ Hz, $C_0 = 10^{-10}$ F, $\Delta\theta = 2 \times 10^{-5}$ radians, $k = 10^7$, $V = 1V$, which are reasonable values for a 25 mil probe spaced at 1000Å, $i(\theta) = 10^{-3}\theta$ amps/radian. Therefore, for $\theta = 10^{-5}$ radian, a signal current of 10^{-8} amps will be generated, which should be readily detectable by the lock-in amplifier method described.

By feeding the current (Eq. 18) into a lock-in amplifier tuned to ω_v, the output of the lock-in is $S_v = A_1\omega_v C_0 V_0 \ (1 + k\theta\Delta\theta \sin \omega_c t)$ for $\omega_v \gg \omega_c$, where A_1 is the gain of lock-in 1. Therefore, the dc component of this signal is a direct measure of C_0. S_v can be fed into a second lock-in tuned to ω_c, the resulting output is $S_c = A_1 A_2 \omega_v C_0 V_0 k\theta\Delta\theta$; thus, $\theta = S_c/\Delta\theta\omega_v C_0 V_0 k A_1 A_2$, where A_2 is the gain of lock-in 2. Direct comparison to Eq. 17 shows that $dC/d\theta$ is measured with this method as $(dC/d\theta) = (2S_c/\Delta\theta\omega_v V_0 A_1 A_2)$. The measurement scheme is shown schematically in Fig. 19. Varying θ until the output of lock-in 2 is a minimum determines $\theta = 0$.

V.B   Design and Assembly

The mechanical design and geometry of the contactless C-V apparatus is shown schematically in Figs. 20 and 21. The sample is mounted in the pivot

$V(t) = V_0 \sin \omega_v t$

$\theta(t) = \theta + \Delta\theta \sin \omega_c t$

$C(t) = C_0(1 + k\theta^2)$

$k = \dfrac{R^2}{4d^2}$

$\omega_v >> \omega_c$

$i = C\dfrac{dV}{dt} + V\dfrac{dC}{dt} = \omega_v V C_0 \cos \omega_v t\,[1 + 2\Delta\theta\, k\,\theta \sin \omega_c t]$

LOCK-IN 1
ω_v

LOCK-IN 2
ω_c

$S_v \propto \omega_v C_0 V_0(1 + 2k\,\theta\,\Delta\theta \sin \omega_c t)$
C and d measurement signal
$\left(d = \dfrac{\varepsilon_0 A}{C_0}\right)$
A = area of probe

$S_c \propto (\omega_v C_0 V_0 k\,\Delta\theta)\,\theta$
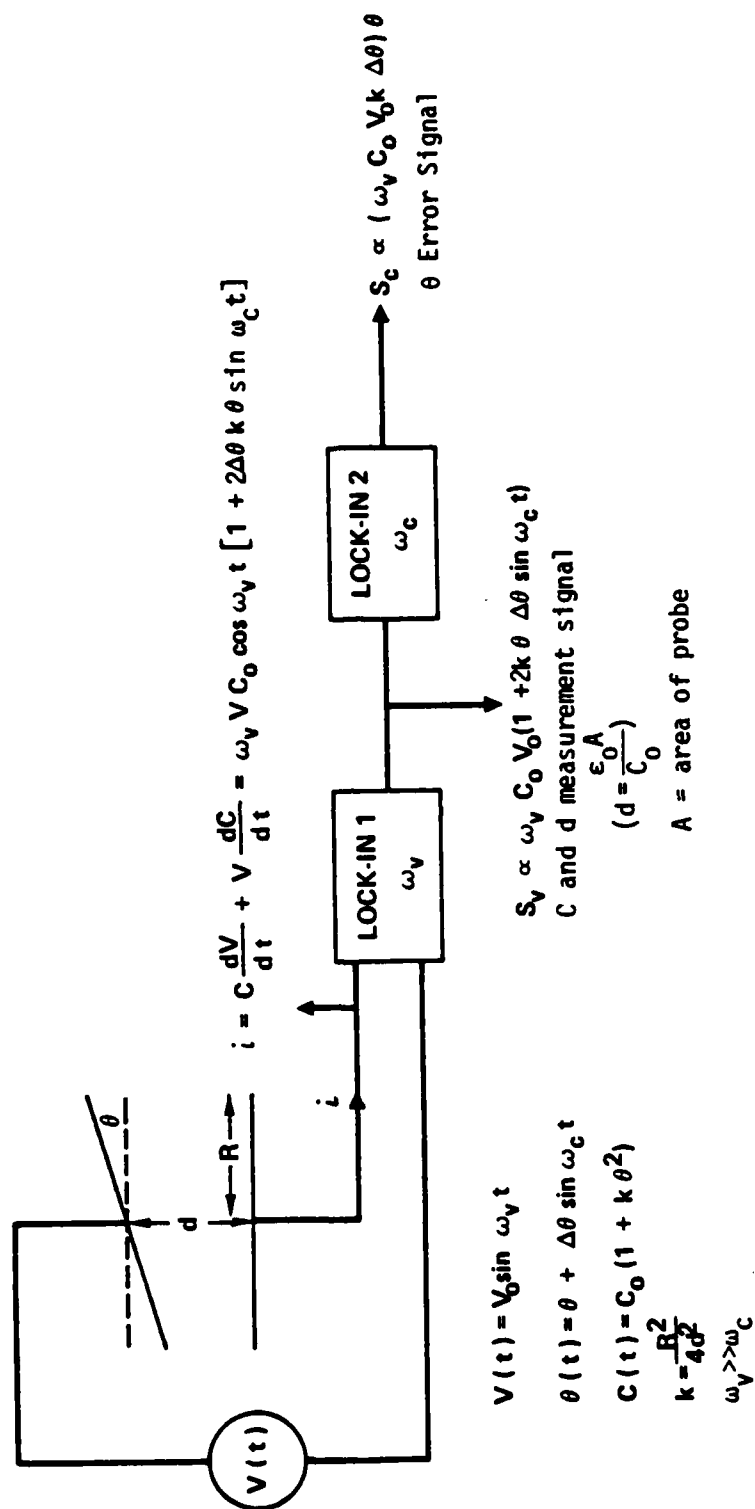θ Error Signal

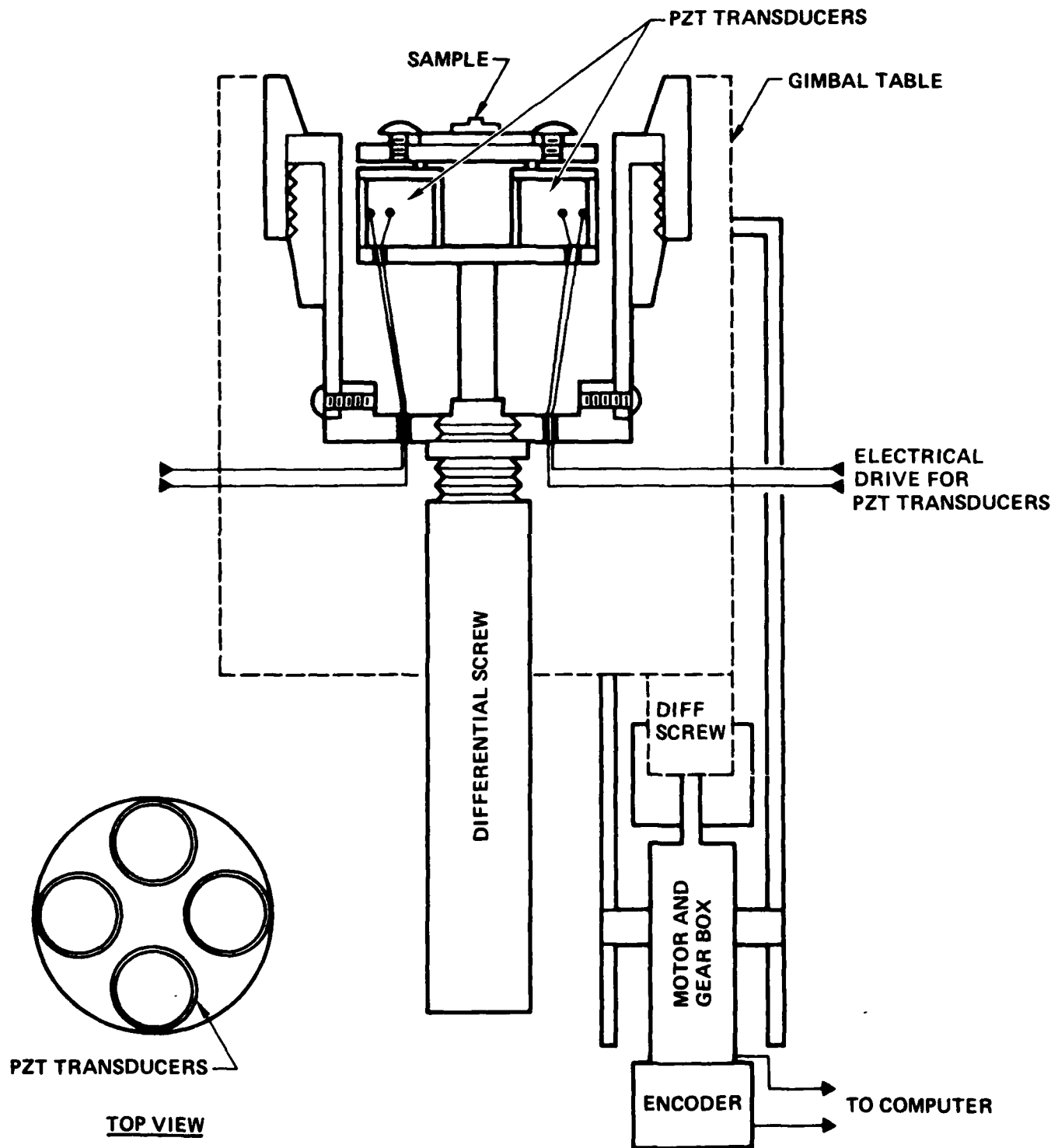Fig. 19 Schematic diagram of contactless C-V measurement scheme.

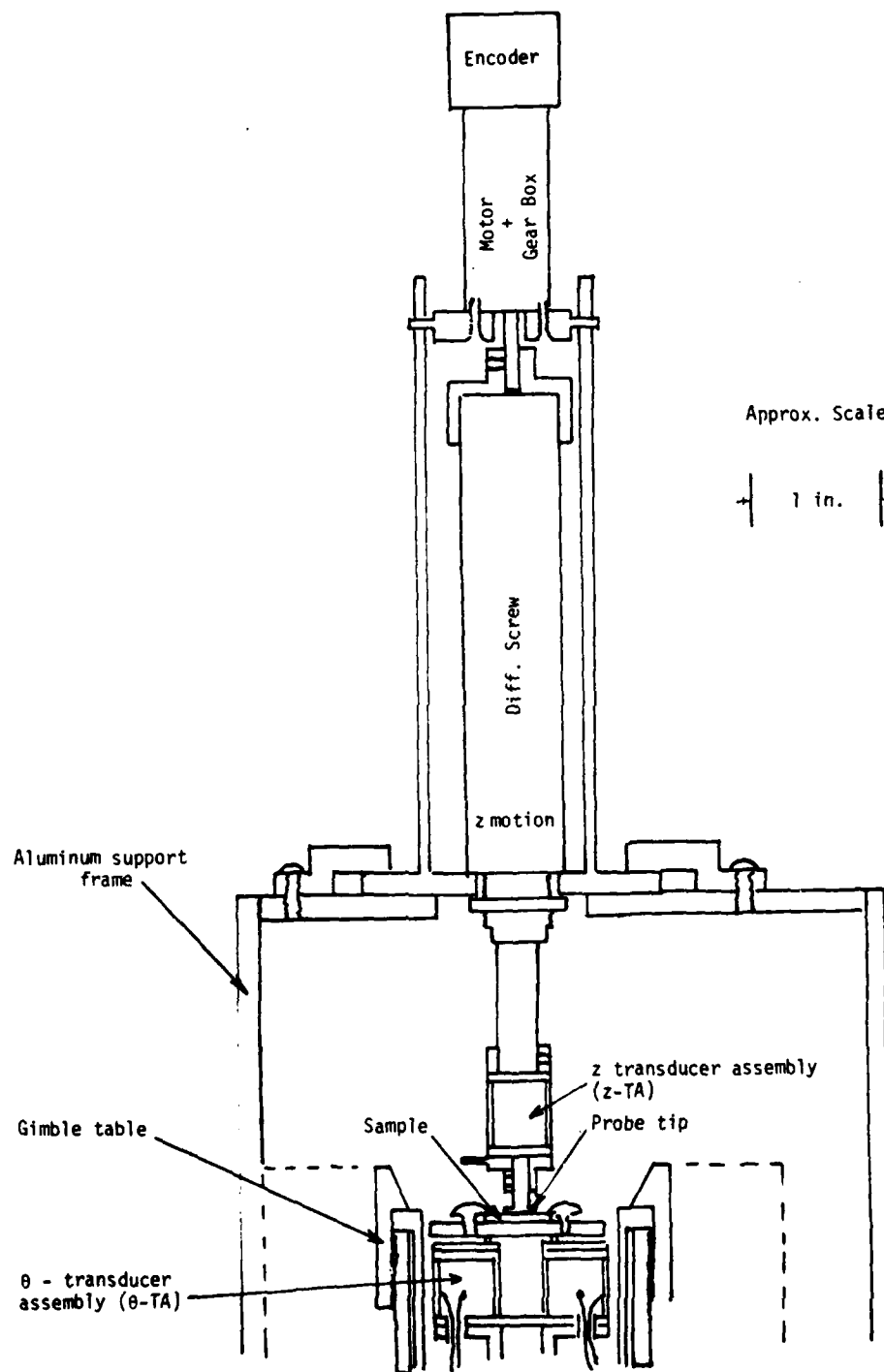Fig. 20 Schematic diagram of θ-motion assembly.

70

Fig. 21 Schematic drawing which shows relationship of z- and θ-motion assemblies.

71

plane of two ~2.5 in. diameter gimbled rings. The ring pivots are 90° apart. Coarse angular adjustment is obtained through the edge pivots by using a differential screw micrometer (coupled to a computer drive). The sample is mounted on an assembly consisting of four piezoelectric transducers in the form of pillars, which in turn are mounted on the end of a differential screw micrometer spindle. This assembly is mounted coaxially in the gimble ring table; the micrometer is adjusted to bring the sample surface to the plane of the gimble pivots. Fine angle adjustment is accomplished by supplying an appropriate electrical drive to the piezoelectric support pillars, the angular tilt is directly coupled to the sample. The micrometers have a controlled movement of <1 μm, and the piezoelectric drives have a maximum movement of ~4 μm. The micrometers are motor driven by computer control to adjust θ and the piezoelectric crystals are driven with an ac voltage to provide the modulation of θ, $\Delta\theta(t)$. The dimensions of the gimble rings and micrometer movements are consistent with a possible $<10^{-5}$ radian adjustment in θ.

The adjustment of d, the gap separation between the 25 mil radius capacitor probe tip and the sample surface, is made by another differential micrometer screw-piezoelectric crystal combination. The crystal is mounted at the end of the micrometer spindle (see Fig. 21). The piezoelectric crystal has an extension of ~3Å/V. The mechanical adjustment can be made in ~2500Å increments, and the piezoelectric drive can be used for adjustments <5000Å. This gap micrometer adjustment would also be by means of a computer controlled motor drive of the micrometer.

Figure 21 is a cross section view showing the relationship between the sample, the θ-motion assembly, and the z-motion assembly. The GaAs sample is mounted on the end plate of the θ-motion transducer assembly (θ-TA), which in turn is attached to the gimble table. The upper part in Fig. 22 is a photograph of θ-TA, shown attached to a differential micrometer screw. When the θ-TA is mounted on the gimble table, this differential screw is adjusted manually to bring the top of the sample into the plane of the gimble pivots. The θ-TA consists of four ceramic piezoelectric transducer (CPT) pillars
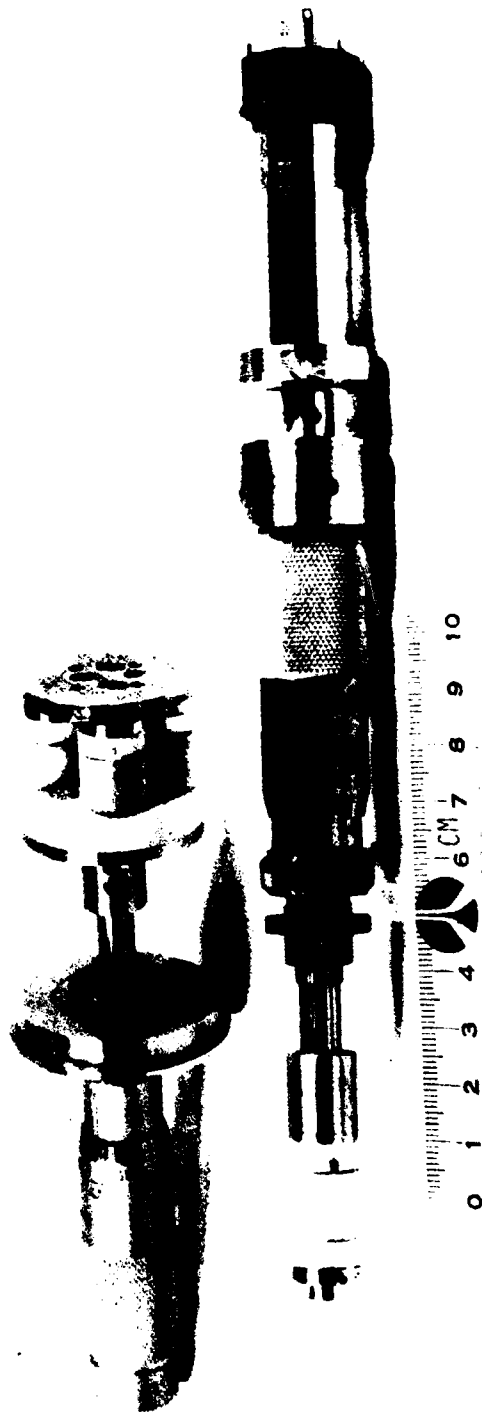
Fig. 22 Photograph of θ-motion (upper) and z-motion (lower) assemblies.

connected electrically so that opposing pairs can be activated to provide a tilt action. Figure 23 shows the gimble table assembly in which the θ-TA is mounted. The two motor driven differential screws provide for a coarse θ adjustment of up to 2.5° (4×10^{-2} rad) with a resolution of 1×10^{-5} radians. A vernier θ motion of up to 5×10^{-4} radians with a resolution of 5×10^{-7} radians is provided by the θ-TA assembly after the coarse mechanical θ alignment. This combination of mechanical and electrical adjustment for θ motion should provide an adequate range for proper operation.

A similar coupling of mechanically- and electrically-induced motion was used for the gap spacing (z-motion) assembly. The z-motion assembly is shown in the lower half of Fig. 22. This assembly consists of a motor driven differential screw to which is attached a CPT pillar. The probe tip (described below) is attached to the opposite end of the CPT to make up the z-transducer assembly (Z-TA). The differential screw has a total motion of 10 mil (250 μm) with a resolvable motion of 1000Å. The Z-TA has a total travel of 3 μm with a resolvable motion of at least 50Å. The z-motion assembly is mounted directly over the θ-motion assembly by means of an aluminum support frame. The entire assembled apparatus is shown in Fig. 24.

In Fig. 25, a block diagram design of the system computerized instrumentation is shown. The system is designed such that after initial coarse manual set-up, it would operate under "closed-loop" computer control to bring the probe tip to within 500Å of the sample surface with a parallel alignment of $<10^{-6}$ radians.

In operation, the computer moves the z-motion drive until lock-in 1 (Fig. 19) gives a signal level which shows the probe is near the sample. The θ-alignment has two orthogonal degrees of freedom, θ_1 and θ_2 accomplished by the gimble table micrometers and the θ-TA. First, θ_1 is varied to minimize θ_e, then θ_2 is varied to produce $\theta_e = 0$. Output C then gives a measure of d. If d needs to be smaller the z-micrometer of Z-TA can be used, followed by any necessary adjustment of θ_1 or θ_2. To control the micrometers, the computer provides drive to the motors attached to the z-micrometer differential
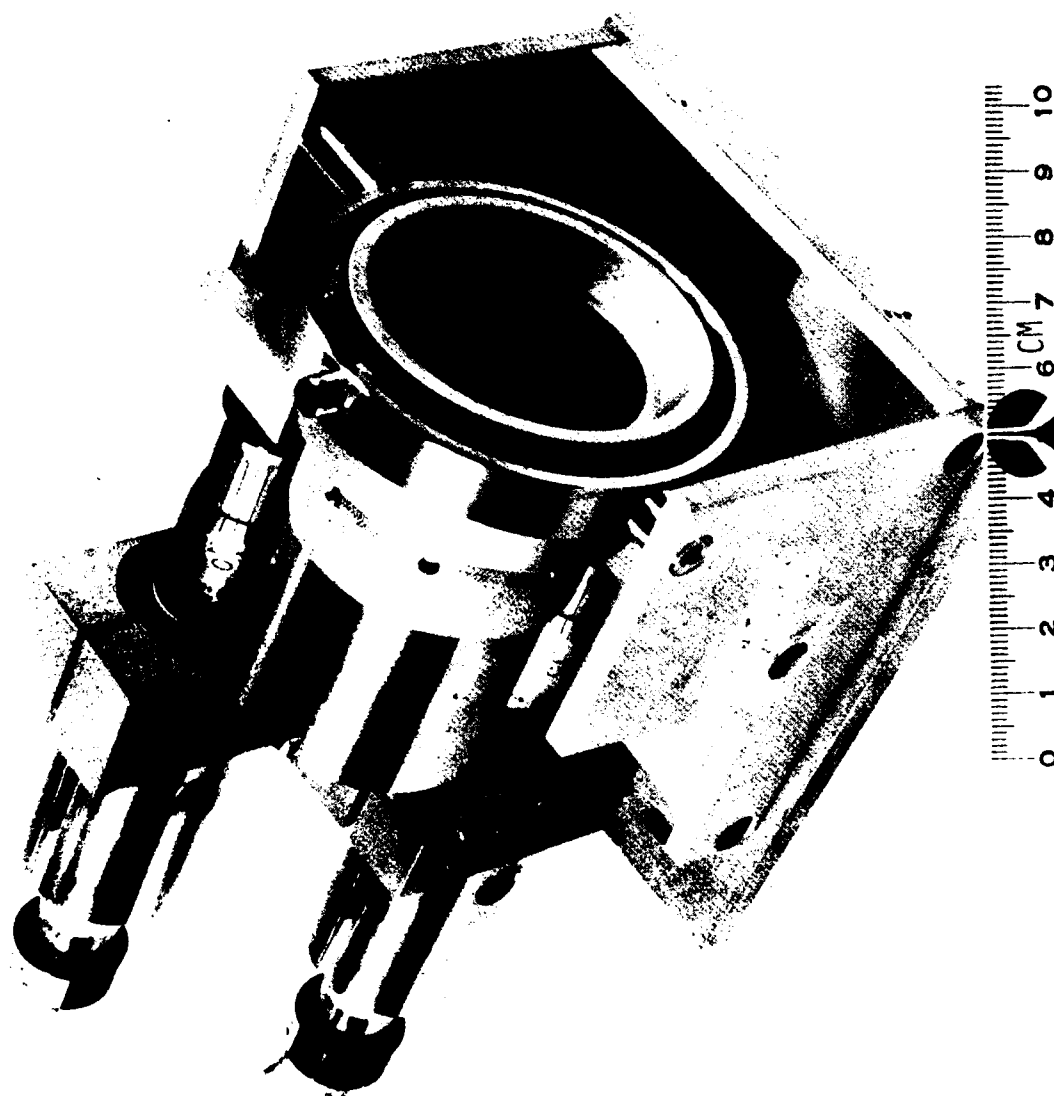
Fig. 23 Photograph of gimbled table with motor-driven differential screws. θ-motion assembly of Fig. 22 mounts in the tube which is attached to the gimbles.
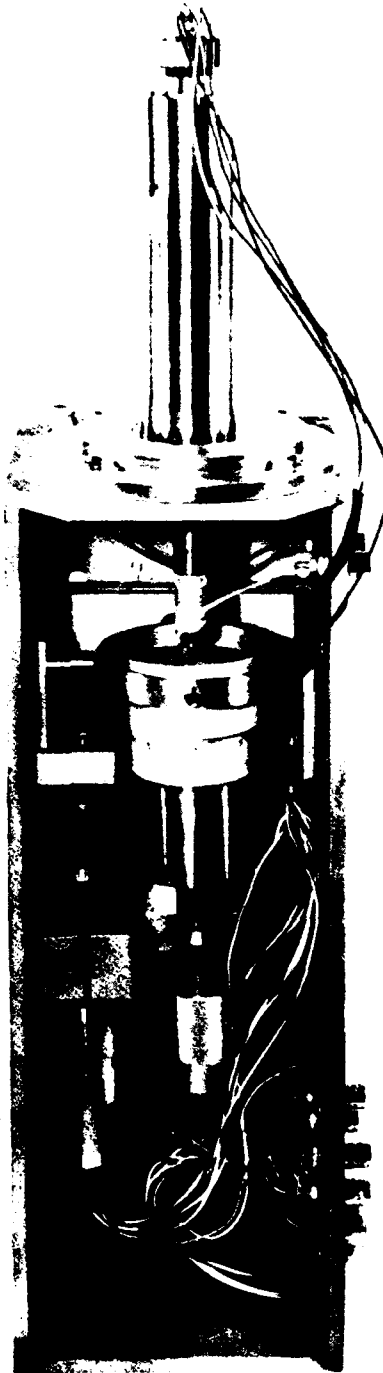
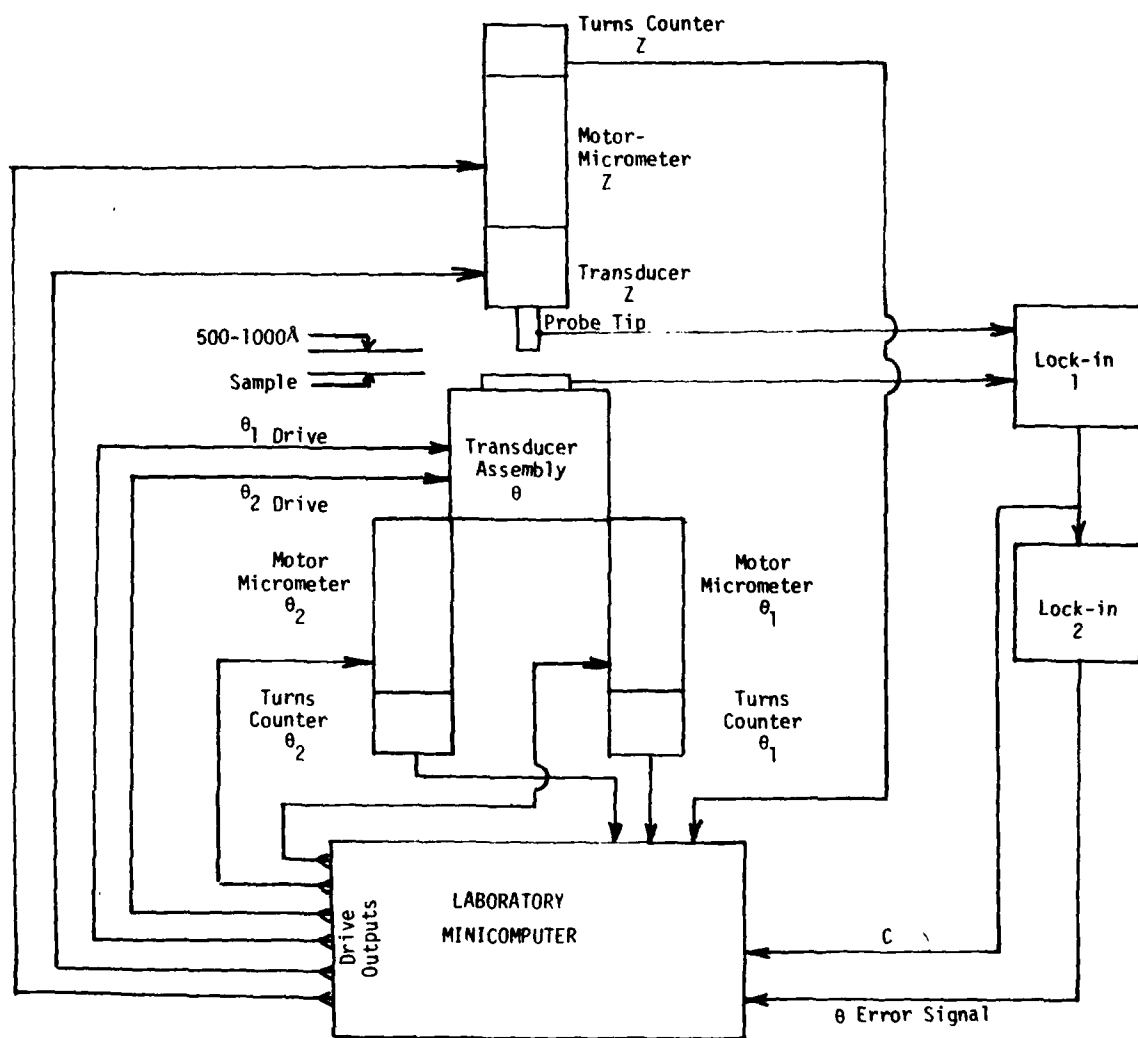Fig. 24 Photograph of assembled contactless C-V apparatus.

Fig. 25 Schematic diagram of contactless C-V apparatus instrumentation.

screw and the θ_1 and θ_2 differential micrometer screws. Feedback to determine micrometer rotation is monitored by turn-counters attached to these motors, whose outputs are read by the computer. The drive for the Z-TA and θ-TA assemblies is a 0-1000 V signal also controlled by the computer. Feedback to measure the effect of Z-TA and θ-TA changes is computer monitored by reading the output of lock-in 1 and lock-in 2, respectively. The Z-TA is designed so a 1 V change in drive corresponds to a 50Å change in d. The θ-TA is designed such that a 1 V change in drive produces a 5×10^{-7} radian change in θ. This alignment sensitivity should be entirely adequate for proper operation of the C-V apparatus.

Probe tips for the C-V apparatus were fabricated. Degenerately doped Si (ρ = 0.004 ohm-cm) slices were sorted for flatness. It is necessary to maintain better than 0.5 µm surface variation per inch to achieve an acceptable probe tip flatness. The silicon wafers used exhibit less than 0.25 µm per inch surface variation in selected areas. Next, mesas were formed by isotropically etching the silicon from the top side; the backside of the wafers is thermally bonded to a glass slide with black wax. Liquified black wax was screened onto the smooth top surface of the wafer through an appropriate metal mask. The mask was lifted off and the wax was allowed to harden. This left a protective pattern of dots on the surface while the backside of the wafer was sealed and protected from the etch. The isotropic silicon etch solution used was nitric, acetic, and hydrofluoric acids ($HNO_3:CH_3OOH:HF$) in the proportions 7:2:1, respectively. This solution provides an etch rate of ~5 µm per minute. The individual mesas were then isolated by wafer sawing and each die was mounted on a metal carrier with either conductive epoxy or preform soldering. A probe tip assembly is shown in Fig. 26.

At the conclusion of this contract the contactless apparatus had been tested in a laboratory bench-top environment. As anticipated the apparatus is very sensitive to vibration. The next development phase of this system would incorporate vibration isolation measures possibly by utilizing a very low resonance spring suspension or an isolation column similar to that used for laser system tables.

78

ERC80-9033

Fig. 26 Photograph of a probe tip fabricated from a highly doped silicon wafer.
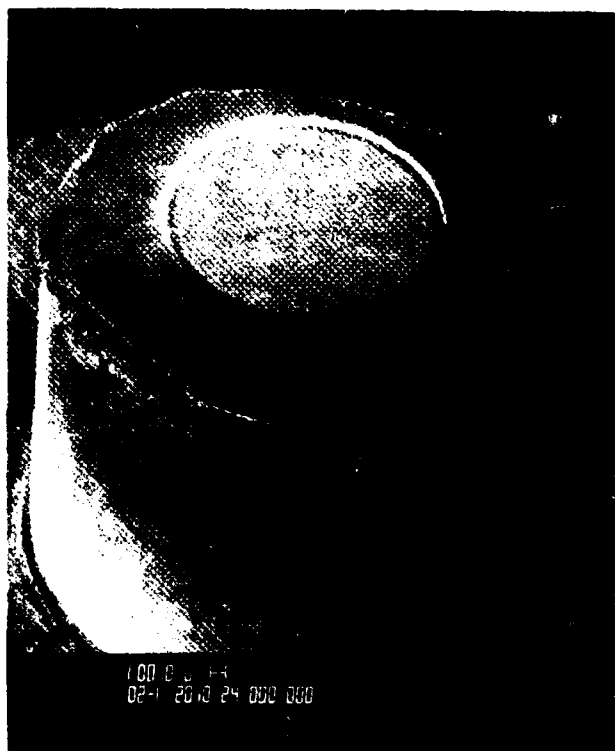
VI. SUMMARY

The surface chemistry and associated surface potential of several
GaAs surfaces has been investigated by XPS. Several surface treatments which
involved oxidation, annealing, gas exposure, chemical processing, and deposi-
tion of materials were studied. The studies primarily involved bulk grown n-
and p-type GaAs samples with both (100) and (110) orientations although a few
samples of VPE grown n-type GaAs (100) were also characterized. No signifi-
cant differences between the bulk grown and VPE grown material were noted.

A primary conclusion is that the interface Fermi-level position,
$\Delta(i)$, can be altered substantially by surface chemistry alteration. The
maximum variation in $\Delta(i)$ was observed for n-type samples and was 0.7 eV. The
relative variation in $\Delta(i)$ is strongly correlated with surface chemistry and
is quite reproducible from sample to sample. For most surface treatments, the
variation in $\Delta(i)$ between n- and p-type samples, subjected to the same surface
treatment as nearly as possible, was highly correlated; an increase in band
bending on an n-type surface corresponded to a decrease in band bending on a
p-type surface and vice versa. The difference in $\Delta(i)$ between the n- and
p-type surfaces remained relatively constant as was ~0.3 eV. Similar results
were obtained for both (100) and (110) oriented samples. An exception to the
highly correlated movement of $\Delta(i)$ on n- and p-type surfaces was provided by
the depositions of a few monolayers of Au (or Pd) onto thermally cleaned sur-
faces. In this case $\Delta(i)$ for both n- and p-type surfaces was observed to be
identical to within experimental error and to be very close to the value
observed in the thermally cleaned p-type surface.

The surface-potential variations observed in this work suggest that
interface states responsible for GaAs Fermi-level pinning may be associated
with multiply charged states of a single defect. The fact that the difference
in $\Delta(i)$ for n- and p-type samples remains nearly constant at ~0.3 eV suggests
that the defect associated levels are shifted in energy by surface treat-
ment. If the same defect is behaving as a donor and acceptor, it must exist

80

in three charge states, positive, neutral, and negative. The energy differ-
ence between the levels associated with a single defect is assumed to arise
from the Coulomb repulsion between two electrons in the same orbital; in Si a
Coulomb shift of ~0.25 eV has been predicted. The behavior of Au (and Pd)
deposited on n-type surfaces suggests that these atoms remove electrons from
neutral defects which makes it possible for the positively charged defects to
acquire electrons and move $\Delta(i)$ to the pinning position observed on the p-type
surface.

Studies associated with the thermal cleaning of GaAs surfaces suggest
a new view of this process. In the temperature range where As_2O_3 is lost from
the surface it is found that little if any oxygen is lost and a substantial
increase in the amount of Ga_2O_3 present on the surface is observed. It is
concluded that a surface chemical reaction $As_2O_3 + 2GaAs \rightarrow Ga_2O_3 + (4/x)As_x\uparrow$,
is associated with the thermal cleaning process rather than the loss of
volatile As oxides from the surface.

REFERENCES

1. K. Siegbahn, et al., ESCA: Atomic, Molecular and Solid State Structure Studied by Means of Electron Spectroscopy, Almquist and Wiksells, Uppsala, 1967.

2. J. Auleytner and O. Hörnfeldt, Arkiv för Fysik 23, 165 (1963).

3. A. Munoz-Yague, J. Piqueras, and N. Fabre, J. Electrochem. Soc. 128, 149 (1981).

4. See for example J. C. Tracy and J. M. Burkstrand, CRC Crit. Rev. Sol. St. Sci. 4, 380 (1973); J. C. Tracy, J. Vac. Sci. Technol. 11, 280 (1974); C. R. Brundle, J. Vac. Sci. Technol. 11, 212 (1974); I. Lindau and W. E. Spicer, J. Electron. Spect. 3, 409 (1974).

5. E. A. Kraut, R. W. Grant, J. R. Waldrop, and S. P. Kowalczyk, Phys. Rev. Lett. 44, 1620 (1980).

6. F. R. McFeely, S. P. Kowalczyk, L. Ley, R. A. Pollak, and D. A. Shirley, Phys. Rev. B7, 5228 (1973).

7. S. P. Kowalczyk, J. R. Waldrop, and R. W. Grant, J. Vac. Sci. Technol. (in press).

8. G. Margaritondo, L. J. Brillson, and N. G. Stoffel, Solid State Comms. 35, 277 (1980).

9. G. Leonhardt, A. Berndtsson, J. Hedman, M. Klasson, R. Nilsson, and C. Nordling, Phys. Stat. Sol. (b) 60, 241 (1973).

10. S. M. Sze, Physics of Semiconductor Devices, Wiley-Interscience, New York (1969), pp. 37.

11. P. Pianetta, I. Lindau, C. M. Garner, and W. E. Spicer, Phys. Rev. Lett. 37, 1166 (1976).

12. C. W. Wilmsen, R. W. Kee, and K. M. Geib, J. Vac. Sci. Technol. 16, 1434 (1979).

13. G. P. Schwartz, B. Schwartz, D. DiStefano, G. J. Gualtieri, and J. E. Griffiths, Appl. Phys. Lett. 34, 205 (1979).

14. C. D. Thurmond, G. P. Schwartz, G. W. Kammlott and B. Schwartz, J. Electrochem. Soc. 127, 1366 (1980).

15. J. A. Cape, W. E. Tennant, and L. G. Hale, J. Vac. Sci. Technol. $\underline{14}$, 921 (1977).

16. R. L. Farrow, R. K. Chang, S. Mroczkowski, and F. H. Pollack, Appl. Phys. Lett. $\underline{31}$, 768 (1977).

17. R. P. H. Chang, T. T. Sheng, C. C. Chang, and J. J. Coleman, Appl. Phys. Lett. $\underline{33}$, 341 (1978).

18. D. W. Langer, F. L. Schuermeyer, R. L. Johnson, H. P. Singh, C. W. Litton, and H. L. Hartnagel, J. Vac. Sci. Technol. $\underline{17}$, 964 (1980).

19. J. R. Waldrop and R. W. Grant, Phys. Rev. Lett. $\underline{43}$, 1686 (1979).

20. W. T. Tsang, M. Olmstead, and R. P. H. Chang, Appl. Phys. Lett. $\underline{34}$, 408 (1979).

21. P. Pianetta, I. Lindau, C. M. Garner, and W. E. Spicer, Phys. Rev. Lett. $\underline{37}$, 1166 (1976).

22. W. E. Spicer, I. Lindau, P. Skeath and C. Y. Su, J. Vac. Sci. Technol. $\underline{17}$, 1019 (1980) and references therein.

23. M. S. Daw and D. L. Smith, J. Vac. Sci. Technol. $\underline{17}$, 1028 (1980).

24. G. A. Baraff, E. O. Kane and M. Schluter, Phys. Rev. B $\underline{21}$, 5662 (1980).

25. F. S. Shishiyanu and B. I. Boltaks, Soviet Phys. - Solid State Vol. $\underline{8}$, 1053 (1966).

APPENDIX

Two papers were published based on work supported by this contract. These papers which are reproduced in this appendix are:

1). "XPS Study of GaAs (100) Surface Oxide Chemistry and Interface Potential" in the Physics of MOS Insulators, edited by G. Lucovsky, S.T. Pantelides, and F.L. Galeener, Pergamon Press, New York, 1980, (a talk on this subject was presented at the Physics of MOS Insulators Conference, June 18-20, 1980, North Carolina State University, Raleigh, N.C.), and

2). "Correlation of GaAs Surface Chemistry and Interface Fermi-Level Position: A Single Defect Model Interpretation", J. Vac. Sci. Technol., Sept./Oct. 1981 issue (in press), (a talk on this subject was presented at the Eighth Annual Physics of Compound Semiconductor Interfaces Conference, January 27-29, 1981, Williamsburg, Va.)

XPS STUDY OF GaAs(100) SURFACE OXIDE CHEMISTRY AND INTERFACE POTENTIAL

R. W. Grant, S. P. Kowalczyk, J. R. Waldrop, and W. A. Hill
Rockwell International Electronics Research Center
Thousand Oaks, California, 91360

Considerable research effort has been expended in recent years searching for a successful GaAs MOS technology. Although promising capacitance-voltage results have been recently reported (1-3), the methods used have, for the most part, relied on technologically complex processing procedures (e.g., molecular beam epitaxy) to obtain the insulator-GaAs interface. It is also noteworthy that the results to date for GaAs MOSFET structures have not been very encouraging. We report experiments in which x-ray photoemission spectroscopy (XPS) has been used to correlate chemistry, electrical potential, and charge at the native-oxide/GaAs interface (n-type material) as a function of various processing treatments. Our results indicate that the lowest interface charge is obtained for the Ga_2O_3/GaAs interface and that the prospect of a MOS structure involving native oxides should not yet be ruled out.

It is well known that x-ray photoemission spectroscopy (XPS) can be used to determine the surface chemistry of a solid sample (4). A much less utilized aspect of the XPS technique is the measurement of surface (or band-bending) potential, V_{BB}, of a semiconductor sample (5). This measurement is illustrated in Fig. 1; a flat-band condition has $V_{BB} = 0$. All binding energies are referenced to the Fermi level, E_F. The conduction-band minimum is E_c, the valence-band maximum is E_v, the core-level binding energy is E_{cl}, $\Delta = E_F - E_v$, W is the depletion width and q is the electronic charge.
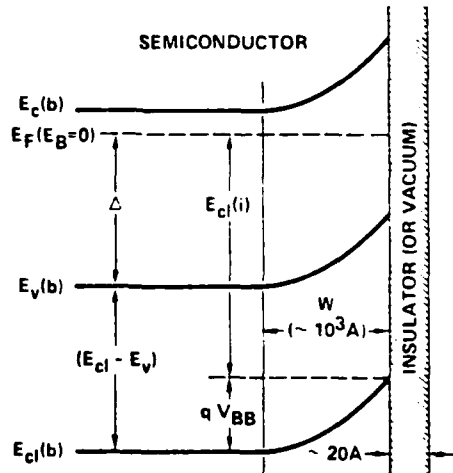

Fig. 1. Schematic energy-band diagram which illustrates the XPS measurement of band bending.

The (b) and (i) notations refer to bulk- and interface-quantities, respectively.
A HP5950A XPS spectrometer which utilizes AlKα radiation (1486.6 eV) was used for
the measurements. The most energetic photoelectrons analyzed in these measure-
ments have escape depths of about 25Å. Thus, if only a thin insulating layer of
$\approx$20Å is present on a semiconductor surface, unscattered photoelectrons from the
underlying semiconductor will be observed and $E_{cl}(i)$ can be determined. For
moderately doped semiconductors ($\leq 10^{17}$cm^{-3}), W$\approx$10^{3}Å and thus band bending will not
complicate the $E_{cl}(i)$ measurement. From Fig. 1 it is seen that

$$qV_{BB} = \Delta + (E_{cl} - E_v) - E_{cl}(i). \tag{1}$$

A knowledge of the semiconductor bulk doping characteristics determines Δ, (E_{cl} -
E_v) can be obtained from XPS measurements. For GaAs, a precise value of

$$E_{As3d}^{GaAs} - E_v^{GaAs} = 40.73 \pm 0.02 \text{ eV}$$

has been recently reported (6).

Changes in surface chemistry during thermal treatment of a chemically etched GaAs
(100) surface were monitored by XPS. The "initial" surface was prepared by etch-
ing in a (4:1:1) H_2SO_4:H_2O_2:H_2O solution. The sample (n-type, $\approx$1x10^{17}cm^{-3}) was
attached to a Mo plate by using In (this involved heating in air to $\approx$160°C) and
was inserted into the XPS spectrometer within a few minutes. Within the XPS system
the relative sample temperature was measured by a thermocouple attached to the
sample heater (in all cases the stated temperature is, therefore, considerably
higher than the actual sample surface temperature, by as much as $\approx$20%). The sample
was heated for five minutes at a specific temperature followed by cooling to $\approx$30°C
for the XPS analysis. Each successive anneal was to a higher temperature; vacuum
during annealing was $\approx$10^{-9} torr. The small amount of initial C surface contamina-
tion became undetectable above $\approx$300°C and O was removed from the surface at $\approx$677°C.
The initial surface exhibited oxidized forms of both As and Ga (upper part of Fig.
2). The chemical shift of the As3d level in As oxide relative to GaAs ($\Delta E_B \approx$3.2 eV)
and of the Ga3d level in Ga oxide relative to GaAs ($\Delta E_B \approx$0.95 eV) suggests that the
oxides are primarily As_2O_3 and Ga_2O_3 (7). The lower part of Fig. 2 shows the same
spectral region after the sample was heated to 650°C. The As_2O_3 has clearly been
removed from the sample surface, however the shoulder on the high binding-energy
side of Ga3d line (which corresponds to Ga_2O_3) has clearly increased in intensity.
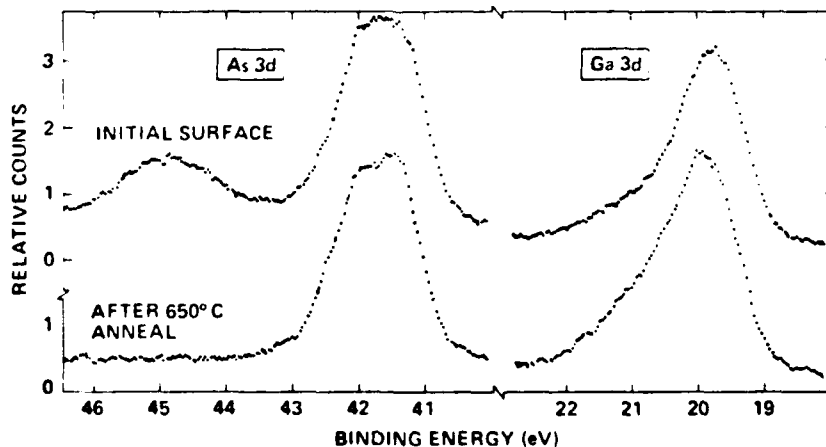

Fig. 2. XPS spectra in the region of the As3d and Ga3d levels. Sample
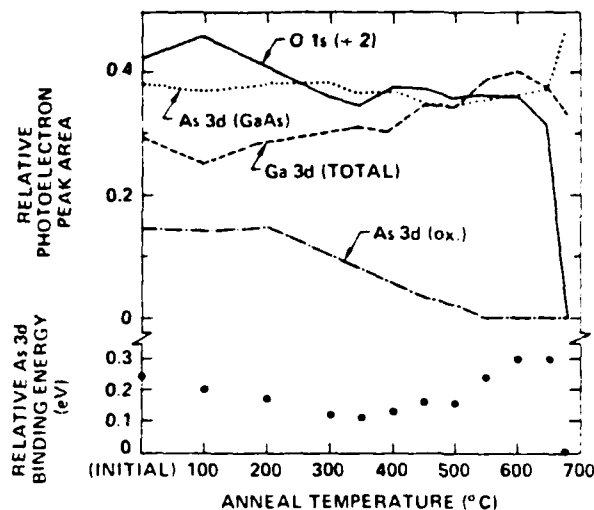is described in text.

Fig. 3. Relative photoelectron peak areas and As3d
binding energy vs. annealing temperature.
Sample described in text.

In Fig. 3 the relative XPS
peak areas above background
are plotted as a function
of annealing temperature.
The oxidized As, labeled
As3d (ox.), decreases slowly
to zero between ≈300 and
550°C. The O 1s line inten-
sity decreases until ≈300°C;
however, in the temperature
range where the oxidized As
is removed from the surface,
the O 1s line intensity is
essentially constant. Also
shown in Fig. 3 are the peak
areas associated with As3d
in GaAs and the total Ga3d
peak area (oxidized Ga + Ga
in GaAs). The As3d(GaAs)
remains relatively constant
up to ≈650°C while Ga3d
(total) is observed to in-
crease significantly in the
300 to 550°C temperature
range. These results suggest
a new view of the surface
chemistry associated with
thermally cleaning a GaAs

surface. It is usually assumed (see e.g., ref. 8) that As oxides are initially
removed from the surface due to the high volatility of these compounds. The XPS
results of Figs. 2 and 3 show that As is lost from the surface as elemental As
(presumably As2 or As4) and in the process additional Ga_2O_3 is formed. We conclude
that a surface chemical reaction

$$As_2O_3 + 2GaAs \rightarrow Ga_2O_3 + \frac{4}{x} As_x\uparrow \qquad (2)$$
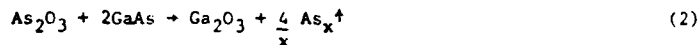
is associated with the removal of As_2O_3 from the GaAs(100) in the 300–550°C temp-
erature range. Additional GaAs is consumed in this process. This same thermally
induced solid-state reaction has been proposed (9) to explain the formation of
elemental As at interfaces between GaAs and relatively thick (~10Å³) anodic oxides.
Interfaces prepared at room temperature which do not initially exhibit elemental As
are observed to form elemental As rapidly at 450°C (9), which, due to the thickness
of the oxide, remains trapped at the interface. Recent condensed phase diagram
calculations (10) have also shown that only elemental As and Ga_2O_3 can exist in
thermodynamic equilibrium with GaAs, consistent with Eq. (2).

There has been considerable recent interest in the electrical effect of the ele-
mental As detected at the thermally annealed native-oxide/GaAs interface (11, 12).
These elemental As atoms may be a major source of interface traps and thus play a
significant role in determining the GaAs MOS characteristics (13). For GaAs MOS
applications, it is important to reduce the interface charge and interface state
density. As mentioned above, XPS can be used to determine V_{BB} and thus the net
interface charge, Q_s. In the lower part of Fig. 3, the E_B for the As3d core level
relative to the thermally cleaned surface, δE_B, is shown (we also define δV_{BB} as
the change in V_{BB} relative to the thermally cleaned surface, $\delta E_B = -\delta V_{BB}$). As the
surface contamination associated with C and O is removed at temperatures below
≈300°C, δE_B is observed to decrease by ≈0.15 eV, which indicates an increase in
V_{BB} and a corresponding larger net negative Q_s. However, in the temperature range
where As is lost from the surface, which is associated with additional Ga_2O_3

87

formation and consumption of GaAs, δE_B increases by ≈ 0.2 eV (V_{BB} decreases by ≈ 0.2 eV) and the net negative Q_S decreases. This behavior is caused by a change in the interface-state density with the possibility that acceptor states are being removed from the interface during the Ga_2O_3 formation process. A marked decrease in δE_B is again observed when the sample temperature is raised high enough to clean the surface (Fig. 3).

In the Table, surface-potential variations for several surface treatments are presented for two additional series of experiments. Both samples were from the same GaAs boule and the initial surface preparation was the same as for the sample discussed previously. The E_{As3d}^{GaAs} scale for sample #1 was established by the evaporation of a thick Au layer onto the sample at the conclusion of the experiment and indexing the observed XPS peak position of the $Au4f_{7/2}$ line to 84.00 ± 0.01 eV (14).

GaAs(100) Surface Potential Variation With Surface Treatment

Sample #	Treatment	E_{As3d}^{GaAs} (eV)	δV_{BB}* (eV)	Remarks
1	500°C; Vacuum 2 days at 25°C	41.95	−0.50	Ga_2O_3
	688°C; 6×10^4L O_2 at 610°C	41.71	−0.26	Ga_2O_3
	695°C	41.45	0.00	Clean, LEED
2	700°C	-----	0.00	Clean, LEED
	6×10^3L H_2O at 25°C	-----	0.00	
	680°C	-----	−0.02	Clean
	6×10^4L O_2 at 600°C	-----	−0.23	Ga_2O_3
	10^5L H_2O at 38°C	-----	−0.44	
	600°C	-----	−0.22	
	10^4L H_2O at 39°C	-----	−0.41	

*$\delta V_{BB} = -\delta E_B$

For sample #1, the initial chemically etched surface was heated to 500°C followed by storage in vacuum for two days at 25°C; this procedure produced a very high E_{As3d}^{GaAs}, and low V_{BB}. Subsequent thermal surface cleaning to obtain a surface with no detectable O or C as determined by XPS and which exhibited a characteristic LEED (low energy electron diffraction) pattern, followed by reoxidation at 610°C to form Ga_2O_3, did not immediately produce a low surface potential. In several experiments, we have observed that room temperature vacuum storage ($\sim 10^{-9}$ torr) for a period of 1-2 days markedly reduced V_{BB} on n-type GaAs(100). A possible explanation is provided by the experiments reported on sample #2 in the Table. An initially clean surface was exposed to H_2O vapor at 25°C; no change in δE_B was observed. This surface was thermally recleaned and oxidized to form Ga_2O_3. A change in δE_B similar to that observed for sample #1 was observed. Subsequent exposure of this surface to small amounts of H_2O vapor for ~1 hour resulted in large values of δE_B similar to that observed in sample #1. Any alteration of the surface chemistry as a result of the H_2O vapor exposure was below detectable limits of the XPS analysis. Because H_2O vapor is a residual gas component of the ion pumped XPS system, exposure to H_2O vapor may offer an explanation for the variation in E_B with the room
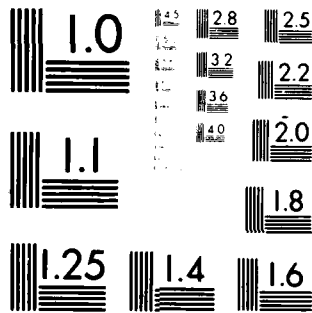
MICROCOPY RESOLUTION TEST CHART

NATIONAL BUREAU OF STANDARDS 1963 A

temperature vacuum storage noted above.

The net interface charge can be calculated by using Eqs. 1 and 3. From the Table, the surface of sample #1 (which was annealed at 500°C and stored in vacuum for 2 days) exhibited E_{As3d}^{GaAs} = 41.95 eV. XPS analysis of this surface showed only Ga_2O_3 (in addition to the GaAs), no oxidized As was observed. For a donor density of $N_D \approx 10^{17} cm^{-3}$, $\Delta \approx 1.39$ eV and thus V_{BB} = 0.17 eV. Q_S can be calculated from (15)

$$Q_s = (2 q \epsilon N_D |V_{BB}|)^{\frac{1}{2}} \tag{3}$$

where ϵ is the permitivity of GaAs. Q_S is found to be $0.8 \times 10^{-7} coul/cm^2 (\approx 5 \times 10^{11}$ electrons/cm²).

The results presented here suggest the possibility of forming a useful GaAs/oxide interface by heat treating a native oxide of moderate thickness (≤ 100Å). If this oxide is annealed in the 500-600°C range, it may be possible to form pure Ga_2O_3, evaporate the elemental As which is formed, and produce a new GaAs interface by consuming additional GaAs during the process. Our observations show that this process reduces Q_S (and hopefully the interface-state density). A MOS structure would be formed by subsequent deposition of a good quality dielectric.

References

1. W. T. Tsang, M. Olmstead and R. P. H. Chang, Appl. Phys. Lett. 34, 408 (1979).
2. R. P. H. Chang and J. J. Coleman, Appl. Phys. Lett. 32, 332 (1978).
3. D. W. Langer, F. L. Schuermeyer, R. L. Johnson, H. P. Singh, C. W. Litton, and H. L. Hartnagel, Physics of Compound Semiconductor Interfaces Conference, Estes Park, Colorado, Jan. 29-31, 1980.
4. K. Siegbahn, et al., ESCA: Atomic, Molecular and Solid State Structure Studied by Means of Electron Spectroscopy, Almquist and Wiksells, Uppsala, 1967.
5. J. Auleytner and O. Hornfeldt, Arkiv för Fysik 23, 165 (1963).
6. E. A. Kraut, R. W. Grant, J. R. Waldrop, and S. P. Kowalczyk, Phys. Rev. Lett., June, 1980 (In Press).
7. P. W. Chye, P. Pianetta, I. Lindau, and W. E. Spicer, J. Vac. Sci. Technol. 14, 917 (1977).
8. C. W. Wilmsen, R. W. Kee, and K. M. Geib, J. Vac. Sci. Technol. 16, 1434 (1979).
9. G. P. Schwartz, B. Schwartz, D. DiStefano, G. J. Gualtieri, and J. E. Griffiths, Appl. Phys. Lett. 34, 205 (1979).
10. G. P. Schwartz, C. D. Thurmond, G. W. Kammlott, and B. Schwartz, Physics of Compound Semiconductor Interfaces Conference, Estes Park, Colorado, Jan. 29-31, 1980.
11. J. A. Cape, W. E. Tennant, and L. G. Hale, J. Vac. Sci. Technol. 14, 921 (1977).
12. R. L. Farrow, R. K. Chang, S. Mroczkowski, and F. H. Pollack, Appl. Phys. Lett. 31, 768 (1977).
13. R. P. H. Chang, T. T. Sheng, C. C. Chang, and J. J. Coleman, Appl. Phys. Lett. 33, 341 (1978).
14. F. R. McFeely, S. P. Kowalczyk, L. Ley, R. A. Pollak, and D. A. Shirley, Phys. Rev. B, 7, 5228 (1973).
15. A. S. Grove, Physics and Technology of Semiconductor Devices, (John Wiley and Sons, Inc., New York, 1967), p. 266.

CORRELATION OF GaAs SURFACE CHEMISTRY AND INTERFACE FERMI-LEVEL POSITION: A SINGLE DEFECT MODEL INTERPRETATION

R.W. Grant, J.R. Waldrop, Steven P. Kowalczyk and E.A. Kraut
Rockwell International
Microelectronics Research and Development Center
Thousand Oaks, CA 91360

ABSTRACT

XPS measurements of core-level binding energies have been used to determine the interface Fermi-level position in (100) and (110) n- and p-type GaAs samples as a function of surface treatment. A variation in interface Fermi-level position of up to 0.7 eV has been observed. The difference in interface Fermi-level position for n- and p-type samples subjected to identical surface treatments remains nearly constant at ≈ 0.3 eV. A single defect model (SDM) is suggested which appears to provide the simplest explanation for the observed interface-potential variations.

I. INTRODUCTION

A generally useful insulator for a GaAs MIS device technology has yet to be developed. The tendency for GaAs-insulator interfaces to exhibit large interface state densities appears to be a major obstacle to achieving inversion or accumulation characteristics suitable for device applications. Recent work[1] has suggested that characteristic GaAs defects (associated with Ga and As vacancies) situated near an oxide-or metal-GaAs interface may be responsible for large mid-gap interface state densities. The present X-ray photoemission spectroscopy (XPS) experiments were undertaken to study the relationship between interface chemistry and Fermi-level position, $\Delta(i)$, with a goal of learning how to adjust and control interface state densities.

We have measured $\Delta(i)$ as a function of several surface treatments for (100) and (110) n- and p-type GaAs samples. A variation in $\Delta(i)$ of up to 0.7 eV has been observed. For n- and p-type samples subjected to identical treatments, the difference in $\Delta(i)$ is nearly constant at ≈ 0.3 eV. It is suggested that a single defect model (SDM) with multiple charge states of the type proposed by Daw and Smith[2] offers the simplest explanation for the experimental observations.

II. EXPERIMENTAL

The use of XPS for interface Fermi-level position measurements has been discussed elsewhere[3],[4], only a brief summary is given here. Fig. 1 shows a schematic energy-band diagram for n-type GaAs with a thin insulator or metal overlayer which has resulted in interface band bending. All binding energies, E_B, are referenced to the Fermi-level (E_F). The conduction-band minimum is E_c^{GaAs}, the valence-band maximum is E_v^{GaAs}, the As3d core-level binding energy is E_{As3d}^{GaAs}, the Fermi-level position relative to E_v^{GaAs} is Δ, W is the depletion width and q is the electronic charge. The (b) and (i) notations refer to bulk- and interface-quantities, respectively. For a flat-band condition $\Delta(b) = \Delta(i)$. The GaAs bulk doping characteristics determine $\Delta(b)$.

A Hewlett-Packard 5950A XPS spectrometer which utilizes monochromatic AlKα radiation (1486.6 eV) was used for the measurements. The spectrometer has an ultra high vacuum sample preparation chamber and the base pressure of the instrument was $\approx 1 \times 10^{-10}$ torr. The As3d- and Ga3d-photoelectrons analyzed in our experiments have escape depths of about 25Å. If only a thin layer of material (thickness comparable to the escape depth) is present on the GaAs surface, unscattered photoelectrons from the underlying GaAs will be observed. The $\approx$ 25Å escape depths of the As3d- and Ga3d-photoelectrons from the GaAs minimize any possible surface chemical-shift effects on the observed core-level binding energies of these photoelectrons. The binding energies of the As3d- and Ga3d-core levels associated with GaAs change by the same amount due to band bending in the GaAs. The As3d line will be used to monitor $\Delta(i)$ because when a surface oxide is present, the As3d binding energy in GaAs is well resolved from the As3d binding energy in the oxide. For moderately doped semiconductors ($\lesssim 10^{17}$ cm^{-3}), W $\approx 10^3$Å and thus band bending will not affect the $E_{As3d}^{GaAs}(i)$ measurements. From Fig. 1 it is seen that

$$\Delta(i) = E_{As3d}^{GaAs}(i) - (E_{As3d}^{GaAs} - E_v^{GaAs}) \ . \tag{1}$$

The term $(E_{As3d}^{GaAs} - E_v^{GaAs})$ is obtained from independent XPS measurements on clean GaAs surfaces and a precise value of

$$E_{As3d}^{GaAs} - E_v^{GaAs} = 40.73 \pm 0.02 \text{ eV} \qquad (2)$$

has been recently reported[4]. It is clear from Eq. 1 that a change in $\Delta(i)$ is equal to the change in $E_{As3d}^{GaAs}(i)$.

Figure. 2 shows an example of a direct observation of a $\Delta(i)$ variation. The As3d core level in n-GaAs (100) for a sample which was thermally cleaned at $\approx 570°C$ in vacuum ($\approx 10^{-9}$torr), oxidized at $\approx 460°C$ by exposure to 2×10^4 L of O_2 to form a Ga_2O_3-GaAs interface[3], and was subsequently stored in vacuum ($\approx 10^{-9}$ torr) at room temperature for 16 hours, is shown in Fig. 2a. This same sample was then thermally cleaned by heating in vacuum ($\approx 10^{-9}$ torr) at $\approx 570°C$ and a few monolayers of Au were evaporated (at $< 8 \times 10^{-9}$ torr) onto the room temperature sample surface (Fig. 2b). The vertical lines in the figure indicate the center of the peak width at half peak height. The large variation (0.7 eV) in $E_{As3d}^{GaAs}(i)$ and thus $\Delta(i)$ is obvious from the figure.

The GaAs samples were bulk grown with n- and p-type doping densities of about 1×10^{17} and 2×10^{16}cm^{-3}, respectively[5]. The samples were cut and polished to obtain (100) and (110) orientations, then etched in a freshly prepared (4:1:1) H_2SO_4:H_2O_2:H_2O solution to remove polishing damage. Freshly etched n- and p-samples with the same crystallographic orientation were mounted on a single Mo plate by using In (this involved heating in air to $\approx 160°C$) and inserted into the XPS spectrometer within a few minutes. The sample temperature was measured by a thermocouple attached to the sample heater (the measured temperatures have been reduced by 20% as an approximate correction for the temperature drop between the thermocouple and sample surface). To calibrate the E_B scale,

a thick Au layer was evaporated onto the sample (at the conclusion of an experiment) and the observed As3d peak positions were indexed to $E_{Au4f_{7/2}}^{Au}$ = 84.00 ± 0.01 eV[6]. The As3d core level binding energies at the interface, $E_{As3d}^{GaAs}(i)$, reported here are accurate to ± 0.05 eV.

Two different types of oxide surfaces were studied in the present work. The first surface was formed by an initial $(4:1:1)H_2SO_4:H_2O_2:H_2O$ chemical etch followed by heating in air to ≈ 160°C. This surface is covered by several monolayers of oxidized Ga and As; the chemical shifts of these surface species suggest that this layer consists primarily of As_2O_3 and Ga_2O_3 (see discussion in Ref. 3). The second type of oxide surface was produced by two methods. The As_2O_3 can be removed from the chemically etched surface to produce a Ga_2O_3-GaAs interface via the surface chemical reaction[3]

$$As_2O_3 + 2GaAs \rightarrow Ga_2O_3 + \frac{4}{x} As_x \uparrow. \tag{3}$$
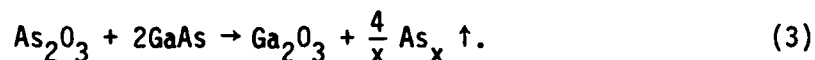
We have observed that As_2O_3 is completely removed from both the (100) and (110) surfaces for annealing temperatures of ≈ 475°C although at a 370°C annealing temperature Su et al[7] report that a small residual amount of As_2O_3 remains on the (110) surface. The Ga_2O_3-GaAs interface was also produced by exposing a thermally cleaned surface to O_2 at ≈ 450°C. All oxides can be removed from the sample surfaces by annealing at ≈ 550°C. Some caution must be exercised to avoid excessive heating, which will cause Ga deposits to form on the surface, but with care reasonably sharp characteristic LEED patterns of the surfaces were obtained.

III RESULTS

Several measurements of $\Delta(i)$ for various surface treatments are summarized in Figs. 3 and 4 for (100) and (110) surfaces respectively. After the initial chemical etch, the surface treatments were carried out sequentially in the XPS sample preparation chamber and the results are shown in Figs. 3 and 4.[8] XPS measurements were performed with the samples at room temperature and in vacuum ($< 10^{-9}$ torr) after each surface treatment. The results indicate that $\Delta(i)$ can be substantially altered by changes in surface chemistry. The Ga_2O_3-GaAs interface on n-type GaAs (100) produces the largest $\Delta(i)$ that we have observed. This large $\Delta(i)$ is obtained only after storing samples in vacuum ($\approx 10^{-9}$ torr) for ≈ 1 day and may be the result of exposure to H_2O vapor from the residual gas[3]. The same large $\Delta(i)$ can be obtained with samples which are either prepared by the surface chemical reaction (Eq. 3) or by oxidizing a thermally cleaned surface in O_2 at $\approx 450°C$. Measurements carried out during the vacuum storage interval indicate that $\Delta(i)$ monotonically shifts from the position observed shortly after preparation of the Ga_2O_3-GaAs interface to the final $\Delta(i)$ shown in Figs. 3 and 4 during a time period of many hours.

The variation in $\Delta(i)$ with surface treatments similar to those described in Figs. 3 and 4 and the nearly constant difference in $\Delta(i)$ observed on the n- and p-type surfaces were reproduced with many (10-15) different samples. The absolute values of $\Delta(i)$ were determined for a much smaller set of samples.   For three n-type (100) and two n-type (110) samples, the average $\Delta(i)$ for the thermally cleaned surfaces was 0.69 eV (0.15 eV range of values) and 0.67 (0.02 eV range of values), respectively. A comparison of $\Delta(i)$ values for the (100) and (110) samples shown in Figs. 3 and 4 indicates that the (110) values are systematically lower by ≈ 0.1 eV however without further work, the significance of this result cannot be evaluated.

IV DISCUSSION

Spicer et al[1] have proposed a universal pair of pinning levels
which in GaAs arise from Ga and As vacancies. In their unified defect
model (UDM), they suggest that these vacancies produce characteristic
donor and acceptor levels at 0.5 and 0.75 eV (relative to E_v^{GaAs}),
respectively. This model was based partly on the observation that the
$\Delta(i)$ are independent of surface treatment for a specific doping type.
Our experimental results agree with Ref. 1 for similar surface conditions
but for treatments associated with the Ga_2O_3-GaAs interface, we observe
different $\Delta(i)$. This seems to unambiguously require a modification
of the UDM.

The fact that the difference between n-type and p-type $\Delta(i)$
remains nearly constant, although the average varies, suggests that the
same defect may be involved throughout with levels shifted by the
surface treatment. Otherwise it would have to be assumed that not only
did the high temperature oxidation followed by vacuum storage add new
defects but that this process also removed the old ones (a new empty
level above the one which had pinned the n-type material would not
increase $\Delta(i)$ if the original level is still present). Furthermore,
it would have to be assumed that the added levels for the n-type and
p-type samples differed in energy by about the same amount as the original
levels. This would require a fortuitous coincidence if two different
defects were involved for both n-type and p-type material. It would even
seem to be a coincidence if one defect which produced n-type and p-type
pinning were replaced by a single different defect which produced n-type
and p-type pinning. It is therefore suggested that the observed highly

correlated movement of $\Delta(i)$ on the n- and p-GaAs surfaces is the result of a single defect (such as an As vacancy[2]) which is responsible for all of the pinning levels and that the defect is affected by surface treatment. Thus, the high temperature oxidation treatment reported here may shift the energy levels associated with the defect by changing the local defect environment.

If the same defect is behaving as a donor and acceptor, it must exist in three charge states, either positive, neutral, or negative[2]. We may then associate an electron level with the addition of the first electron (+/0) and a higher level with the addition of the second (0/-). The energy difference in such levels is customarily called U and is assumed to arise from the Coulomb repulsion between two electrons in the same orbital. The differences in $\Delta(i)$ observed for GaAs are in fact on the order of a typical Coulomb shift; Baraff et al[9] predict a Coulomb U of $\simeq 0.25$ eV for the Si vacancy. The defect in GaAs cannot be a negative U center as is the vacancy in Si because for a negative U center the neutral state would be unstable. This would lead to a single $\Delta(i)$ for both n- and p-type GaAs since there is only a single energy level at which an electron is added or removed.

In n-type material, we assume that enough defects are in the negative charge state to produce the band bending necessary to pin $\Delta(i)$ at the (0/-) level; in p-type material enough defects are in the positive charge state to pin $\Delta(i)$ at the (+/0) level. Since (0/-) and (+/0) levels originate from the same defect, the number of each of these levels is of course equal on a particular surface.

The n- and p-GaAs surfaces on which several monolayers of Au were evaporated seem to be an anomaly. On these surfaces both n-type and

97

p-type specimens have the same $\Delta(i)$ which is, within experimental error, the same as the $\Delta(i)$ observed on the thermally cleaned p-type surface. This suggests that the gold atoms have taken electrons from the neutral defects to produce positive defects and compensating negatively charged gold centers. This process in itself does not change $\Delta(i)$, but the positively charged defects can now take on electrons in n-type material which moves $\Delta(i)$ to the (+/0) level, in agreement with experiment. The fact that a heavy coverage of gold is required to accomplish this suggests that only a small fraction of the gold atoms are active (less than the number of defects, but enough to increase the band bending to the (+/0) level), perhaps those which enter the specimen interstitially. Previous experimental work has indicated that Au can form shallow acceptor levels in GaAs and cause n to p conversion[10].

The model discussed above of single defects near or at a GaAs surface is compatible with a slight difference in $\Delta(i)$ between crystallographic faces for the same surface treatment. Thus, a single defect model (SDM) of Fermi-level pinning in GaAs accounts in a natural way for all of our experimental data and we believe, all of the data in Ref. 1. It is probably the simplest model which will accomplish this, but it is not conclusively proven. Furthermore, our results give no indication as to what the defect may be although an As vacancy would seem to be a reasonable possibility.

The model proposed here could have important implications for interface-state density control. It suggests that by means of surface treatments it may be possible to adjust $\Delta(i)$ within some interval. However, the observation that the interface-potential difference between a pair of n- and p-type samples remains nearly constant at ≈ 0.3 eV suggests that

the interface-state density may be rather large despite a surface treatment that minimizes band bending on one or the other sample. This is because the minimum density of defects in the SDM is that required to trap the charge associated with the surface which has the largest band bending of the pair.
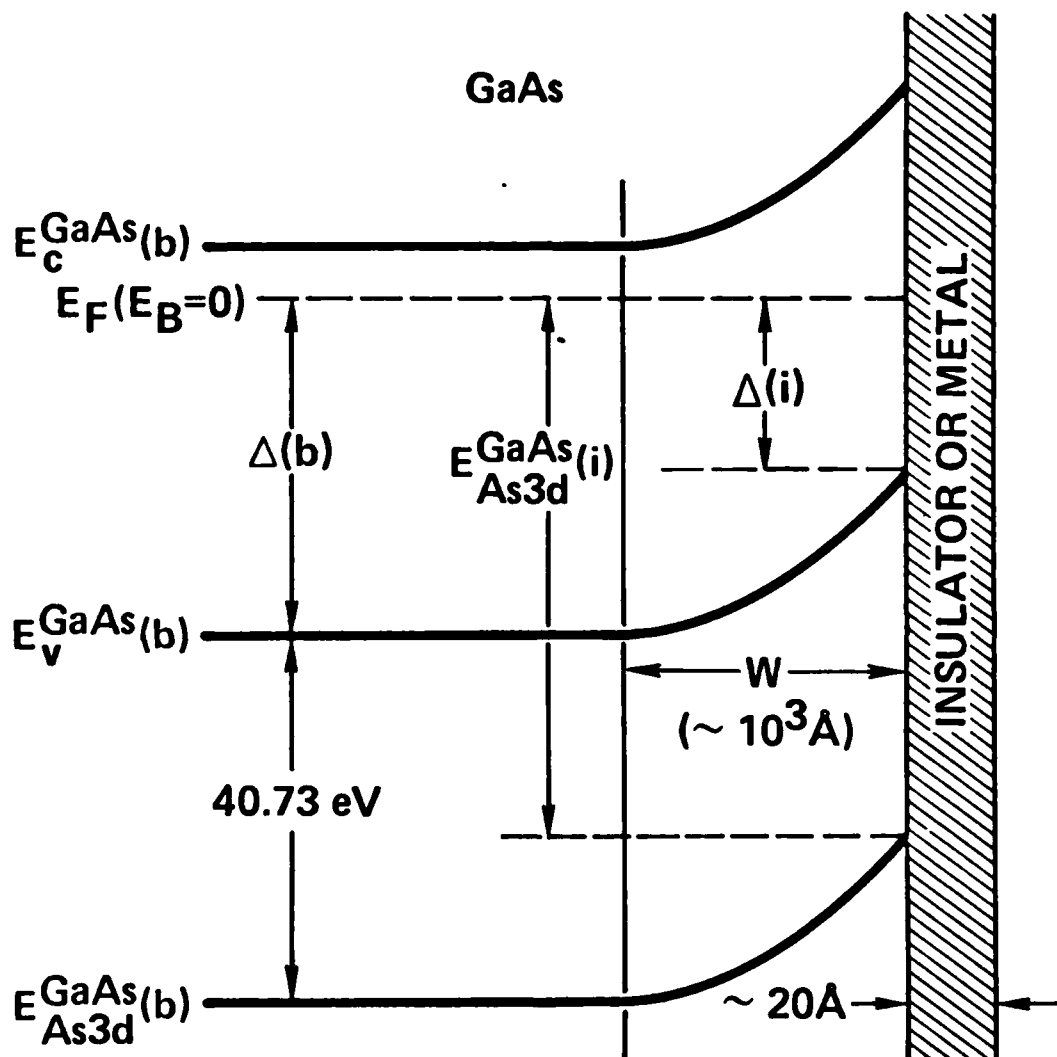
ACKNOWLEDGEMENTS

REFERENCES

1. W.E.Spicer, I. Lindau, P. Skeath and C.Y. Su, J. Vac. Sci. Technol. 17, 1019 (1980) and references therein.

2. M.S. Daw and D.L. Smith, J. Vac. Sci. Technol. 17, 1028 (1980).

3. R.W. Grant, S.P. Kowalczyk, J.R. Waldrop and W.A. Hill, in The Physics of MOS Insulators, edited by G. Lucovsky, S.T. Pantelides and F.L. Galeener (Pergamon Press, New York, 1980) p. 202.

4. E.A. Kraut, R.W. Grant, J.R. Waldrop and S.P. Kowalczyk, Phys. Rev. Lett. 44, 1620 (1980).

5. Obtained from Crystal Specialties, Inc.

6. F.R. McFeely, S.P. Kowalczyk, L.Ley, R.A. Pollak and D.A. Shirley, Phys. Rev. B 7, 5228 (1973).

7. C.Y. Su, I. Lindau, P.R. Skeath, P.W. Chye and W.E. Spicer, J. Vac. Sci. Technol. 17, 936 (1980).

8. The Al overlayer data shown in Fig. 4 were obtained on an independent n- and p-type sample set which was thermally cleaned prior to the Al deposition.

9. G.A. Baraff, E.O. Kane and M. Schlüter, Phys. Rev B 21, 5662 (1980).

10. F.S. Shishiyanu and B.I. Boltaks, Soviet Phys. - Solid State Vol. 8, 1053 (1966).

<u>FIGURE CAPTIONS</u>

Fig. 1   Schematic energy-band diagram which illustrates the XPS
         measurement of $\Delta(i)$ for GaAs.

Fig. 2   XPS spectra in the region of the As3d core level for a
         n-GaAs(100) sample with two different surface treatments.
         a) Sample was thermally cleaned at $\approx 570°C$, oxidized at
         $\approx 460°C$ by exposure to 2×10^4 L O_2 and stored in vacuum
         for 16 hours.
         b) The same sample was thermally cleaned at $\approx 570°C$
         followed by the deposition of 2-5 monolayers of Au.
         The E_B difference of 0.7 eV between the two vertical lines
         is a direct measure of the $\Delta(i)$ difference.

Fig. 3 $\Delta(i)$ for several GaAs (100) surface treatments.

Fig. 4 $\Delta(i)$ for several GaAs (110) surface treatments.

GaAs

$E_c^{GaAs(b)}$

$E_F(E_B=0)$

$\Delta(i)$

$\Delta(b)$

$E_{As3d}^{GaAs(i)}$

$E_v^{GaAs(b)}$

INSULATOR OR METAL

W
($\sim 10^3$A)

40.73 eV

$E_{As3d}^{GaAs(b)}$

$\sim$ 20A

E_c^{GaAs}

INTERFACE FERMI-LEVEL POSITION, Δ (i) (eV)

1.2

1.0

0.8

0.6

0.4

0.2

E_v^{GaAs}

n

p

42.0

41.8

41.6

41.4

41.2

41.0

40.8

As 3d BINDING ENERGY (eV)

CHEMICAL ETCH

$\approx$ 470°C ANNEAL (Ga_2O_3)

$\approx$ 550°C ANNEAL (CLEAN, LEED)

$\approx$ 430°C, 2×10^4 L O_2 (Ga_2O_3)

12 HR VACUUM

$\approx$ 540°C ANNEAL (CLEAN, LEED)

$\approx$ 1 MONOLAYER Al

$\approx$ 5 MONOLAYERS Al

SURFACE TREATMENT

105